A Study on the Development of Microwave Atomic Force Microscope

2012

Lan ZHANG

Contents

ACKNOWLEDGEMENT

I would like to express my sincere gratitude to my supervisor, Professor Yang Ju, for his tireless supports, encouragement and inspiration through my study. His invaluable support and care made possible the completion of this study.

I want to say thanks to Professor Kazuo Sato for his irreplaceable suggestions, say thanks to Professor Eiichi Tanaka for his incomparable kindness, and say thanks to Professor Kenji Fukuzawa for his invaluable help. Also, say thanks very much to Assoc. Prof. Tadashige Ikeda for his special help.

I am also grateful to Lectuer Yasuyuki Morita for the many valuable suggestions and enjoyable discussions. I further extend my appreciations to Assist. Prof. Atsushi Hosoi for his help.

Many thanks also go to all my friends and colleagues who made my life so full and happy by their warm friendship and understanding during those past years.

The scholarship provided by Mitsubishi UFJ Trust and Banking Corporation of Japan is gratefully acknowledged.

My special thanks go to my parents for their loving support and encouragement.

ABSTRACT

With the development of nanotechnology, different types of scanning probe microscope (SPM) have been developed for satisfying the requirement of nanotechnology. Recently, for the development of next generation devices and the analysis of biological tissues, the quantitative measurement of electrical properties of materials in an infinitesimal scanning area has become into a great needing.

On the other hand, microwave microscopy has been proposed for determining electrical properties of materials, because the response of materials in microwave range is directly relative to the electromagnetic properties of materials. However, nanometer scale resolution and quantitative evaluation have not been successful so far due to the difficulty in controlling the standoff distance between the probe and measured sample.

To solve the problem of microwave signals are affected by the standoff distance, we proposed a novel microwave atomic force microscopy (M-AFM). The M-AFM is a combination of the principles of the scanning probe microscope and the microwave-measurement technique. By combining the advantages of AFM with microwave-based measurement, the M-AFM has the ability to sense the topography and microwave image simultaneously with a high spatial resolution. It could be used for characterizing the electrical properties of materials on the nanometer scale.

The M-AFM probe consists of an AFM cantilever integrated with a parallel plate waveguide. To decrease the loss of microwave, gallium arsenide (GaAs) was used as the substrate. The GaAs cantilever was fabricated by micro electro mechanical system (MEMS) technique. As a result, the average dimensions of the fabricated cantilever and the body of the M-AFM probes are typically 252×31×14 μm and 2742×723×339 μm, respectively. Based on these dimensions, the characteristic impedance of the M-AFM probes is, on average, 49.3 Ω. In this way, the M-AFM probe could match well with the co-axial line, which has an impedance of 50 Ω.

In order to confirm the spatial resolution of the fabricated M-AFM probes, the

Abstract

AFM topography of two grating samples having 2000 line/mm and 18 nm step height were measured by the fabricated M-AFM probe. AFM measurements were performed by comparing with the commercial Si AFM probe. It is indicated that GaAs microwave probe has a capability to catch AFM topography of grating samples and having a high accuracy for lateral and height evaluation, similar as the commercial AFM probe.

Then, we created an M-AFM-obtained microwave image using a compact microwave instrument that was optimally synchronized with an AFM scanner. The distinguishing features of M-AFM are its ability to maintain a constant standoff distance between the probe tip and the sample surface and to measure the microwave signal interacted with the sample. Therein, both the topography and electrical-property images of the sample can be simultaneously characterized. Therefore, M-AFM is able to measure, *in situ*, the distribution of electrical properties on a nanometer scale. As shown in the experimental results, we successfully generated a microwave image of a 200-nm Au film coating on a glass wafer substrate with a spatial resolution of 120 nm, and, moreover, we measured the voltage difference between these two materials to be 19.2 mV. We also successfully created a microwave image of an Au/Au step sample with a spatial resolution on nanometer order, which indicates that the microwave measurement is not affected by the surface shape of the material and the standoff distance was well controlled by the atomic force.

Moreover, for quantitative measurements, based on the microwave theory, analytical and explicit evaluation equations for the local conductivity were proposed. To calibrate the undetermined constants, only two reference samples are needed. By substituting the measured voltage for any other materials into the evaluation equations, the conductivity of the material can be determined quantitatively.

Facing a novel device, we put the M-AFM technique into some practical applications. Firstly, under the non-contact mode, the surface topography and microwave image of a single Au nanowire were obtained by the M-AFM probe, simultaneously. In contrast to the traditional four-point method, which requires some nanowires to be in suitable positions for conductivity measurements by dispersing the

nanowires onto an insulated substrate with electrode arrays, the M-AFM can spot the nano-structures directly and measure the microwave image and topography simultaneously. Secondly, we carried out a group of experiment to verify the M-AFM with the capacity of measuring the electrical information of underlying materials. Some special samples with different thickness of dielectric films (SiO_2) which plays the role of oxide layer creating on the material surface were fabricated. Based on the results, the M-AFM can be used to measure the electrical property of material under a thin oxide layer with a limited thickness of 60 nm, and the thickness and electromagnetic parameters of the oxide layer should be considered in a quantitative measurement. Thirdly, under the non-contact AFM mode, a microwave image of osteoblast-like cell on nanometer-scale spatial resolution was created by the M-AFM. By analysis the results, quantification such as number and distribution of organelles and proteins of osteoblast-like cell as well as their dimension and electrical information can be characterized.

1. Introduction

1.1 Atomic Force Microscope (AFM)

1.1.1 Brief History of AFM

The individual surface atoms of flat samples could be made visible in real space until the introduction of the Scanning Tunneling Microscope (STM) in 1981 by Binnig, Rohrer, Gerber, and Weibel.[1] This powerful instrument has provided a breakthrough in our possibilities to investigate matter on the atomic scale. Within one year of its invention, the STM has helped to solve one of the most intriguing problems in surface science: the structure of the Si surface. Because of their fabulous contribution, G. Binnig and H. Rohrer were rewarded with the Nobel Prize in physics in 1986. A huge number of conductors and semiconductors have been investigated on the atomic scale and marvelous images of this world of atoms have been created within the first few years after the inception of the STM. Today, the STM is an invaluable asset in the surface scientist's toolbox.

Despite the great success of the STM, it has a serious limitation. The STM requires electrical conduction of the sample material, because the STM needs the tunneling current which is flowing between a pin contact with or very nearing the sample. Thus, the STM can only image electrically conductive samples, which limits its application to imaging metals and semiconductors. But even conductors except for a few special materials, like highly oriented pyrolytic graphite can not be studied in ambient conditions by STM but have to be investigated in an ultra-high vacuum (UHV). In ambient conditions, the surface layer of solids constantly changes by adsorption and desorption of atoms and molecules. UHV is required for clean and well defined surfaces. Taking the above condition into account, Binnig speculated the atomic force between the tip and sample, the Atomic Force Microscope (AFM)[2][3] was invented by him in 1986. Because electrical conductivity of the sample is not required in AFM, the AFM can image virtually any solid surface without the need for surface

preparation. Consequently, thousands of AFMs are in use in universities, public and industrial research laboratories all over the world.

1.1.2 Principle of Atomic Force Microscope

The AFM consists of a cantilever with a sharp probe-tip at its end that is used to scan the specimen surface (see **Fig. 1-1**). The cantilever is typically silicon or silicon nitride with a tip radius of curvature on the order of nanometers. When the tip is brought into proximity of a sample surface, forces between the tip and the sample lead to a deflection of the cantilever according to Hooke's law. Depending on the situation, forces that are measured in AFM include mechanical contact force, van der Waals forces, capillary forces, chemical bonding, electrostatic forces, magnetic forces , etc. Along with force, additional quantities may simultaneously be measured through the use of specialized types of probe. The deflection is measured using a laser spot reflected from the top surface of the cantilever into an array of photodiodes.

Laser light from a solid state diode is reflected off the back of the cantilever and collected by a position sensitive detector (PSD) consisting of two closely spaced photodiodes whose output signal is collected by a differential amplifier. Angular displacement of the cantilever results in one photodiode collecting more light than the other photodiode, producing an output signal (the difference between the photodiode signals normalized by their sum) which is proportional to the deflection of the cantilever. It detects cantilever deflections <10 nm (thermal noise limited). A long beam path (several centimeters) amplifies changes in beam angle.

If the tip was scanned at a constant height, a risk would exist that the tip collides with the surface, causing damage. Hence, in most cases a feedback mechanism is employed to adjust the tip-to-sample distance to maintain a constant force between the tip and the sample. Traditionally, the sample is mounted on a piezoelectric tube that can move the sample in the z direction for maintaining a constant force, and the x and y directions for scanning the sample. Alternatively a tripod configuration of three piezoelectric crystals may be employed, with each responsible for scanning in

the *x, y* and *z* directions. This eliminates some of the distortion effects seen with a tube scanner. In newer designs, the tip is mounted on a vertical piezoelectric scanner while the sample is being scanned in *x* and *y* using another piezoelectric block. The resulting map of the area *z=f(x,y)* represents the topography of the sample.

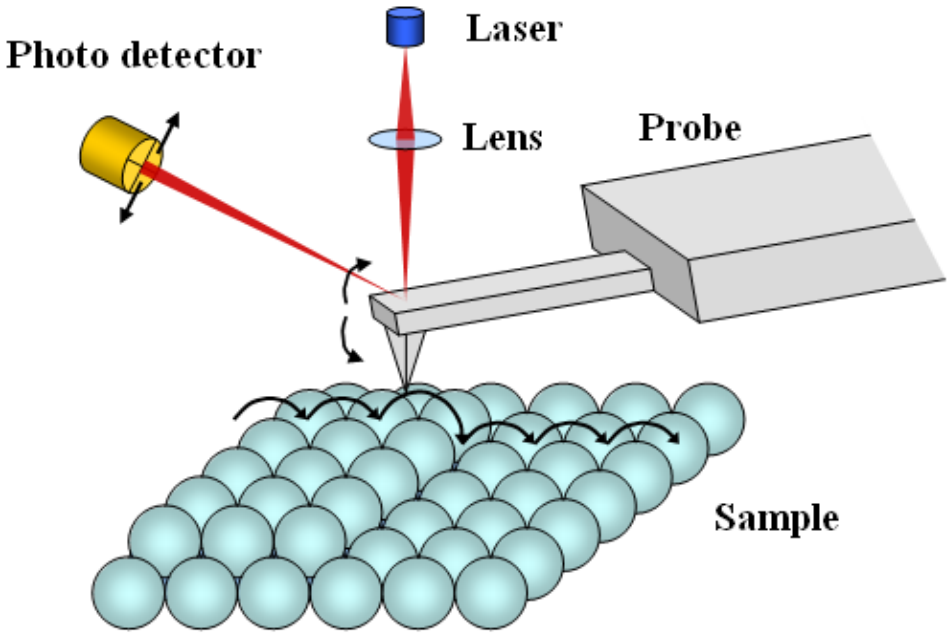

Fig. 1-1 Atomic Force Microscope.

1.1.3 Modulation of Atomic Force Microscope

1.1.3.1 Contact Mode

In the static mode operation, the static tip deflection is used as a feedback signal. Because the measurement of a static signal is prone to noise and drift, low stiffness cantilevers are used to boost the deflection signal. However, close to the surface of the sample, attractive forces can be quite strong, causing the tip to snap-in to the surface. Thus static mode AFM is almost always done in contact where the overall force is repulsive. Consequently, this technique is typically called contact mode. In contact

mode, the force between the tip and the surface is kept constant during scanning by maintaining a constant deflection.

1.1.3.2 Tapping Mode

In ambient conditions, most samples develop a liquid meniscus layer. Because of this, keeping the probe tip close enough to the sample for short-range forces to become detectable while preventing the tip from sticking to the surface presents a major problem for non-contact dynamic mode in ambient conditions. Dynamic contact mode (also called intermittent contact or tapping mode) was developed to bypass this problem. In tapping mode (also called AC Mode or intermittent contact mode) the cantilever is driven to oscillate up and down at near its resonance frequency by a small piezoelectric element mounted in the AFM tip holder similar to non-contact mode. Tapping mode is gentle enough even for the visualization of supported lipid bilayers or adsorbed single polymer molecules under liquid medium. With proper scanning parameters, the conformation of single moleculescan remain unchanged for hours.

1.1.3.3 Non-Contact Mode

In this mode, the tip of the cantilever does not contact the sample surface. The cantilever is instead oscillated at a frequency slightly above its resonant frequency where the amplitude of oscillation is typically a few nanometers (<10 nm). The van der Waals forces, which are strongest from 1 nm to 10 nm above the surface, or any other long range force which extends above the surface acts to decrease the resonance frequency of the cantilever. This decrease in resonant frequency combined with the feedback loop system maintains a constant oscillation amplitude or frequency by adjusting the average tip-to-sample distance. Measuring the tip-to-sample distance at each (*x,y*) data point allows the scanning software to construct a topographic image of the sample surface. Non-contact mode AFM does not suffer from tip or sample

degradation effects that are sometimes observed after taking numerous scans with contact AFM. This makes non-contact AFM preferable to contact AFM for measuring soft samples. In the case of rigid samples, contact and non-contact images may look the same. However, if a few monolayers of adsorbed fluid are lying on the surface of a rigid sample, the images may look quite different. An AFM operating in contact mode will penetrate the liquid layer to image the underlying surface, whereas in non-contact mode an AFM will oscillate above the adsorbed fluid layer to image both the liquid and surface.

In amplitude modulation, changes in the phase of oscillation can be used to discriminate between different types of materials on the surface. Amplitude modulation can be operated either in the non-contact or in the intermittent contact regime. In frequency modulation (FM mode), changes in the oscillation frequency provide information about tip-sample interactions. Frequency can be measured with very high sensitivity and thus the frequency modulation mode allows for the use of very stiff cantilevers. Stiff cantilevers provide stability very close to the surface and, as a result, this technique was the first AFM technique to provide true atomic resolution.

1.2 Microwave Technique for Materials Characterization

The microwave methods for materials characterization generally fall into resonant methods and non-resonant methods. Resonant methods are used to get knowledge of dielectric properties at single frequency or several discrete frequencies, while non-resonant methods are often used to get a general knowledge of electromagnetic properties over a frequency range. By modifying the general knowledge of electrical properties over a certain frequency range obtained from non-resonant methods with the accurate knowledge of electrical properties at several discrete frequencies obtained from resonant methods, accurate knowledge of materials properties over a frequency range can be obtained.

1.2.1 Resonant Methods

Resonant methods usually have higher accuracies and sensitivities. They are most suitable for low-loss samples. Resonant methods generally include the resonator method and the resonant-perturbation method. The resonator method is based on the fact that the resonant frequency and quality factor of a dielectric resonator with given dimensions are determined by its permittivity and permeability. Resonant method is usually used to measure low-loss dielectric whose permeability is μ_0. The resonant-perturbation method is based on resonant-perturbation theory. For a resonator with given electromagnetic boundaries, when part of the electromagnetic boundary condition is changed by introducing a sample, its resonant frequency and quality factor will also be changed. From the changes of the resonant frequency and quality factor, the electrical properties of the sample can be derived.

1.2.2 Non-Resonant Methods

In non-resonant methods, the electrical properties of materials are fundamentally deduced from their impedance and the wave velocities in the materials. As shown in **Fig. 1-2**, when an electromagnetic wave propagates from one materials into another (from free space to sample), both the characteristic wave impedance and the wave velocity change, resulting in a partial reflection of the electromagnetic wave from the interface between the two materials. Measurements of the reflection from such an interface and the transmission through the interface can provide information for the deduction of permittivity and permeability relationships between the two materials.

Non-resonant methods mainly include transmission/reflection methods and reflection methods. In a transmission/reflection method, the material properties are calculated on the basis of the reflection form the sample and the transmission through the sample, and in reflection methods, electromagnetic waves are directed to a sample under study, and the properties of the material sample are deduced from the reflection coefficient at a defined reference plane.

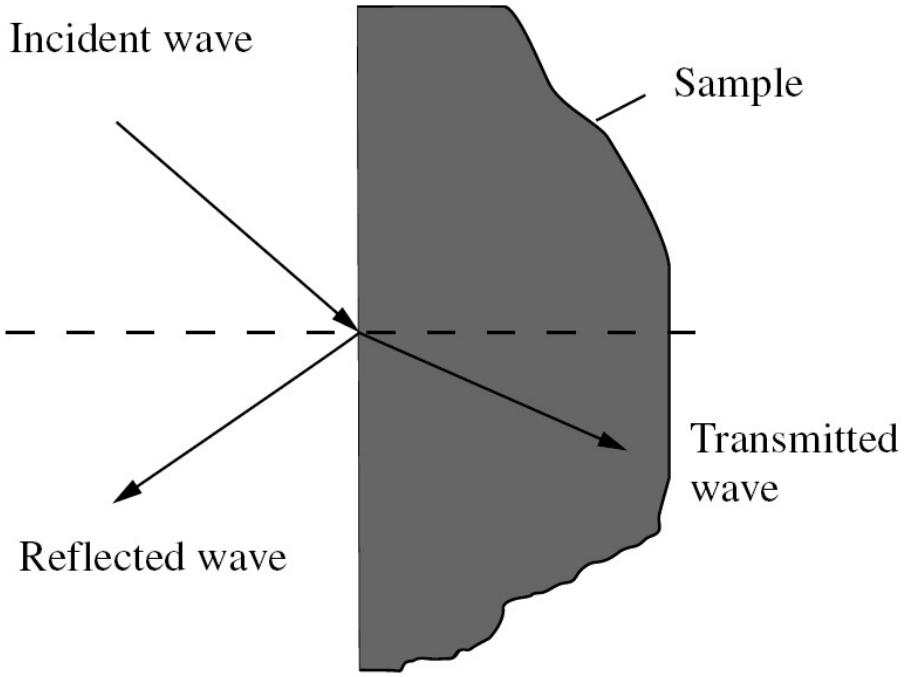

Fig. 1-2 Boundary condition for material characterization using a non-resonant method.

1.2.2.1 Transmission/Reflection Method

In a transmission/reflection method, the sample under test is inserted into a segment of transmission line, such as waveguide or coaxial line. From the relevant scattering equations relating the scattering equations relating the scattering parameters of the segment of transmission line filled with the sample under study to the permittivity and permeability of the sample, the electromagnetic properties of sample can be obtained.

1.2.2.2 Reflection Method

In a reflection method, the properties of a sample are obtained from the reflection due to the impedance discontinuity caused by the presence of the sample in a transmission structure.

The reflection method is a type of non-resonant method. From the view of transmission line, in a reflection method, the sample under test is introduced into a

certain position of a transmission line, and so the impedance loading to the transmission line is changed. The properties of the sample are derived from the reflection due to the impedance discontinuity caused by the sample loading.

In a reflection method, the measurement fixture made from a transmission line is usually called measurement probe or sensor. In order to increase the measurement accuracy and sensitivity, or to satisfy special measurement requirements, the measurement probes are often specially designed (Taking this thesis for example, to investigate the surface topography and electrical property of conductive and dielectric materials simultaneously on a nanometer scale. In my work, the sensor with the name of microwave atomic force microscope (M-AFM) probe is a composed of scanning probe microscope and microwave-measurement technique together).

1.2.2.3 Near-Field Scanning Probe

In the reflection methods, there is a special method named Near-field scanning probe should be introduced. Scanning techniques for local characterization of conducting and insulating films are attracting much interest. Many efforts have been made on developing microwave near-field scanning techniques, and various types of near-filed microwave microscopes have been developed for different purposed. Under the reflection method, the properties of a sample are obtained from the reflectivity due to the presence of the sample.

In principle, any type of transmission lines can be used to develop near-field microwave microscopes. In a near-field microwave microscope developed form parallel-board waveguide, the most important part is an aperture in the form of a narrow slit (the following mentioned nano-slit plays this role in M-AFM probe). When a sample surface is in the near-filed zone of the slit, the microwave is reflected mostly from the region under the slit. Since reflection from a sample surface is determined by the resistivity, by measuring the amplitude and phase of the reflected wave while raster scanning the surface, it is possible to map the microwave resistivity of the surface. For conductive layer with thicknesses much larger that the skin depth,

we can get surface impedance, while for thin layer, we can get sheet resistance. In the determination of microwave resistivity, it is necessary to measure layer thickness independently.

1.3 Developed AFM-Based and Microwave Technique for Measuring the Electrical Properties

Electrical properties are the most significant intrinsic characteristics of substances; they strongly affect the work functions of different materials, especially in nanometer-scale materials and devices. Thus, measuring electrical properties has become an urgent need in many areas of modern technology. For instance, in the electronics industry, critical feature sizes are becoming smaller, and it is necessary to evaluate the electrical properties of the materials with the spatial resolution on a nanometer scale to establish the knowledge to predict the behavior of materials in real devices. In addition, newly developed materials, such as conducting plastic thin films and biomaterials, which may possibly have some uncertain physical properties, will be important in the field of surface science and biological applications. Despite being intensely studied for years, their electrical properties, especially their conductivity and permittivity, are still poorly understood.

As the first section of this chapter saying, atomic force microscopy (AFM) has played an important role in nano-scale science and technology because it is one of the most versatile instruments available for imaging and manipulating structures on the nanometer scale. [4-7] Several attempts based on atomic force microscopy have been made to characterize the electrical information of materials on the nanometer scale, such as conducting atomic force microscopy (C-AFM),[8][9] scanning capacitance microscopy (SCM)[10][11] and electrostatic force microscopy (EFM).[12][13] Although C-AFM can produce a nano-scale electrical characterization of thin-films, the AFM tip must contact the conducting substrate to apply a current, so during the probing process, the AFM tip will scratch the surface of the sample. SCM can characterize electrical information by measuring the capacitance between the tip of

the probe and the sample. However, it suffers from a limited spatial resolution and is sensitive to the thickness of the specimen. EFM, including Kelvin probe force microscopy (KFM)[14], scanning surface potential microscopy (SSPM)[15] and scanning Maxwell-stress microscope (SMM)[16], can measure the surface electrical potential of materials by detecting the electrostatic force between the probe tip and the sample. However, the van der Waals forces and chemical bonding forces, as well as the electrostatic forces are included in the measured data. Hence, the sample surface chemistry and atmospheric conditions greatly impact the measured electrical potential.

On the other hand, microwave measurements have been of great interest to many researchers because microwaves can propagate easily in air, and the sample response is directly related to the electrical properties of the material.[17] Thus, to obtain the microscopic electrical information, a variety of microwave microscopes have been developed [18][19]. Steinhauer et al. developed a non-destructive and non-invasive near-field scanning microwave microscope (NSMM), which can image the local permittivity and tenability of a dielectric thin film with a spatial resolution of 1 μm.[20] Zhang and co-authors improved the NSMM to investigate the local perpendicular dielectric information of single-phase multi-ferroic thin films and single crystal materials.[21] Ferd Duewer et al. introduced scanning evanescent microwave microscopy (SEMM),[22][23] which measures the changes of the tip-sample capacitance at the resonant frequency and the quality factor of microwave absorption. They succeeded in imaging the topography and surface resistance of metallic samples. However, to evaluate the electrical properties of materials using microwaves, it is necessary to keep the stand-off distance between the microwave probe and the sample constant because microwave signals in the near-field are extremely sensitive to this distance. Otherwise, it would be difficult to distinguish whether the changes in the signal are due to the difference of the material properties or the variation of the stand-off distance. In particular, to evaluate the electrical properties of materials with high resolution on the nanometer scale, it is indispensable to control the stand-off distance precisely on the order of nanometers.

Recently, to solve the problem of how microwave signals are affected by the stand-off distance, a technique of combining AFM with microwave microscopy has been studied.[24-27] K. Lai et al. invented a microwave impedance microscope (MIM),[24][25] which fed a microwave signal to a silicon nitride cantilever with a Pt tip that was used to investigate the nano-scale dielectric inhomogeneity in a non-invasive manner. The Weide group combined an NSMM with an AFM (NSMM-AFM)[26][27] by adding a microwave signal to a commercial probe. The NSMM-AFM can measure the topography and dielectric constant of thin film simultaneously. However, it is noted that MIM and NSMM-AFM do not use matched probes or cantilevers as the microwave-guide connected with the source of microwave signals. Thus, the microwave signals may not propagate along the probe and emit from the tip apex of the probe. Therefore, these techniques can only measure the changes of the probe-sample system impedance but not the intrinsic electrical properties of the measured materials.

To summarize, these AFM-based methodologies and microwave microscopy techniques can only image relative electrical properties, rather than the absolute values of the intrinsic electrical properties, such as the conductivity, permittivity, and permeability. Thus, the need remains for a microscopy technique that can provide a simultaneous measurement of topography and electrical properties on the nanometer scale.

1.4 Research Objective

Recently, we proposed a novel microwave atomic force microscopy (M-AFM). [28-32] By combining the advantages of AFM with microwave-based measurement, the M-AFM has the ability to sense the topography and microwave image simultaneously with a high spatial resolution. It could be used for characterizing the electrical properties of materials on the nanometer scale.

In previous studies, M-AFM probes have enabled us to measure the topography of a grating sample with high-resolution in air in the non-contact AFM mode.[28] These

results demonstrate that the M-AFM probe has a similar ability to image the surface topography of materials in comparison with a conventional Si AFM probe. To confirm the emission of microwaves at the tip of the M-AFM probe, a network analyzer was connected to the M-AFM probe by a coaxial line.[29] When the test samples approached the tip of probe, the reflected microwave signals were measured by the network analyzer, which indicates that the nano-slit at the tip of probe can act as a sensor to emit and receive microwave signals. Moreover, the effects of using Al and Au as waveguide coating materials for the propagation of microwave signals in the M-AFM probe has also been studied.[30] However, because it is difficult to synchronize the network analyzer that is used to measure the microwave signals with the AFM scanner that is used to create the AFM image, a microwave AFM image has not yet been achieved. Therefore, in my work, a compact microwave instrument was constructed which can be appropriately synchronized with an AFM scanner. Consequently, the microwave AFM image of different measured sample was realized.

Although microwave imaging has been realized,[31] whether the microwave image is independent from the geometrical configuration of the surface needs to be investigated further. In the following work, a new sample with two steps of same material (Au/Au) was measured with the M-AFM. The results indicated that our M-AFM can sense the electrical properties of measured materials without the influence of the geometrical configuration.

Moreover, even though the possibility of evaluating the conductivities of metallic materials has been quantitatively demonstrated,[32] the measurement of the distribution of the conductivities and the quantitative evaluation of the conductivities from microwave images has not yet been realized. Thus, for quantitative measurements, based on the microwave theory, analytical and explicit evaluation equations for the local conductivity were proposed. To calibrate the undetermined constants, only two reference samples are needed. By substituting the measured voltage for any other materials into the evaluation equations, the conductivity of the material can be determined quantitatively.

Facing a novel device, we put the M-AFM technique into some practical

applications. Firstly, under the non-contact mode, the surface topography and microwave image of a single Au nanowire were obtained by the M-AFM probe, simultaneously. In contrast to the traditional four-point method, which requires some nanowires to be in suitable positions for conductivity measurements by dispersing the nanowires onto an insulated substrate with electrode arrays, the M-AFM can spot the nano-structures directly and measure the microwave image and topography simultaneously. Secondly, we carried out a group of experiment to verify the M-AFM with the capacity of measuring the electrical information of underlying materials. Some special samples with different thickness of dielectric films (SiO_2) which plays the role of oxide layer creating on the material surface were fabricated. Based on the results, the M-AFM can be used to measure the electrical property of material under a thin oxide layer with a limited thickness of 60 nm, and the thickness and electromagnetic parameters of the oxide layer should be considered in a quantitative measurement. Thirdly, under the non-contact AFM mode, a microwave image of osteoblast-like cell on nanometer-scale spatial resolution was created by the M-AFM. By analysis the results, quantification such as number and distribution of organelles and proteins of osteoblast-like cell as well as their dimension and electrical information can be characterized.

1.5 Organization of This Dissertation

The remainder of this thesis consists of six chapters.

In Chap. 2, firstly, the principle of microwave atomic force microscope (M-AFM) was defined as that, the M-AFM is a combination of the principles of the scanning probe microscope and the microwave-measurement technique. Secondly, the working mode of M-AFM and the mechanism of microwave signals transmission were explained. Thirdly, the fabrication process of the M-AFM probe was provided. Then, we used the SEM to observe the fabricated probes and EDX to check the coating metal on the surface of M-AFM probe. Finally, by using the standard grating samples, the basic function (the capability of mapping the topography of measured sample) of

M-AFM was proofed.

In Chap.3, we depicted the integrated test system of the M-AFM. A Au/Glass step sample was scanned and the microwave image of the measured sample was obtained. and .To testify the To demonstrate that M-AFM can sense the microwave image based on electrical characteristic of the measured materials and is not affected by the surface shape of the sample an Au/Au step sample was scanned.

Chapter 4 mainly put the focus on the discussion of quantitative measurement of the electrical properties of materials on nanometer scale. Based on the microwave theory, we proposed the novel analytical and explicit evaluation equations for evaluating the local conductivity. Only two reference samples were used to calibrate the undetermined constants in the equations, and then, any other conductivity of the material can be determined quantitatively.

In Chap. 5, we put the M-AFM technique into three kinds of application field. Firstly, we used the M-AFM probe to implement a microwave image of a single Au nanowire. Secondly, some special samples with different thickness of dielectric films which plays the role of oxide layer creating on the material surface were scanned by the M-AFM probe. Thirdly, under the non-contact AFM mode, a microwave image of osteoblast-like cell on nanometer-scale spatial resolution was created by the M-AFM.

Finally, the conclusions of this thesis are summarized and discussed in Chap. 6.

A work flowchart of this research is illustrated in **Fig. 1-3.**

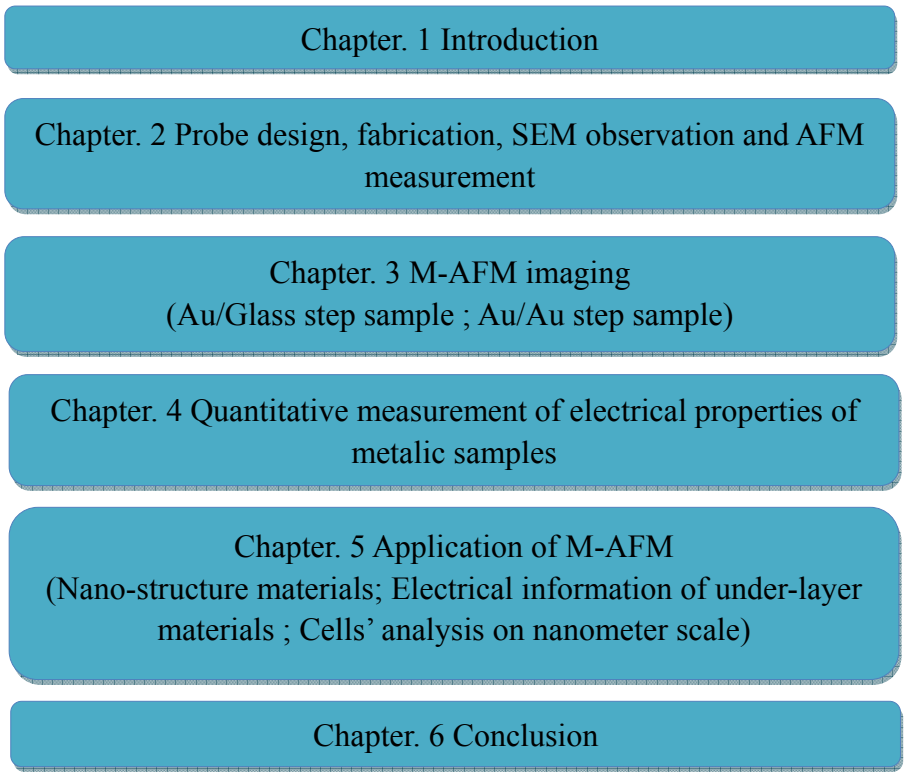

Fig. 1-3 The work flowchart of this research.

REFERENCES:

1**.** Binnig, G; Rohrer, H; Gerber, C; Weibel, E. Surface Studies by Scanning Tunneling Microscopy. *Phys. Rev. Lett.* **1982,** *49*, 57-61.

2. Binnig, G.; Quate, C. F.; Gerber, C. Atomic Force Microscope. *Phys. Rev. Lett.* **1986,** *56*, 930-933.

3. Rugar, D.; Hansma, P. Atomic Force Microscopy. *Phys. Today* **1990,** *43*, 23-30.

4. Meli, M. V.; Badia, A.; Grütter, P.; Lennox, R. B. Self-Assembled Masks for the Transfer of Nanometer-Scale Patterns into Surfaces: Characterization by AFM and LFM. *Nano lett*. **2002,** *2*, 131-135.

5. Chen, L. W.; Cheung, C. L.; Ashby, P. D.; Lieber, C. M. Single-Walled Carbon Nanotube AFM Probes: Optimal Imaging Resolution of Nanocluster and Biomolecules in Ambient and Fluid Environments. *Nano lett*. **2004,** *4*, 1725-1731.

6. Wen, C. K.; Goh, M. C. AFM Nanodissection Reveals Internal Structure Details of Single Collagen Fibrils. *Nano lett*. **2004,** *4*, 129-132.

7. Wade, L. A.; Shapiro, I. R.; Ma, Z. Y.; Quake, S. R.; Collier, C. P. Correlating AFM

Probe Morphology to Image Resolution for Single-Wall Carbon Nanotube Tips. *Nano lett*. **2004,** *4*, 725-731.

8. Olbrich, A.; Ebersberger, B.; Boit, C. Conducting Atomic Force Microscopy for Nanoscale Electrical Characterization of Thin SiO_2. *Appl. Phys. Lett.* **1998,** *73*, 3114-3116.

9. Xu, D. G.; Watt, G. D.; Harb, J. N.; Davis, R. C. Electrical Conductivity of Ferritin Proteins by Conductive AFM. *Nano lett*. **2005,** *5*, 571-577.

10. Kopanski, J. J.; Marchiando, J. F.; Lowney, J. R. Scanning Capacitance Microscopy Measurements and Modeling: Progress towards Dopant Profiling of Silicon. *J. Vac. Sci. Technol.* B **1996**, *14*, 242-247

11. Smoliner, J.; Brezna, W.; Klang, P.; Andrews, A. M.; Strasser, G. Quantitative Scanning Capacitance Microscopy on Single Subsurface InAs Quantum Dots. *Appl. Phys. Lett.* **2008,** *92*, 092112.

12. Stern, J. E.; Terris, B. D.; Mamin, H. J.; Rugar, D. Deposition and Imaging of Localized Charge on insulator surfaces using a force microscope. *Appl. Phys. Lett.* **1988,** *53*, 2717-2719.

13. Hu, Z. H.; Fischbein, M. D.; Drndić, M. Local Charge Transport in Two-dimensional PbSe Nanocrystal Arrays Studied by Electrostatic Force Microscopy. *Nano lett*. **2005,** *5*, 1463-1468.

14. Nonnenmacher, M.; O'Boyle, M. P.; Wickramasinghe, H. K. Kelvin Probe Force Microscopy. *Appl. Phys. Lett.* **1991,** *58*, 2921-2923.

15. Fujihara, M.; Kawate, H. Scanning Surface Potential Microscope for Characterization of Langmuir-Blodgett Films. *Thin Solid Films* **1994,** *242*, 163-169.

16. Yokoyama, H.; Inoue, T. Scanning Maxwell Stress Microscope for Nanometer-scale Surface Electrostatic Imaging of Thin Films. *Thin Solid Films* **1994,** *242*, 33-39.

17. Ju, Y.; Inoue, K.; Saka, M.; Abé, H. Contactless Measurement of Electrical Conductivity of Semiconductor Wafers Using the Reflection of Millimeter Waves. *Appl. Phys. Lett.* **2002,** *81*, 3585-3587.

18. Ash, E. A.; Nicholls, G. Super-resolution Aperture Scanning Microscope. *Nature*

1972, *237*, 510-512.

19. Rosner, B. T.; Van der Weide, D. W. High-frequency Near-field Microscopy. *Rev. Sci. Instrum.* **2002,** *73*, 2505-2525.

20. Steinhauer, D. E.; Vlahacos, C. P.; Wellstood, F. C.; Anlage, S. M.; Canedy, C.; Ramesh, R.; Stanishevsky, A.; Melngailis, J. Imaging of Microwave Permittivity, Tunability, and Damage Recovery in (Ba, Sr)TiO_3 Thin Films. *Appl. Phys. Lett.* **1999,** *75*, 3180-3182.

21. Zhang, X. Y.; Wang, X. C.; Xu, F.; Ma, Y. G.; Ong, C. K. High Frequency Dielectric Properties Distribution of $BiFeO_3$ Thin Using Near-filed Microwave Microscopy. *Rev. Sci. Instrum.* **2009,** *80*, 114701.

22. Duewer, F.; Gao, C.; Takeuchi, I.; Xiang, X. D. Tip-sample Distance Feedback Control in a Scanning Evanescent Microwave Microscope. *Appl. Phys. Lett.* **1999,** *74*, 2696-2698.

23. Gao, C.; Hu, B.; Zhang, P.; Huang, M. M.; Liu, W. H.; Takeuchi, I. Quantitative Microwave Evanescent Microscopy of Dielectric Thin Films Using a Recursive Image Charge Approach. *Appl. Phys. Lett.* **2004,** *84*, 4647-4649.

24. Lai, K.; Kundhikanjana, W.; Peng, H.; Cui, Y.; Kelly, M. A.; Shen, Z. X. Tapping Mode Microwave Impedance Microscopy. *Rev. Sci. Instrum.* **2009,** *80*, 043707.

25. Kundhikanjana, W.; Lai, K. J.; Wang, H. L.; Dai, H. J.; Kelly, M. A.; Shen, Z. X. Hierarchy of Electronic Properties of Chemically Derived and Pristine Graphene Probed by Microwave Imaging. *Nano lett*. **2009,** *9*, 3762-3765.

26. Van der Weide, D. W. Localized Picosecond Resolution with a Near-field Microwave/Scanning-force Microscope. *Appl. Phys. Lett.* **1996,** *70*, 677-679.

27. Karbassi, A.; Ruf, D.; Bettermann, A. D.; Paulson, C. A.; Van der Weide, D. W.; Tanbakuchi, H.; Stancliff, R. Quantitative Scanning Near-field Microwave Microscopy for Thin Film Dielectric Constant Measurement. *Rev. Sci. Instrum.* **2008,** *79*, 094706.

28. Ju, Y.; Kobayashi, T.; Soyama, H. Development of a Nanostructural Microwave Probe Based on GaAs. *Microsyst. Technol.* **2008,** *14*, 1021-1025.

29. Ju, Y.; Hamada, M.; Kobayashi, T.; Soyama, H. A Microwave Probe

Nanostructure for Atomic Force Microscopy. *Microsyst. Technol.* **2009,** *15*, 1195-1199.

30. Hosoi, A; Hamada, M; Fujimoto, A; Ju, Y. Properties of M-AFM Probe Affected by Nanostructural Metal Coatings. *Microsyst. Technol.* **2010,** *16*, 1233-1237.

31. Zhang, L.; Ju, Y.; Hosoi, A.; Fujimoto, A. Microwave Atomic Force Microscopy Imaging for Nanometer-scale Electrical Property Characterization. *Rev. Sci. Instrum.* **2010,** *81*, 123708.

32. Fujimoto, A.; Zhang, L.; Hosoi, A.; Ju, Y. Structure Modification of M-AFM Probe for the Measurement of Local Conductivity. *Microsyst. Technol.* **2011,** 17, 715–720.

2.The Principle, Fabrication and Evaluation of Microwave AFM

2.1 The Principle of M-AFM

2.1.1 Microwave AFM

The microwave atomic force microscope (M-AFM) is a combination of the principles of the scanning probe microscope and the microwave-measurement technique.[1-5] M-AFM can maintain the constant stand-off distance between the M-AFM-probe tip and scanned sample surface, by detecting the deflection of the atomic force between them, and measure the electrical properties of materials with nanometer scale spatial resolution.

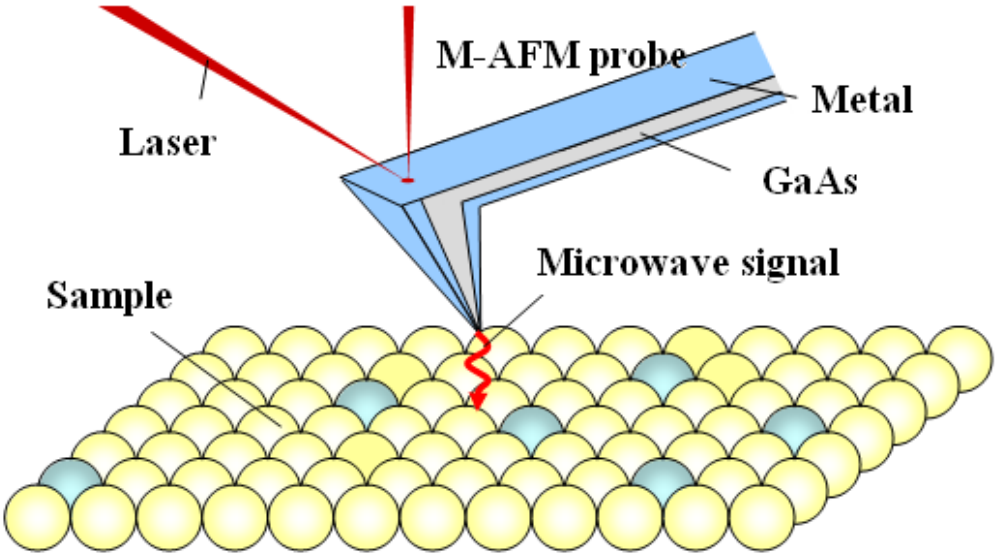

Fig. 2-1 Schematic diagram of the M-AFM probe that was used to measure the electrical properties of materials in this study.

Figure 2-1 shows the schematic diagram of the M-AFM probe that was used to measure the electrical properties of materials in this study. Different with the normally commercial AFM probes, the M-AFM probe is having a special structure. That is, a

pair of metal films was fabricated on surfaces of the M-AFM cantilever by EB (electron beam) vapor method. The metal films play a role of parallel-board microwave-signal waveguide, which can make the microwave signal propagate in the body of M-AFM cantilever and emit at the probe-tip apex. Then, by detecting the response of microwave signal reflected from the vicinity of the sample, the electrical properties can be evaluated on the nanometer scale.

2.1.2 The Working Mode of Microwave AFM

To make the M-AFM can provide a non-contact scanning function with advantage of non-destructive and non-invasive, and keep a high sensitivity for detecting atomic force acting between the M-AFM probe and measured sample. The frequency modulation (FM) mode,[6] which belongs to non-contact AFM mode, was employed in our experiment. In FM-AFM, a cantilever with eigenfrequency f_0 and spring constant k is subject to controlled positive feedback such that it oscillates with a constant amplitude A as shown in **Fig. 2-2.**

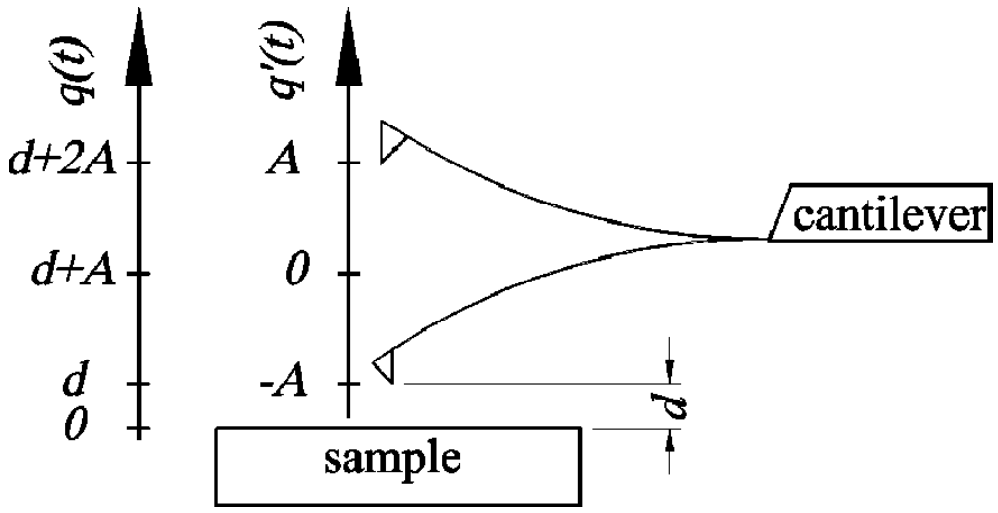

Fig. 2-2 Schematic view of an oscillating cantilever at its upper and lower turnaround points. The minimum tip-sample distance is d and the amplitude is A.

The deflection signal first enters a band-pass filter. Then the signal splits onto three branches: one branch is phase shifted, route through an analog multiplier, and feed

back to the cantilever via an actuator; one branch is used to compute the actual oscillation amplitude-this signal is used to calculate a gain input g for the analog multiplier; and one branch is used to feed a frequency detector. The frequency f is determined by the eigenfrequency f_0 of the cantilever and the phase shift φ between the mechanical excitation generated at the actuator and the deflection of the cantilever. If $\varphi=\pi/2$, the loop oscillates at $f=f_0$.

Forces between tip and sample cause a change in $f=f_0+\Delta f$. The eigenfrequecy of a harmonic oscillator is given by $(k^*/m^*)^{0.5}/(2\pi)$, where k^* is the effective spring constant and m^* is the effective mass. If the second derivative of the tip-sample potential $k_{ts}=\partial^2 V_{ts}/\partial z^2$ is constant for the whole range covered by the oscillating cantilever, $k=k+k_{ts}$. If $k_{ts}<<k$, the square root can be expanded a Taylor series and the shift in eigenfrequency is approximately given by

$$\Delta f = \frac{k_{ts}}{2k} f_0 \tag{2-1}$$

The case in which k_{ts} is not constant is treated in the next section. By measuring the frequency shift Δf, one can determine the tip-sample for gradient.

The oscillator circuit is a critical component in FM-AFM. The function of this device is understood best by analyzing the cantilever motion. The cantilever can be treated as a damped harmonic oscillator that is externally driven. For sinusoidal excitations $A_{drive}e^{i2\pi f_{drive}t}$ and a quality factor $Q>>1$, the response of the oscillation amplitude of the cantilever is given by

$$\frac{A}{A_{drive}} = \frac{1}{1-f_{drive}^2/f_0^2 + if_{drive}/(f_0 Q)} \tag{2-2}$$

the f_{drive} is the driving frequency of AFM, the absolute value of the amplitude $|A|$ is given by

$$|A| = \frac{|A_{drive}|}{\sqrt{\left(1-f_{drive}^2/f_0^2\right)^2 + f_{drive}{}^2/(f_0^2 Q^2)}} \tag{2-3}$$

and the phase angle φ between the driving and resulting signal is

$$\varphi = \arctan\left(\frac{f_{drive}}{Qf_0\left(1 - f_{driver}^2 / f_0^2\right)}\right) \tag{2-4}$$

where the Q is value of the cantilever.

In the closed feedback loop, the driving frequency can no longer be chosen freely but is determined by f_0 of the cantilever, the phase shift φ, and the tip-sample forces. The purpose of the oscillator circuit is to provide controlled positive feedback (with a phase angle of $\varphi=\pi/2$) such that the cantilever oscillates at a constant amplitude. The cantilever deflection signal is first routed through a band-pass filter which cuts off the noise from unwanted frequency bands. The filtered deflection signal branches into an RMS-to-DC converter and a phase shifer. The RMS-to-DC chip computes a DC signal that corresponds to the RMS value of the amplitude. The signal is added to the inverted set-point RMS amplitude, yielding the amplitude error signal. The amplitude error enters a proportional and optional integral controller, and the resulting signal g is multiplied with the phase-shifted cantilever deflection signal q'' with an analog multiplier chip. This signal drives the actuator. The phase shifter is adjusted so that the driving signal required for establishing the desired oscillation amplitude is minimal.

The oscillation frequency is the main observable in FM-AFM, and it is important to establish a connection between frequency shift and the forces acting between tip and sample. While the frequency can be calculated numerically, an analytic calculation is important for finding the functional relationships between operational parameters and the physical tip-sample forces. The motion of the cantilever (spring constant k, effective mass m^*) can be described by a weakly disturbed harmonic oscillator. **Figure 2-2** shows the deflection $q'(t)$ of the tip of the cantilever: it oscillates with an amplitude A at a distance $q(t)$ from a sample. The closest point to the sample is $q=d$ and $q(t)=q'(t)+d+A$. The Hamiltonian of the cantilever is

$$H = \frac{P^2}{2m^*} + \frac{kq^2}{2} + V_{ts}(q) \tag{2-5}$$

where *p=m*dq'/dt.* The unperturbed motion is given by

$$q'(t) = A\cos(2\pi f_0 t) \tag{2-6}$$

FM-AFM operated in the AFM system solved some of problems that appear in the imaging of reactive surfaces with the static AFM. The periodic motion of the cantilever prevents the tip degradation during the lateral scan due to the shear force caused by adhesion, and eliminates the jump to contact instability through the restoring force of the cantilever, kA_0 the condition is

$$\max\left|-\frac{dV_{ts}}{dz}\right| = \left|F_{ts}^{\max}\right| < kA_0 \tag{2-7}$$

where V_{ts} is the tip-sample interaction, z the tip-surface separation, F_{ts} contains the tip-surface interaction forces, k the cantilever spring constant and A_0 the oscillation amplitude.

Figure 2-3 shows the principle of frequency character of changes in mechanical resonance of the cantilever. The curve of the right ones is vibration characteristics of the cantilever resonance in a state free. In this case, resonance frequency of the cantilever f_0 is given by the following equation.

$$f_0 = \frac{1}{2\pi}\sqrt{\frac{k}{m}} \tag{2-8}$$

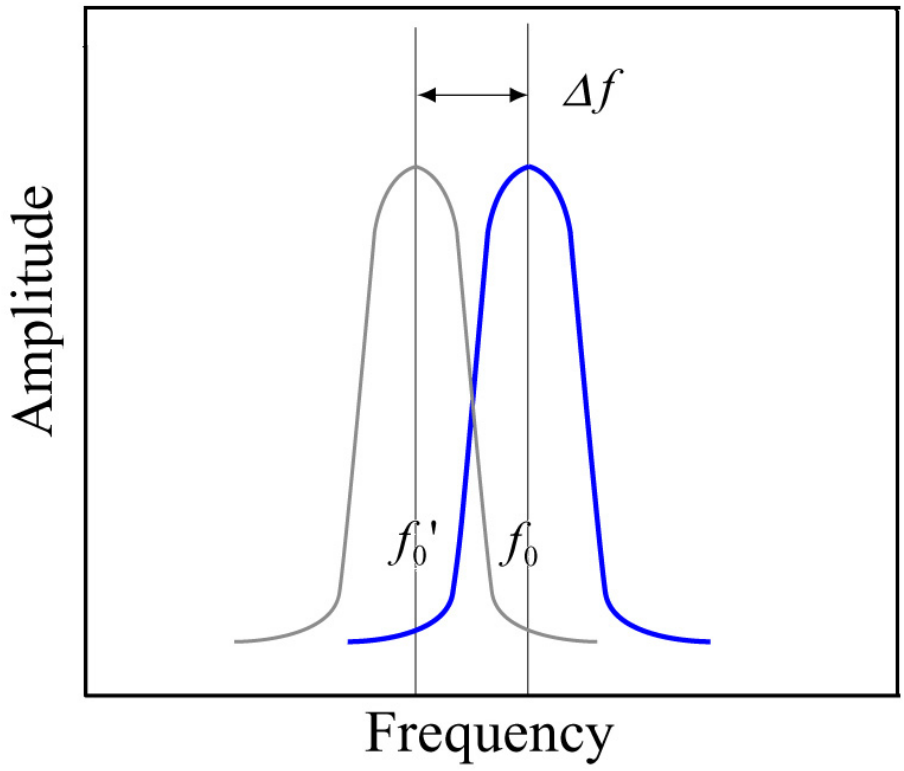

Fig. 2-3 Resonance frequency–oscillation amplitude curve of cantilever.

Here, k is the spring constant of the probe cantilever, m is the effective mass of the probe cantilever. When the AFM probe was approached to the sample surface in a very closer proximity state, and due to the gradient of the atomic force interaction between the tip and sample surface, the effective spring constant of the cantilever was changed. As a result, the resonant frequency changes as the left curve in **Fig. 2-3**, the following equation is given by the changed resonant frequency f_0':

$$f_0' = \frac{1}{2\pi}\sqrt{\frac{k - \frac{\partial F}{\partial z}}{m}} \tag{2-9}$$

Here, $\partial F/\partial z$ is the gradient between the AFM probe tip and sample surface. Therefore, by measuring the changes in resonant frequency, an approximate gradient of the atomic force acting on the cantilever (F') can be determined as follows:

$$-\frac{\partial F}{\partial z} = 2k\,\frac{\Delta f}{f_0} \tag{2-10}$$

Thus, in the other words, the non-contact measurement method is possible, due to force gradient can be decided by detecting the frequency changes of AFM probe cantilever.

In the FM mode, the cantilever is oscillated at a frequency slightly above its resonant frequency where the amplitude of oscillation is typically a few nanometers (<10 nm). The van der Waals forces, which are strongest from 1 to 10 nm above the surface, or any other long range force which extends above the surface acts to decrease the resonance frequency of the cantilever. During the scanning process, if the tip-to-sample distance was kept constant, the aforementioned force, thereby the oscillation frequency, at each scanning point would be different due to the uneven surface. In a practical scanning process, the feedback loop system can sense the transient decrease in oscillation frequency immediately and maintains a constant oscillation frequency by adjusting the average tip-to-sample distance. Measuring the tip-to-sample distance at each scanning point allows the computer to construct a topographic image of the sample surface. However, there is another question should be discussed, it is noted that taking the basic principle of M-AFM into account and as above mentioned, the microwave signals should be propagated in the probe cantilever, weather the deflection of cantilever will affect the microwave evaluation results. As view as the diagram (see **Fig. 2-2**), which shows the oscillating cantilever at its upper and lower turnaround points. During the scanning process, the absolute tip-sample distance (the deflection $q'(t)$ of the tip of the cantilever (see following image)), it oscillates with an amplitude A at a distance $q(t)$ from a sample, and $q(t)= q'(t)+d+A$. However, the deflection phenomena will not affect the microwave measurement, for comparing with the scanning speed the cantilever, microwave signals having a higher frequency (94 GHz in this study, the value which is around 400 times of the oscillating-cantilever frequency), which means at one probing point, the measured microwave signal is a mean value.

2.1.3 Microwave Transmission Mechanism

To make the microwave signals can be transmitted in the AFM probe holder and cantilever, it is important to form a microwave-signal waveguide on the surface of the probe. In order to meet the needs of light weight, mass production easy, wide bandwidth, and suit for semiconductor substrate, etc., a method of parallel-board microwave-signal waveguide was employed in this study. **Figure 2-4** shows the transmission mechanism image of parallel-board microwave-signal waveguide.

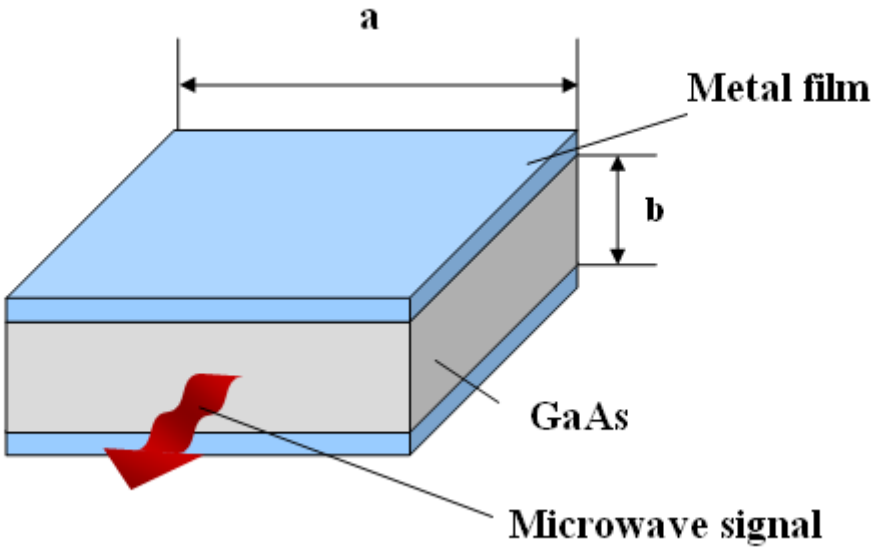

Fig. 2-4 The Schematic image of parallel-board microwave-signal waveguide.

Characteristic impedance (*Zc*) of the parallel-board microwave-signal waveguide is represented by the following equations.[7]

$$Z_c = \frac{b}{a} Z \tag{2-10}$$

$$Z = \sqrt{\frac{\mu}{\varepsilon}} \tag{2-11}$$

Here, a is the width of the conductor, b is the height distance of conductor plate spacing, Z is the characteristic impedance of the medium, μ is the permeability of the medium, ε represents the dielectric constant of the medium.

The characteristic impedance of M-AFM should be considered to match well with

the external microwave signals' source and waveguide (In my work, the characteristic impedance of external waveguide is 50 Ω, thus the characteristic impedance *Z*c of M-AFM also designed with a value of 50 Ω).

Moreover, it is necessary to choose a material suit for microwave transmission in it. Recently, the single crystal silicon (Si) and silicon nitride (SiN) substrate were used in fabricating for AFM probe widely. Since the perspective of that Si and SiN can keep the high mechanical strength and very easy to be fabricated. However, we need a material which can keep a characteristic of excellent microwave transmission. Comparing with Si and SiN, the compound semiconductor Gallium arsenide (GaAs) having excellent insulating and with low transmission losses. Therefore, the GaAs as a substrate was used to be fabricated the M-AFM probe in this study.

2.2 Fabrication of M-AFM Probe

2.2.1 Fabricating the Tip of M-AFM Probe

To restrain the attenuation of microwave in the M-AFM probe, GaAs was used as the substrate of the probe. On the other hand, to obtain the desired structure, wet etching was used to fabricate the tip of the probe. Different with the dry etching, a side-etching will occur under the etching mask. Utilizing this property, a micro tip can be fabricated by etching a wafer, of which a small mask was introduced on the surface in advance. In the case of single crystalline wafer, such as Si and GaAs, the chemical activities are different for different crystalline planes, thereby, the etch rates are also different. Therefore, the side plane obtained at the side of the mask pattern is the most inactive plane (that is the plane having the most low etching speed) which is parallel to the side of the mask pattern. Consequently, the result of etching is strong affected by the direction of mask pattern. On the other hand, GaAs has a sphalerite structure that is more complex than that of Si, which has a similar structure as diamond. Therefore, the prediction of the etch effects is very difficult[2][3].

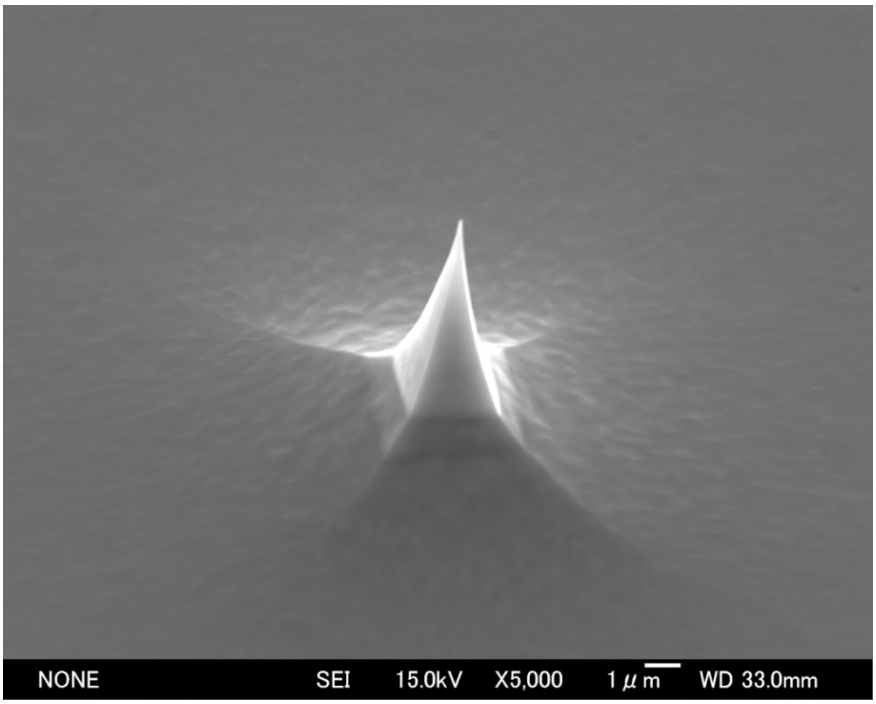

Fig. 2-5 Fabricated tip of GaAs probe.

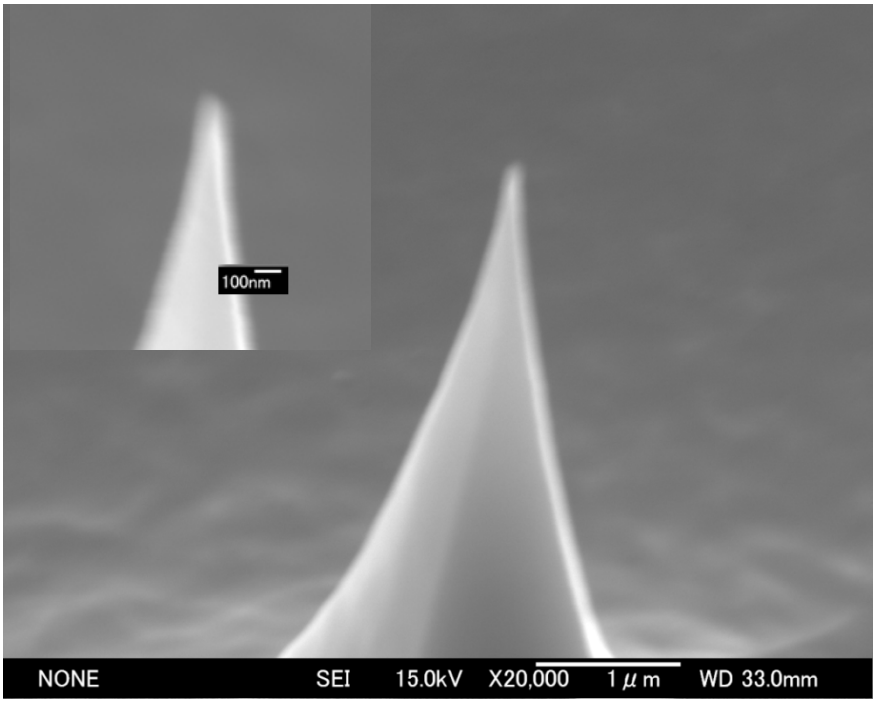

Fig. 2-6 GaAs probe tip with high magnification of apex part. The key component in an AFM is the tip, which should be as very sharp as possible.

In our study, it was found that only the square resist pattern can form a sharp tip

(**Fig. 2-5** and **Fig. 2-6**). In the case of hexagonal pattern, the reason that tip was not formed well may be due to the side of the etching mask to be too short. The reason for triangular pattern may due to that there is no crystalline plane parallel to the side of the etching mask. In addition, it was also found that one side of the square mask being 45° to the <011> direction can form a tip with a higher aspect ratio comparing with the case of one side of the resist pattern being parallel to <011> direction[4].

2.2.2 Fabrication of M-AFM Probe

The process of probe fabrication is shown in **Fig. 2-7** in details: (a) Patterning the etching mask for tip generation; (b) Forming the tips by wet etching; (c) Patterning the stencil mask for the waveguide and evaporating the metal film; (d) Removing resist and film; (e) Patterning the etching mask for the beam of cantilever; (f) Forming the beam of cantilever by wet etching; (g) Patterning the etching mask on back side for the fabrication of the holder; (h) Forming the holder; (i) Evaporation of metal film on the back side; (j) Introducing slit aperture at the tip of the probe.

In the experiment, no doped semi-insulted GaAs wafer having (100) oriented surface and 350 μm thickness was used. At first, the tips were formed by etching the wafer for 100 seconds to reach the etching depth of 7.7 μm. After that, Au film used to construct the waveguide was evaporated on the substrate. The film thickness was about 50 nm (**Fig. 2-7(c)**). After the deposition, the pattern of the waveguide was formed by lift-off process, where the film on the resist mask corresponding to the area without waveguide pattern was removed (**Fig. 2-7(d)**). Then, in order to form the beam of the cantilever, the beam etching mask was patterned. Here, by considering the chemical activities at different crystalline planes, the length direction of the etching mask was patterned along the <011> direction. In consequence, the side-etching occurred under the resist mask, and mesa type planes appeared at the both sides of the beam (45º inclined plane). On the other hand, inverse-mesa type plane was formed at the end of the beam (60-75º inclined plane). Etching depth of the beam was about 20 μm.

In the same conditions as the beam fabrication process, holder was formed by back side etching (**Fig. 2-7(f)**). Here, the etching mask was patterned on the bottom surface, and etching was carried out until the substrate was penetrated. The stirring was performed by magnetic stirrer in order to etch the sample uniformly. In the step (i) as shown in **Fig. 2-7**, Au film was deposited on bottom surface of the probe to propagate a microwave signal in the probe. The thickness of the film was 50 nm, which is the same as that on the top surface of the probe. Both plane surfaces of the waveguide which were evaporated Au film are connected at the end of the beam. However, there is no Au film on the sides of the beam, since the formed inclined planes at the beam sides are not face to the direction of the evaporation. Finally, by using FIB fabrication, a slit at the tip of probe was formed to open the connection of the Au film on the two surfaces of the probe. Consequently, a homogeneous parallel plate waveguide was formed and microwaves are able to propagate along the probe and emit at the tip apex of the M-AFM probe.

It should be mentioned that dimensions of the GaAs substrate and the Au films of the M-AFM probe decide the characteristic impedance of the waveguide, in order to make certainly that microwave signals can propagate properly in the M-AFM probe for maximum sensitivity, the waveguide should have a characteristic impedance of 50 Ω (to match the characteristic impedance of a coaxial transmission line). Thus, the cantilever and the body of the M-AFM probe were designed with the dimensions of 250×30×15 μm and 2740×720×340 μm respectively.

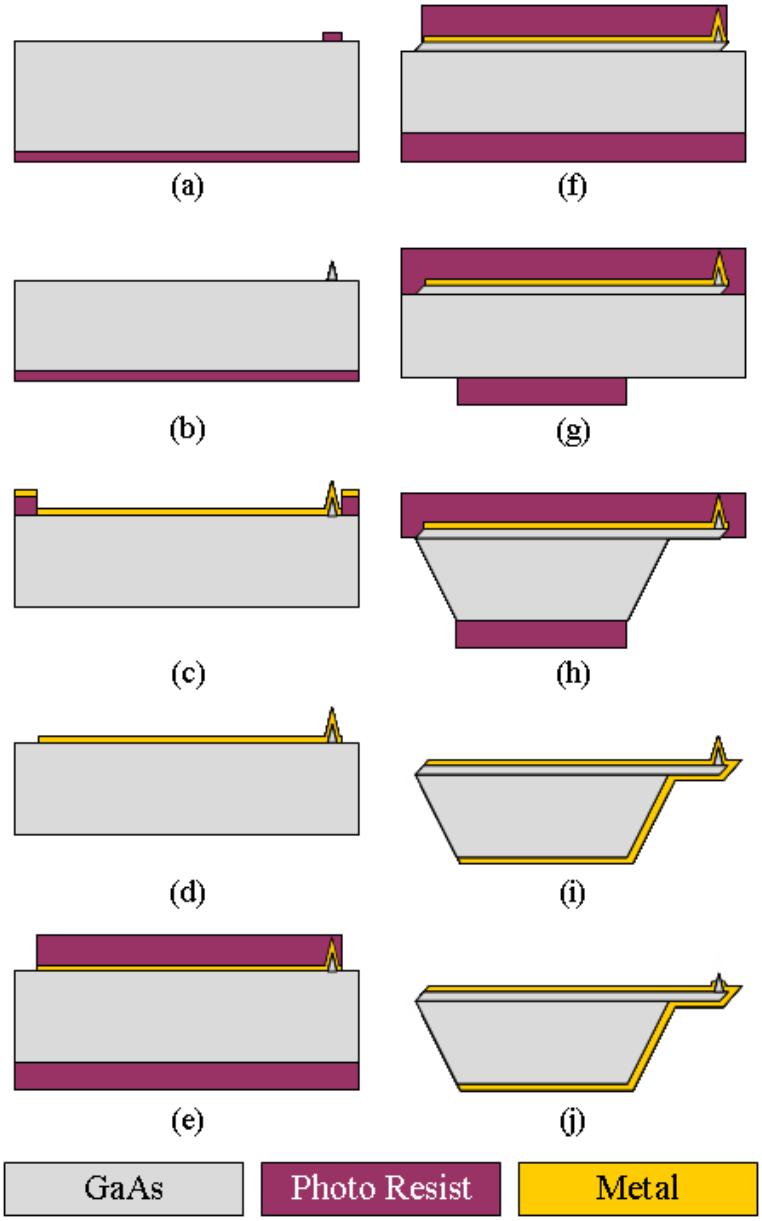

Fig. 2-7 Fabrication processes of the M-AFM probe. (a) Patterning the etching mask for the generation of tip. (b) Forming the tip by wet etching. (c) Patterning the resist mask for the waveguide. (d) Evaporating the metal film. (e) Removing the resist and metal film. (f) Patterning the etching mask for the beam of cantilever. (g) Forming the beam of cantilever by wet etching. (h) Patterning the etching mask on back side for fabrication of the holder. (i) Forming the holder. (j) Evaporation of metal film on the back side. (k) Introducing the micro slit at the tip of probe.

2.2.3 SEM Observation for Fabricated M-AFM Probes

The SEM images of the fabricated M-AFM probes are depicted in **Fig. 2-8 to Fig. 2-11**. **Figure 2-8** shows the SEM photograph of the fabricated M-AFM probes. There 44 probes were fabricated in one process for one substrate. **Figure 2-9** shows the as-fabricated cantilever of the M-AFM probe. The dimensions of the M-AFM probe depend on several small variations of experimental parameters, including the developing time of the resist pattern, the wet etching rate, and the EB evaporation rate. The average dimensions of the cantilever and the body of the M-AFM probes are typically 252×31×14 μm and 2742×723×339 μm, respectively. Thus, the characteristic impedance of the M-AFM probes is, on average, 49.3 Ω. **Figure 2-10** depicts an SEM photograph of the FIB-fabricated nano-slit that has been patterned across the cantilever through the center of the probe tip. The observed tip is located near the front edge of the cantilever. As can be observed in **Fig. 2-11**, the tip is approximately 7 μm high, and the nano-slit is approximately 100 nm in width.

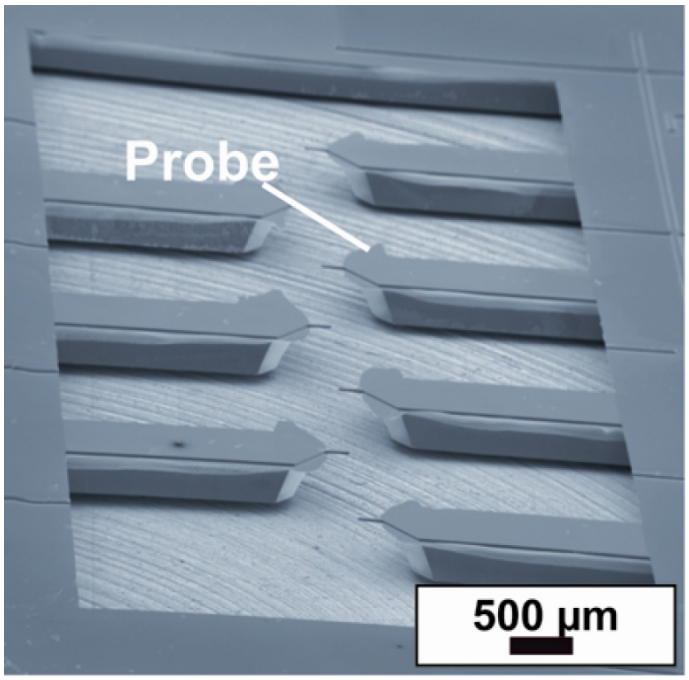

Fig. 2-8 The fabricated M-AFM probes.

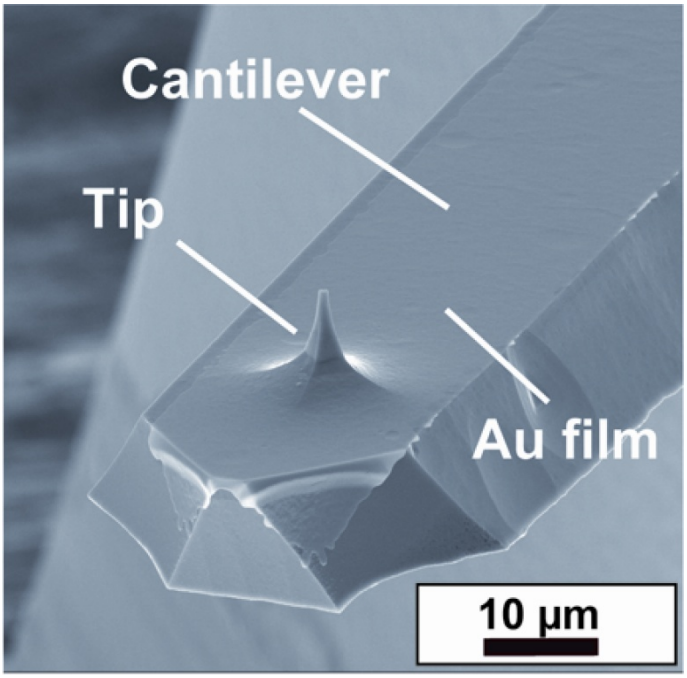

Fig. 2-9 The cantilever of the M-AFM probe.

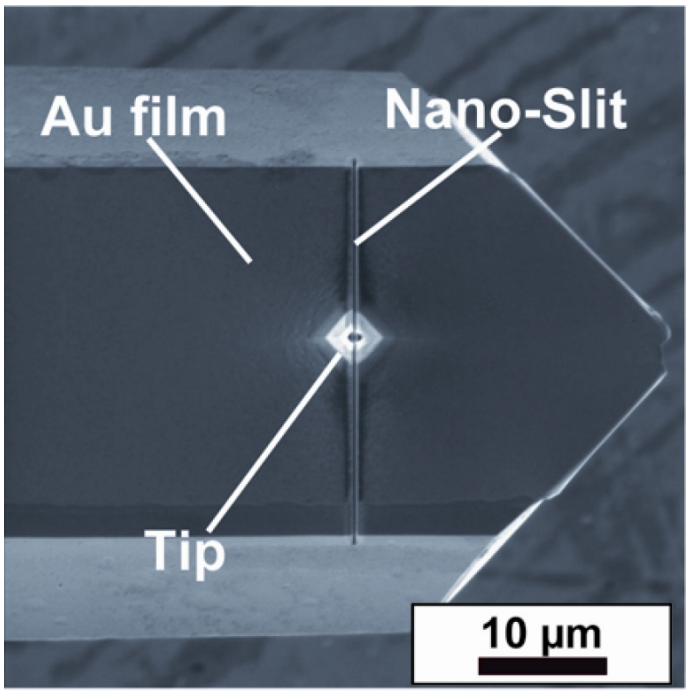

Fig. 2-10 The 100-nm-wide-FIB-fabricated nano-slit that is across the cantilever and through the center of the tip.

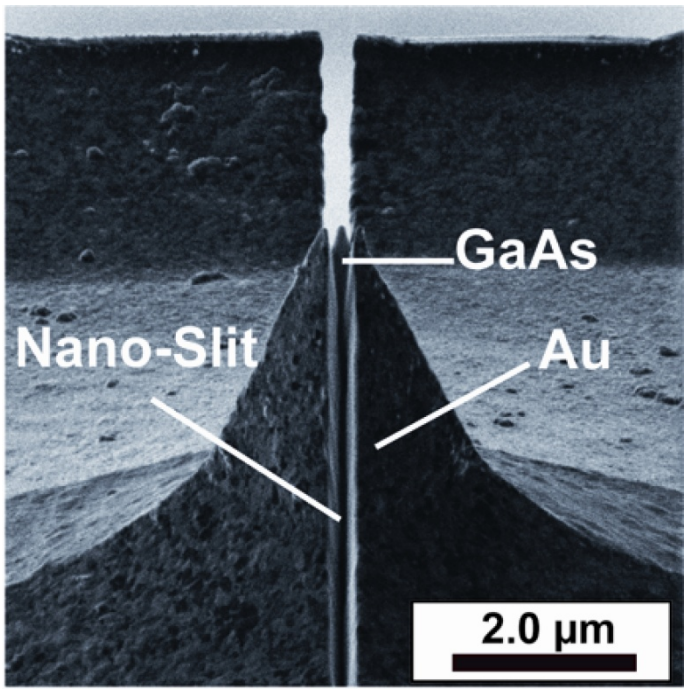

Fig. 2-11 The high-magnification image of the M-AFM-probe tip.

2.3 Microwave AFM Probe Evaluation

2.3.1 EDX for Checking the Coating Metal on the Surface of M-AFM Probe

In order to make the microwave signal can propagate efficiently in the M-AFM probe holder and the cantilever, metal films were deposited on the top and bottom surfaces of the probe to form a parallel-board microwave-signal waveguide. The metal film is required to be connected at the end of the beam, and should be absent at the sides of the beam. It is important to form the waveguide with high precision to evaluate the electrical properties of materials because the standoff distance between an AFM probe and a sample is in nanometer scale and in a practical measurement. However, the microwave probe obtained by the anisotropic etching has a steep slope between the cantilever and the body of the probe, and it is difficult to obtain the uniform film on this part. As previous introduced, the metal film is deposited on the AFM probe by EB process, because the deposition method has an advantage that it is possible to obtain

the metal film on an inhomogeneous surface. However, some fabricated probes are nagged by the situation of that the propagation of microwave signals in the microwave probe may interrupt by the open circuit at the top or other parts of the probe. Thus, in my work, The Energy Dispersive X-ray Spectrometry (EDX) method was used to be check weather that the fabricated M-AFM probes were possessing a suit coating film.

EDX is an analytical technique used for the elemental analysis or chemical characterization of a sample.[8][9] Almost, all fundamental elements' atom can be detected. Its characterization capabilities are due to the fundamental principle that each element has a unique atomic structure allowing X-rays that are characteristic of an element's atomic structure to be identified uniquely from one another. Quantitative analysis (determination of the concentrations of the elements present) entails measuring line intensities for each element in the sample and for the same elements in calibration standards of known composition. Then, the element distribution of sample can be obtained.

Firstly, we checked the coating metal on the bottom surface of M-AFM probe holder by EDX technique. The M-AFM-probe holder was covered by the metal Au could be confirmed by the EDX profile (lower image in **Fig. 2-12**). The EDX spectrum taken from the surface of the M-AFM-probe holder, and the phase shows that Au element takes the most part of atomic concentration. Secondly, based on same examine situation, the bottom surface of M-AFM cantilever was detected (in **Fig. 2-13**). Similar with the detected results of EDX spectrum over the bottom surface of M-AFM probe holder. The Au element is taking main part in atomic concentration. To verify the precision of analysis, we did repeated tests at the different place over the M-AFM probe holder and cantilever, the similar results were obtained finally.

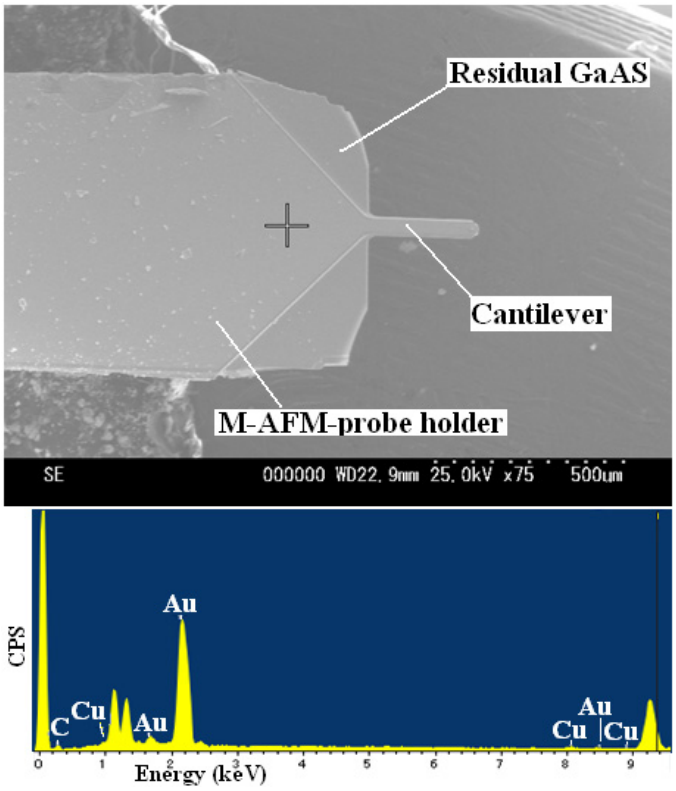

Fig. 2-12 SEM image of M-AFM-probe holder and cantilever, the crossing marker is the detection position, and the EDX spectrum over the detection position.

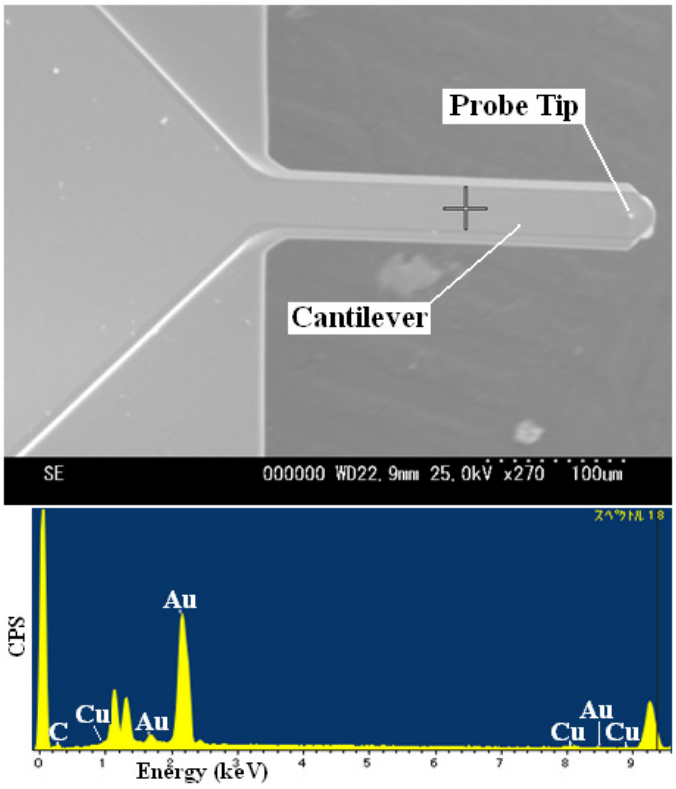

Fig. 2-13 SEM image of M-AFM cantilever, the crossing marker is the detection position, and the EDX spectrum over the detection position.

Figure 2-14 shows the SEM image of top part of M-AFM-probe and the EDX spectrum over the residual GaAs wafer substrate. During the forming the beam of cantilever (as the previous chapter mentioned), due to obtain a suit dimension of cantilever by wet etching, the GaAs wafer substrate will remain at the top part of M-AFM holder sometimes (see SEM image of **Fig. 2-14**). However, the extruding length of this residual GaAs structure is much shorter the cantilever, thus, it will not affect the AFM scanning results.

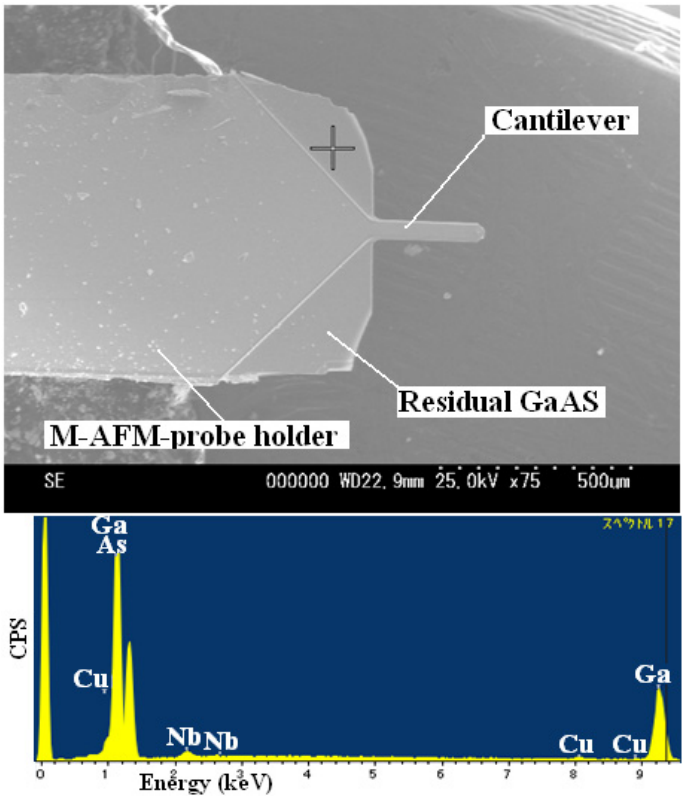

Fig. 2-14 SEM image of M-AFM-probe; EDX spectrum was used to examine the chemical characterization of residual GaAs wafer substrate.

There is potential difference, between the parallel-board microwave-signal waveguide (lower and upper metal films located on surfaces of M-AFM-probe cantilever), which can make sure the microwave signals can propagate in the M-AFM probe. If the sides of M-AFM cantilever were coated by the metal during the EB process, the microwave signals will be interrupted by the short circuit. Thus, as the **Fig. 2-15** shown**,** we checked the chemical characterization over the sides of M-AFM

cantilever. In the EDX spectrum profile gallium and arsenide phase take the most part of atomic concentration. However, the gallium and arsenide phase was detected as well as some metal element (Au and Cu in EDX spectrum). The main reason for the detection of metal element was due to the under a relatively low magnification factor (with a 270 times), the crossing marker was difficult to be pointed at a very accuracy place and the metal film on the bottom surface of M-AFM probe cantilever will affect the detection result more or less, inevitable.

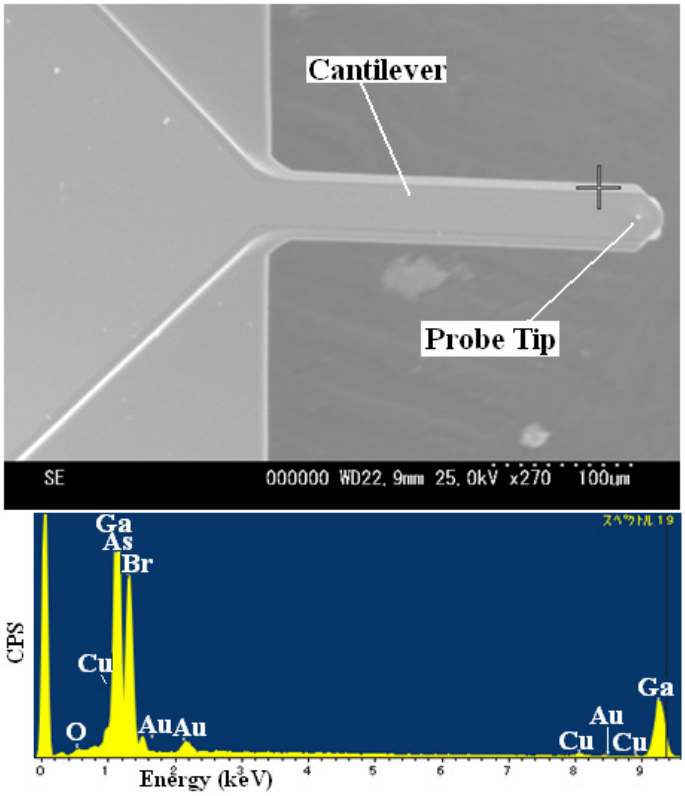

Fig. 2-15 SEM image of M-AFM-probe; EDX spectrum was used to examine the chemical characterization of GaAs (side surface).

Figures 2-16 to **2-18** are the SEM images of M-AFM-probe holder, cantilever and the EDX profiles for checking the surface chemical composing of them. The similar detected results over the three different checking positions were presented. As shown in the EDX spectrum profiles in **Fig.2-16**, **Fig.2-17** and **Fig.2-18**, the Au element is taking main part in atomic concentration.

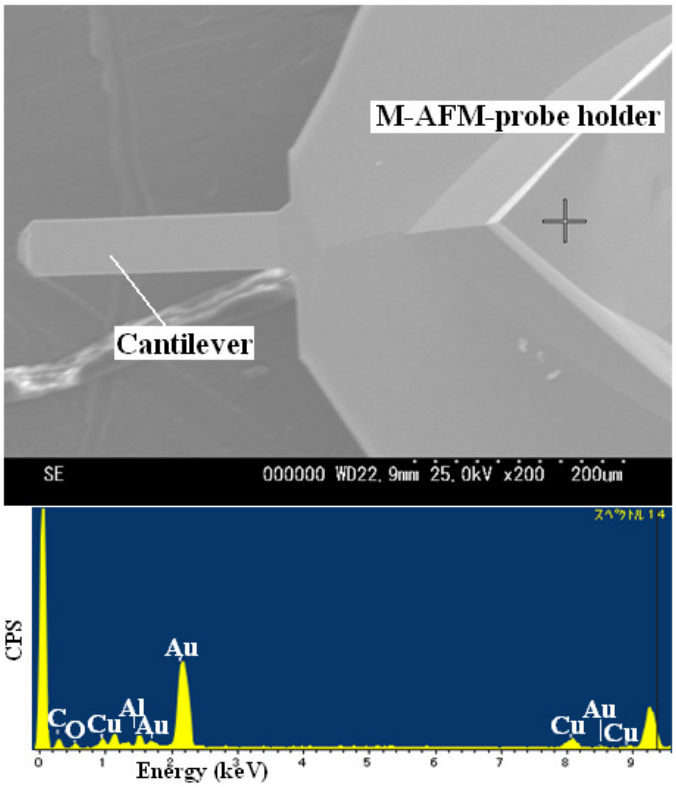

Fig. 2-16 SEM image of M-AFM-probe holder and cantilever, the crossing marker is the detection position, and the EDX spectrum over the detection position.

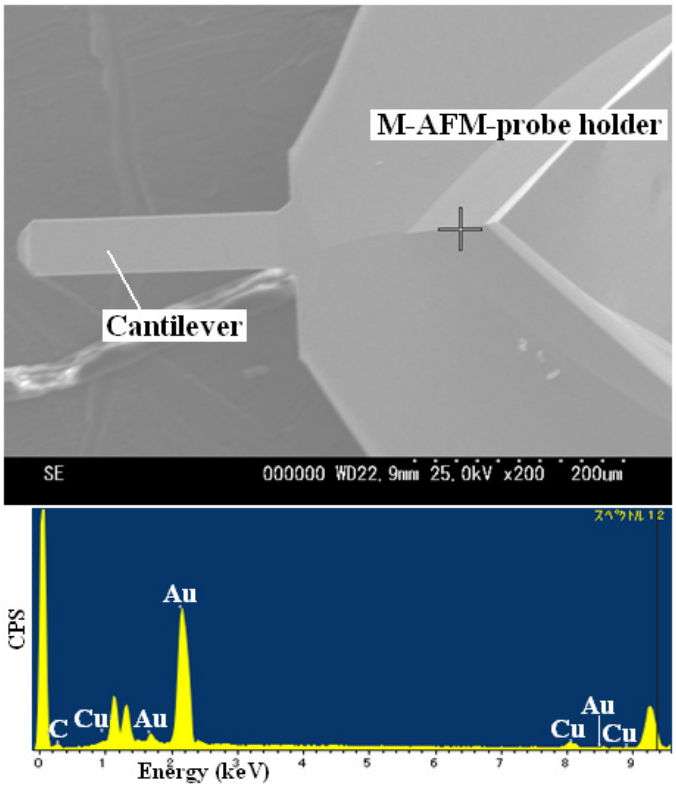

Fig. 2-17 SEM image of M-AFM-probe holder and cantilever, the crossing marker is the detection position, and the EDX spectrum over the detection position.

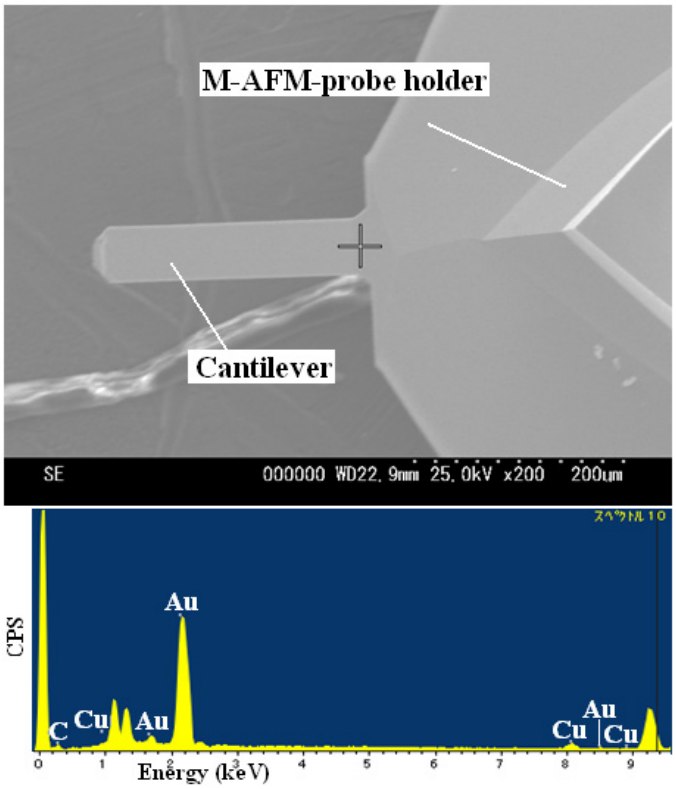

Fig. 2-18 SEM image of M-AFM-probe holder and cantilever, the crossing marker is the detection position, and the EDX spectrum over the detection position.

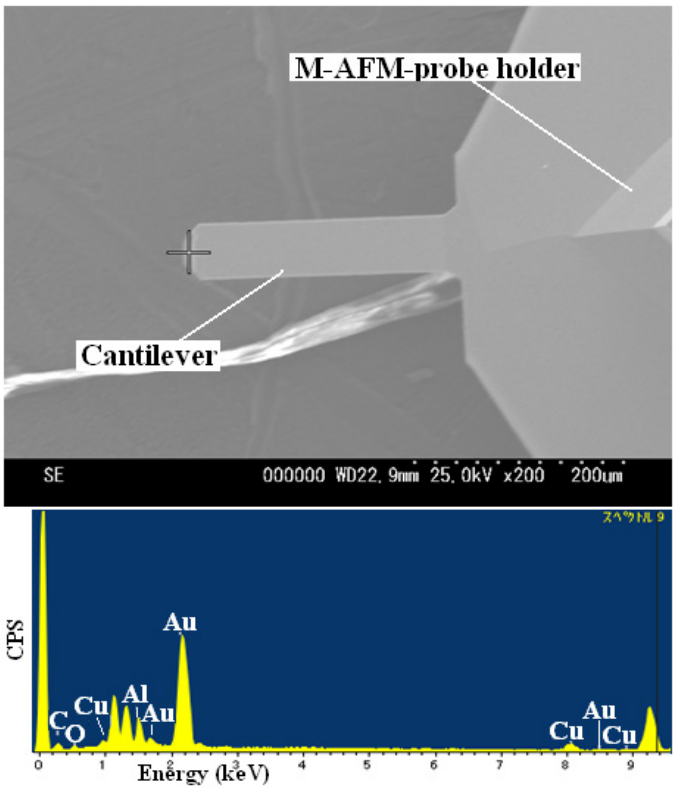

Fig. 2-19 SEM image of top part of the M-AFM-probe, the detection position located at the end of the cantilever beam, and the EDX spectrum over the detection position.

To generate a whole microwave signals transmission waveguide, the metal film on M-AFM-probe is required to be connected at the end of the cantilever beam. As the SEM image of **Fig. 2-19** shown, the detecting of chemical characterization for the end of the cantilever beam also have been done by the EDX method. In the EDX profile (see lower image of **Fig. 2-19**), Au element is possessing very high proportion in atomic concentration, thus, the end of the cantilever beam was coated by the metal Au was verified.

2.3.2 Measuring Topography by M-AFM Probe

In order to confirm the spatial resolution of the fabricated M-AFM probes, the AFM topography of two grating samples having 2000 line/mm and 17.9 nm step height were measured by a commercial Si AFM probe, a GaAs probe without nano-slit and a M-AFM probe with nano-slit, respectively.

Table 2-1 The properties of AFM probes in the atmosphere:

Probe	The resonance frequency (kHz)	*Q*-value	Spring constant (N/m)
A commercial Si probe	262	370	Typical value: 42
A GaAs probe without the nano-slit	185	510	Typical value: 134
A M-AFM probe with the nano-slit	201	333	Typical value: 134

A JSPM-5400 was used for measurement of the sample under the noncontact mode (frequency modulation (FM) mode). The properties of three kinds of probe are given in **Table 2-1**, the resonance frequency was swept and the *Q* value was defined by the following relation, $Q=f_0/(f_+-f_-)$, where f_0 is the peak frequency, f_+ and f_- the shifted

frequency from f_0 at 70.7% of peak intensity. The Q value indicates a resonance sharpness of the cantilever; the higher the Q value, the better stabilization of the oscillation.

Whether during the scanning process, the AFM system can keep in a non-contact mode, or to say, the probe can lift without having an adhesion with the measured sample. There are several experimental condition should be concerned. Firstly, the physical and surface characteristics of measured sample take very influence on it in the scanning process. For instance cohesive material, cohesionless material and elastic material were prepared as the sample, the results are very different. Secondly, the experimental environment (the testing temperature and humidity) also will affect the experimental process. Especially, for scanning living cells, the AFM probe should be put into the solution, this testing environment needs that probe cantilever with a very proper design parameter to fit this experimental needing.

Taking my experiment into account, our samples are solid materials without the special properties of cohesiveness. Moreover, under the FM-AFM testing mode, the commercial Si probe (which was used in this work with a series number of OMCL-AC160TS-C2, fabricated by Olympus) can keep in a non-contact testing situation without have a tap or contact with the measured sample surface. Based on the values as shown in **Table 2-1,** the typical spring constant value of M-AFM probe cantilever is 134 N/m, this value is larger than 100 N/m and is three times around the one of Si probe cantilever. The larger spring constant of cantilever means the M-AFM can provide larger oppose force to the van der Waals adsorption in attractive region (via Hook's law: $F = -k \times z$, where F is the force, k is the stiffness of the cantilever, and z is the distance of cantilever is bent) and keep the oscillate (with an amplitude of A) to be smaller, under the same testing situation. Thus, during the scanning process, the M-AFM probe can keep a non-contact scan, and protect the surface of measured sample.

The AFM system is also integrated with a scanner indicator, which can synchronously provide the status information of the probe to the user, during the

scanning process. When we found the probe has an adhesion with the sample, we can stop the scanning process, and take a proper adjustment.

Figures 2-21 to 2-23 show the topographies of the standard sample (the sketch as shown in **Fig. 2-20**) having 2000 lines/mm obtained by the commercial Si probe, GaAs probe without the nano-slit, and M-AFM probe with the nano-slit under the non-contact mode, respectively. The measurements were performed in the air, and the AFM worked in non-contact mode, with a working environment temperature of 25.0 °C and a relative humidity of 50%. The resonance frequency of Si probe and M-AFM probes (without nano-slit and with nano-slit) were 262 kHz, 185 kHz and 201 kHz, respectively, and the *Q*-value of them were 370, 510 and 333. The scan area was 2×2 μm^2, scanning speed was 3 μm/s, and the white spots in these figures are due to micro-dust on the sample surface.

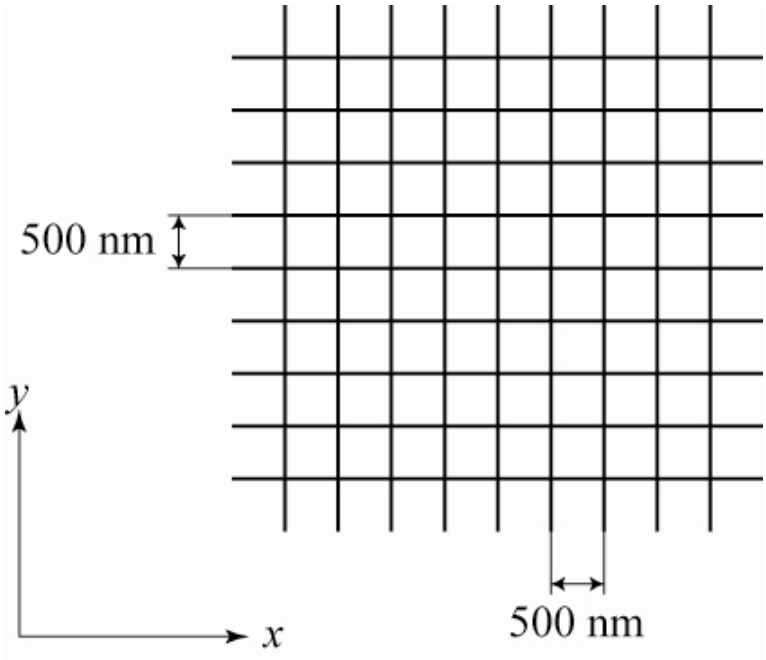

Fig. 2-20 The standard sample for the AFM measurement.

Figure 2-21(a and b) show the non-contact mode AFM topography and three-dimensional image obtained by using the commercial Si cantilever. Even though the *Q*-value is lower than that of the GaAs probe without the nano-slit, the commercial Si probe still can obtain a little higher resolution topography due to the higher aspect ratio of the tip.

Comparing the obtained images of **Fig. 2-22, Fig. 2-23** with the ones in **Fig. 2-21**, the results illustrate that M-AFM probe has a similar capability for sensing surface topography of materials as that of commercial AFM probes.

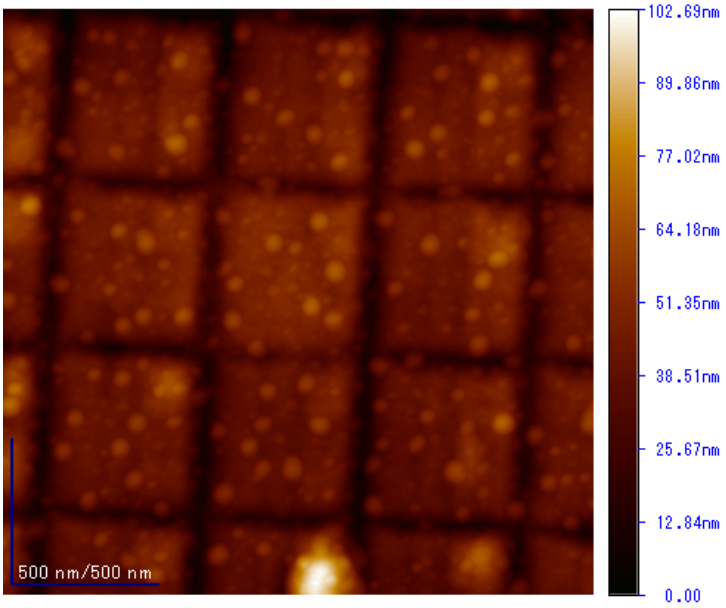

Fig. 2-21(a) Surface topography of the grating sample obtained by the commercial Si probe.

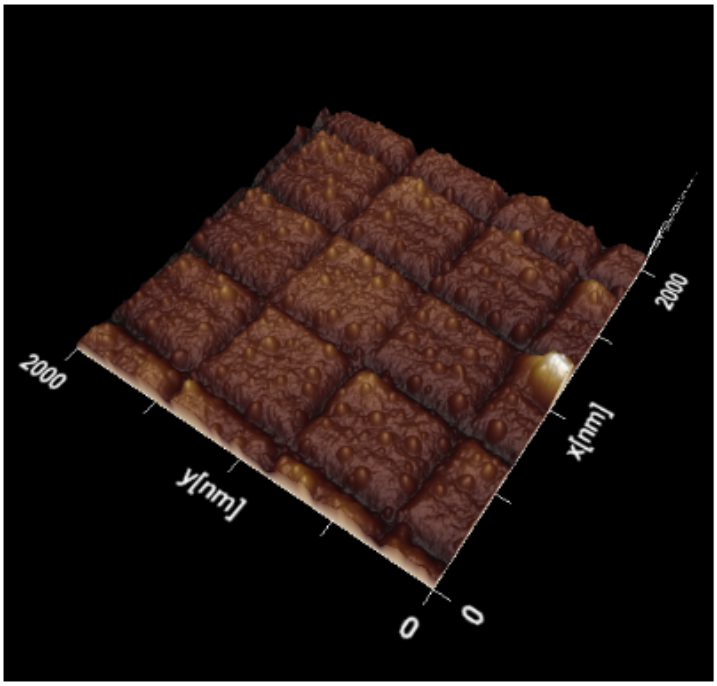

Fig. 2-21(b) A three-dimensional image that corresponds to **Fig. 2-21(a)**.

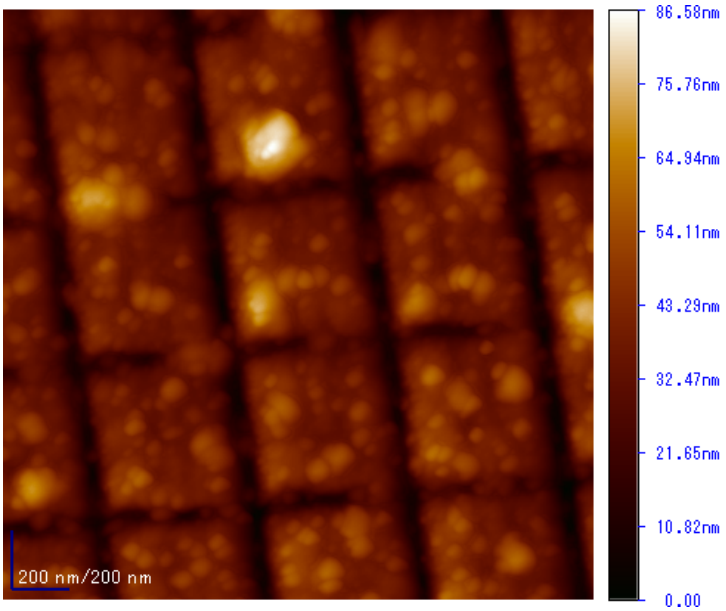

Fig. 2-22(a) Surface topography of the grating sample obtained by the GaAs probe without the nano-slit.

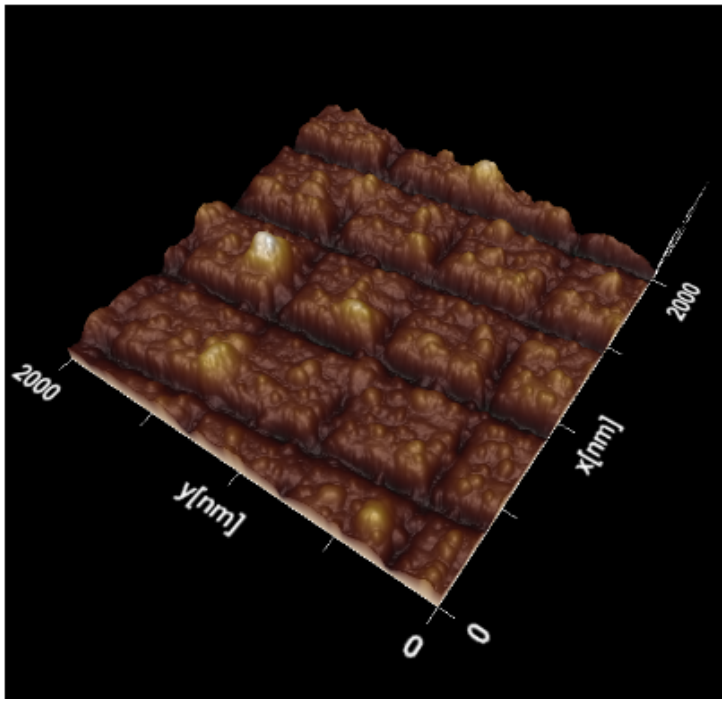

Fig. 2-22(b) A three-dimensional image that corresponds to **Fig. 2-22(a)**.

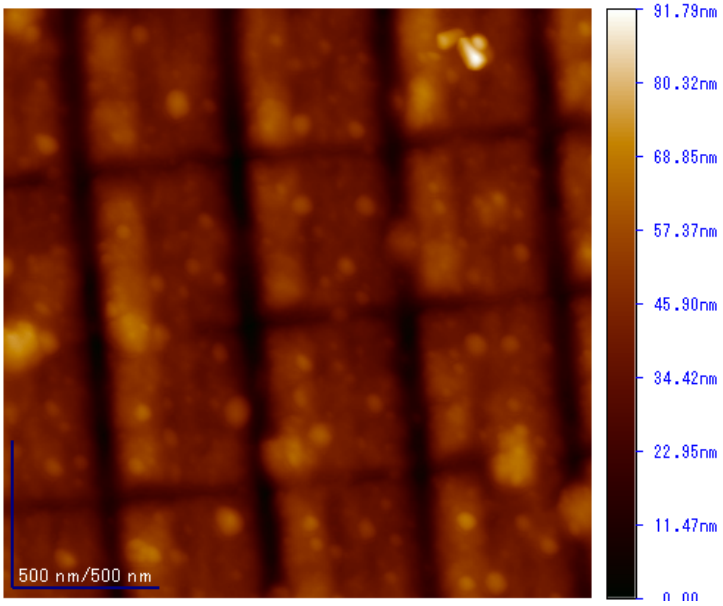

Fig. 2-23(a) Surface topography of the grating sample obtained by the M-AFM probe with the nano-slit.

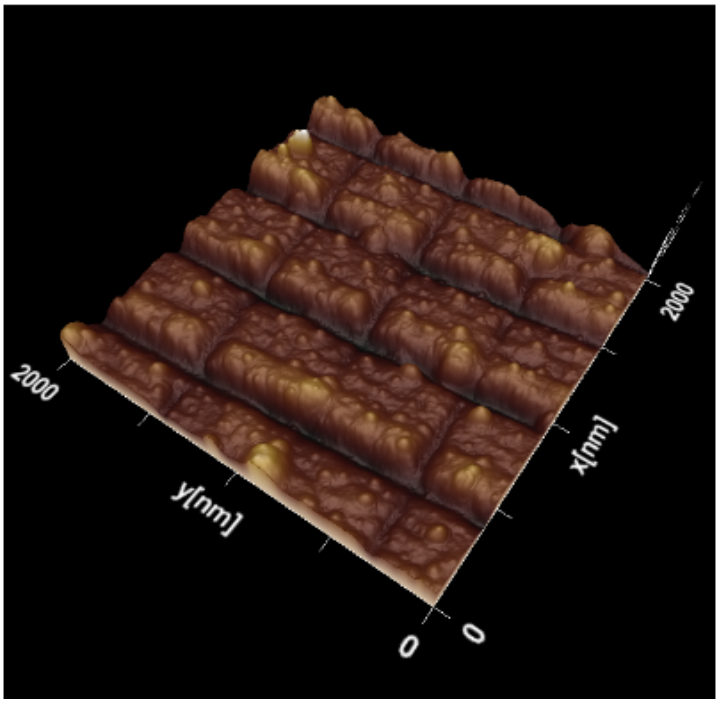

Fig. 2-23(b) A three-dimensional image that corresponds to **Fig. 2-23(a)**.

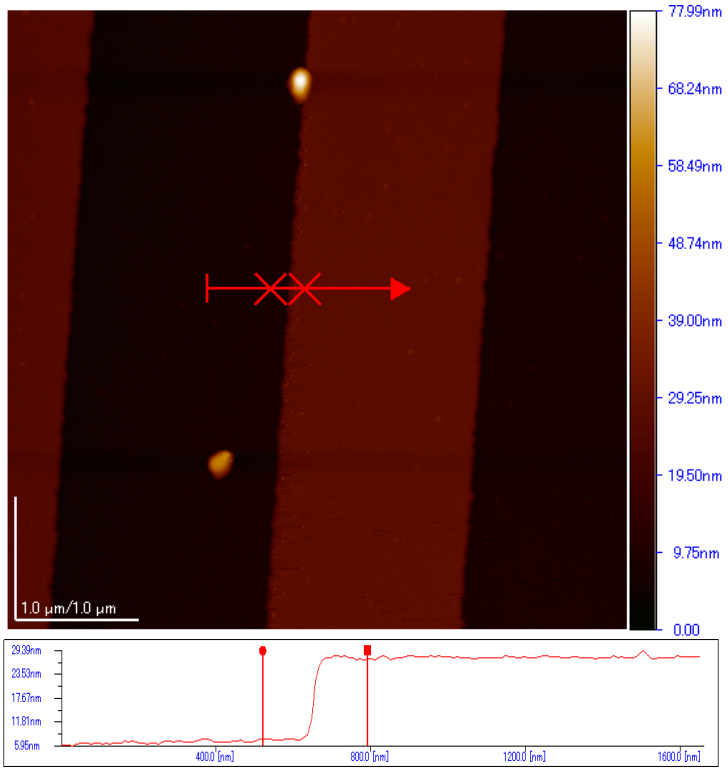

Fig. 2-24(a) Topography of the grating sample obtained by the commercial Si probe with the analysis of crossing profile.

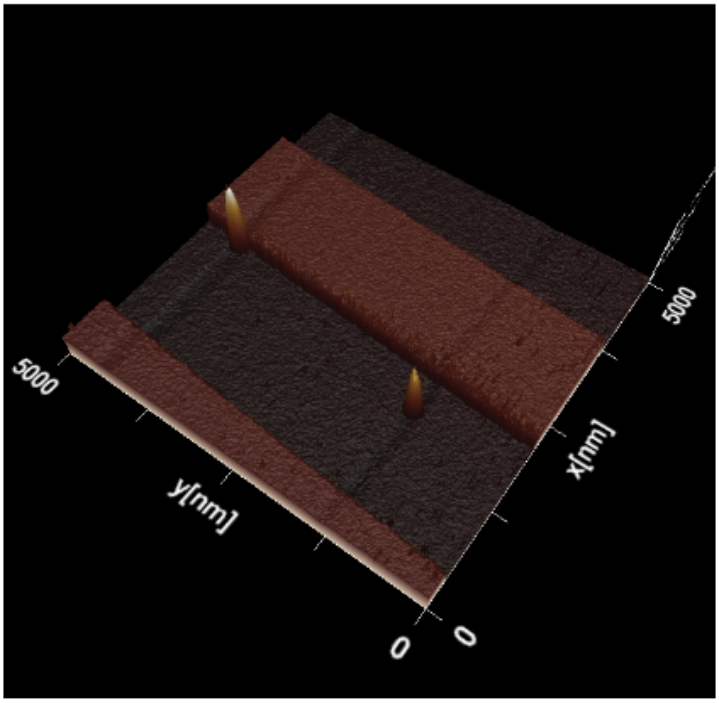

Fig. 2-24(b) A three-dimensional image that corresponds to **Fig. 2-24(a)**.

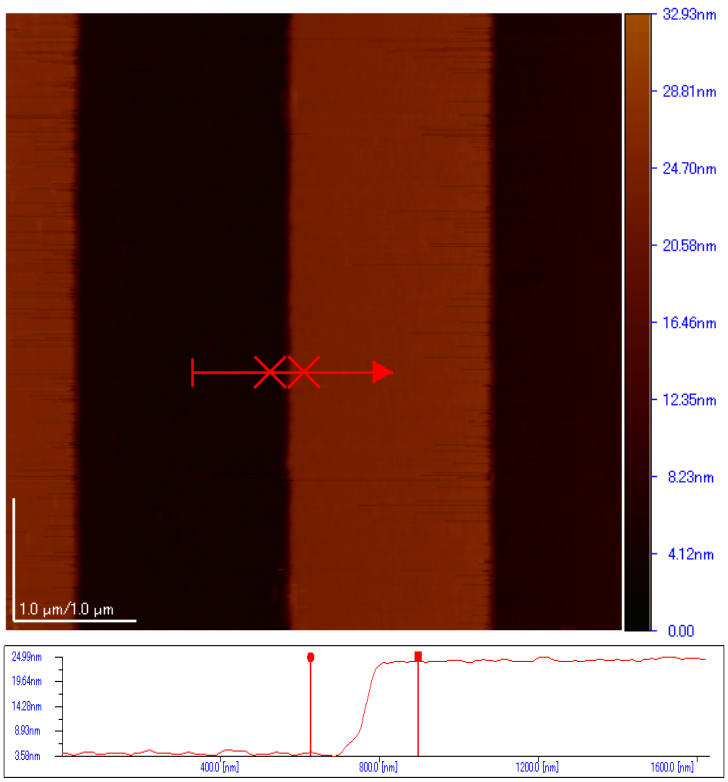

Fig. 2-25(a) Topography of the grating sample obtained by the commercial Si probe with the analysis of crossing profile.

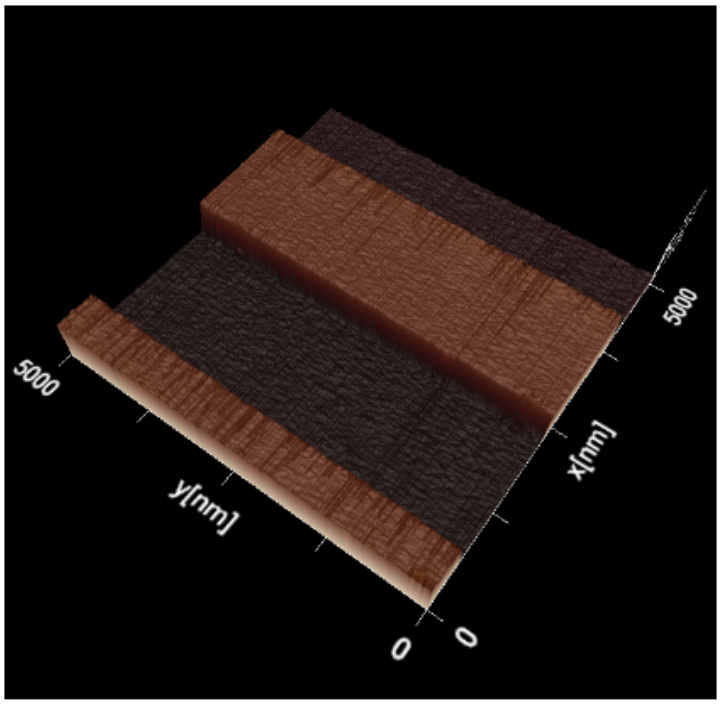

Fig. 2-25(b) A three-dimensional image that corresponds to **Fig. 2-25(a)**.

In order to evaluate the accuracy of height measurement, a grating sample having

17.9 nm±1nm step height was measured by using the commercial Si probe and the M-AFM probe, respectively. **Figures 2-24** and **2-25** show the AFM topographies and the cross-section profiles of the grating sample obtained by the commercial Si probe and the fabricated M-AFM probe, respectively.

From the slope of the step of the cross-section profile in the figures, it is confirmed that the fabricated M-AFM probes have the capability to catch the AFM topography with the resolution of nanometer order. The height of the step of the grating sample obtained by each probe was 19.17 nm and 19.67 nm, respectively. The fabricated M-AFM probe has also high resolution although the resolution was inferior as compared to the commercial Si probe. The reason why the resolution degraded with the fabricated probe is that the tip of the probes was cut by FIB fabrication. From these results, it is considered that the control of the standoff distance between the probe and the sample with high precision was achieved by the fabricated M-AFM probe.

2.4 Summary

(a) The microwave atomic force microscope (M-AFM) is a combination of the principles of the scanning probe microscope and the microwave-measurement technique. M-AFM can maintain the constant stand-off distance between the M-AFM-probe tip and scanned sample surface, by detecting the deflection of the atomic force between them, and measure the electrical properties of materials with nanometer scale spatial resolution.

(b) Microwave-AFM probes were fabricated on the GaAs wafer by using the wet etching process. A waveguide was introducing on the probe by evaporating Au film on the both surfaces of the probes. The open structure (the nano-slit) of the waveguide at the tip apex of the M-AFM probe was obtained by using FIB fabrication.

(c) SEM was used to observe the fabricated M-AFM probes. The average dimensions of the cantilever and the body of the M-AFM probes are typically 252×31×14 μm and 2742×723×339 μm, respectively. Based on these dimensions, the characteristic

impedance of the M-AFM probes is, on average, 49.3 Ω. In this way, the M-AFM probe could match well with the co-axial line, which has an impedance of 50 Ω. The observed tip is located near the front edge of the cantilever and the tip is approximately 7 μm high, and the nano-slit is approximately 100 nm in width.

(d) The metal film on the surface of M-AFM probe is required to be connected at the end of the beam, and should be absent at the sides of the beam. We checked the coating metal on the bottom surface of M-AFM probe holder by EDX technique. Based on the EDX profile results shown, the fitting spots on M-AFM-probe holder were well covered by the metal Au could be confirmed.

(e) AFM measurements were performed by comparing with the commercial Si AFM probe. It is indicated that GaAs microwave probe has a capability to catch AFM topography of grating samples and having a high accuracy for lateral and height evaluation.

REFERENCES:

1. Ju, Y.; Kobayashi, T.; Soyama, H. Development of a Nanostructural Microwave Probe Based on GaAs. *Microsyst. Technol.* **2008,** *14*, 1021-1025.

2. Ju, Y.; Hamada, M.; Kobayashi, T.; Soyama, H. A Microwave Probe Nanostructure for Atomic Force Microscopy. *Microsyst. Technol.* **2009,** *15*, 1195-1199.

3. Hosoi, A; Hamada, M; Fujimoto, A; Ju, Y. Properties of M-AFM Probe Affected by Nanostructural Metal Coatings. *Microsyst. Technol.* **2010,** *16*, 1233-1237.

4. Zhang, L.; Ju, Y.; Hosoi, A.; Fujimoto, A. Microwave Atomic Force Microscopy Imaging for Nanometer-scale Electrical Property Characterization. *Rev. Sci. Instrum.* **2010,** *81*, 123708.

5. Fujimoto, A.; Zhang, L.; Hosoi, A.; Ju, Y. Structure Modification of M-AFM Probe for the Measurement of Local Conductivity. *Microsyst. Technol.* **2011,** 17, 715–720.

6. Giessibl, F. J. Advances in Atomic Force Microscopy. *Rev. Mod. Phys.* **2003**, 75, 949.

7. Pozer, D. M. *Microwave Engineering 2nd ed.* (Jone Wiley and Sons: New York 1998)**,** p. 32.

8. Lin, C. C; Juo, T. J.; Chen, Y. J.; Chiou,, C. H.; Wang, H. W.; Liu, Y. L. Enhanced Cyclic Voltammetry Using 1-D Gold Nanorods Synthesized via AAO Template Electrochemical Deposition. *Desalination*. **2008**, *233*, 113-119.

9. Yue, Y. M.; Chen, M. J.; Ju,Y.; Zhang, L. Stress-induced Growth of Well Aligned Cu2O Nanowire Arrays and Their Photovoltaic Effect. *Scripta Mater.* **2012**, *66*, 81-84.

3. Microwave Imaging for Materials on Nanometer-scale

3.1 Experimental Setup

Figure 3-1 schematically depicts the integrated test system of the M-AFM.[1][2] In our M-AFM system, the initial microwave signals, which are working at a frequency f ＝16.66 GHz, are generated by a microwave generator. Next, the frequency of the microwave signals is extended by a six-frequency multiplier, which results in a stable testing frequency f＝94 GHz. The microwave signals propagate through an isolator and a circulator and then propagate into the M-AFM probe. The transmission line that connects the circulator and the probe changes from a rectangular waveguide into a coaxial line, which then changes into the parallel-plate waveguide (in the M-AFM probe). A detector is connected to the circulator, to measure the microwave signals that are received by the tip of the probe and indicate the voltage data that are converted from the reflected microwave signals. The measured signals are synchronized with positional information that is obtained from the AFM scanner, which is then used to create a microwave image. At the same time, by evaluating the output voltage data, the electrical properties of the measured materials can be determined. **Figure 3-2** presents the photo image of M-AFM system.

A coaxial line was used to connect the M-AFM probe to the compact microwave instrument; more specifically, a coaxial line with an inner diameter of 1 mm was fixed on the probe holder, which is used to set up an AFM probe for an AFM measurement.[3][4] A schematic image of modified probe holder is shown in **Fig. 3-3**, and an enlarged view of the probe connection is shown in **Fig. 3-4.** The outer and inner conductors of the coaxial line are connected to the bottom and top surfaces of the M-AFM probe, respectively. Therefore, microwave transmission line changes from the coaxial line to the parallel board waveguide (special structure of M-AFM possessing). By using this holder, the M-AFM probe can be set-up repeatedly and a

measurement of the microwave response and AFM surface profile can be realized simultaneously.

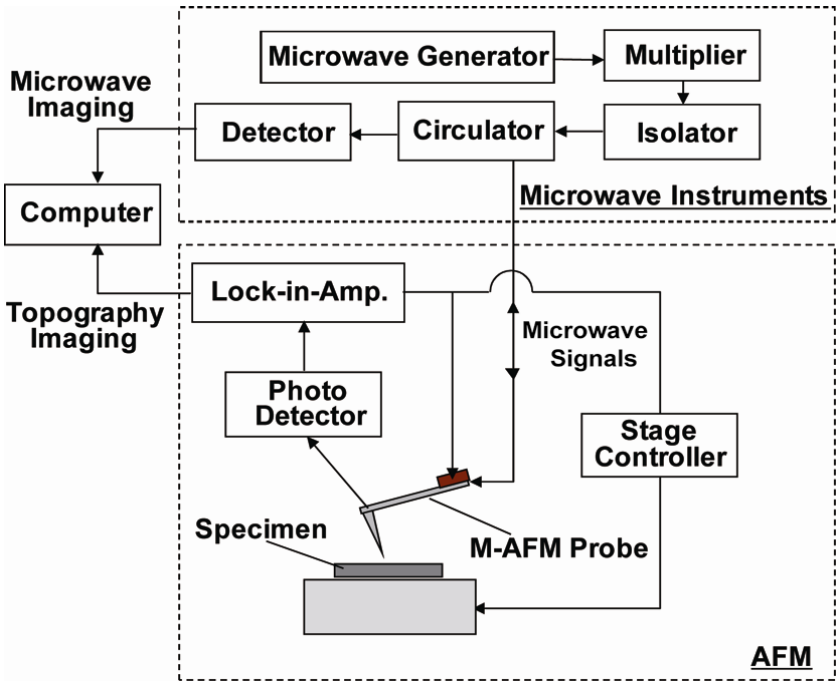

Fig. 3-1 Diagram of the M-AFM system.

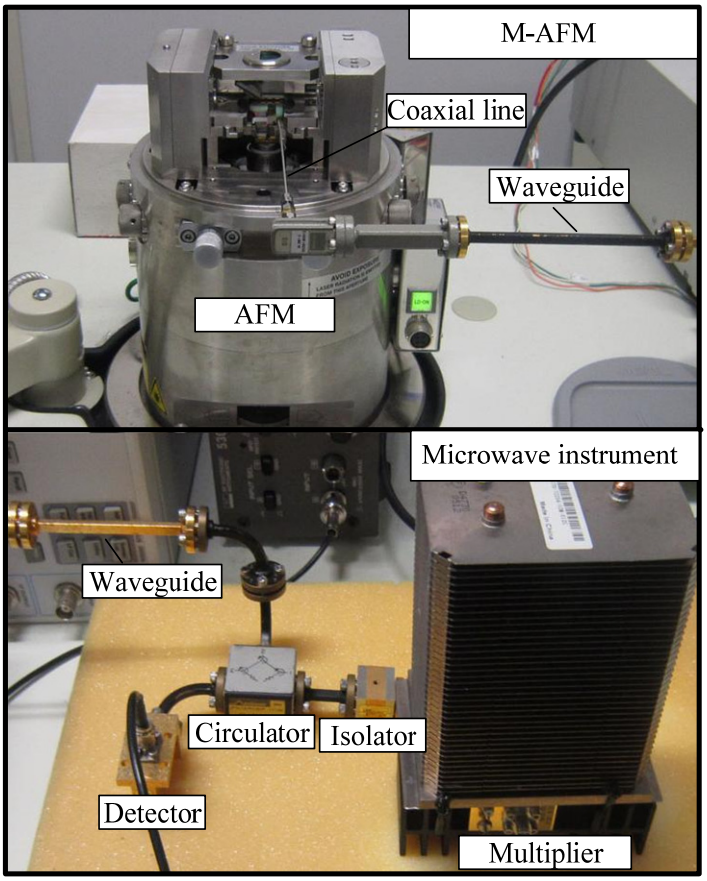

Fig. 3-2 Photo of the M-AFM system.

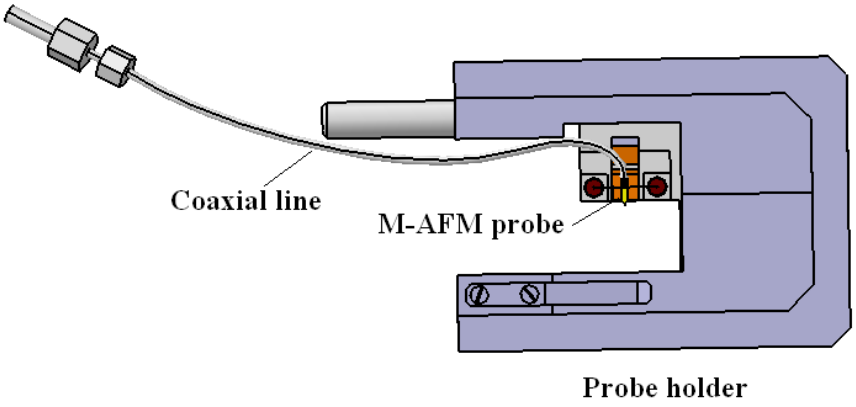

Fig. 3-3 A schematic diagram of the modified probe holder.

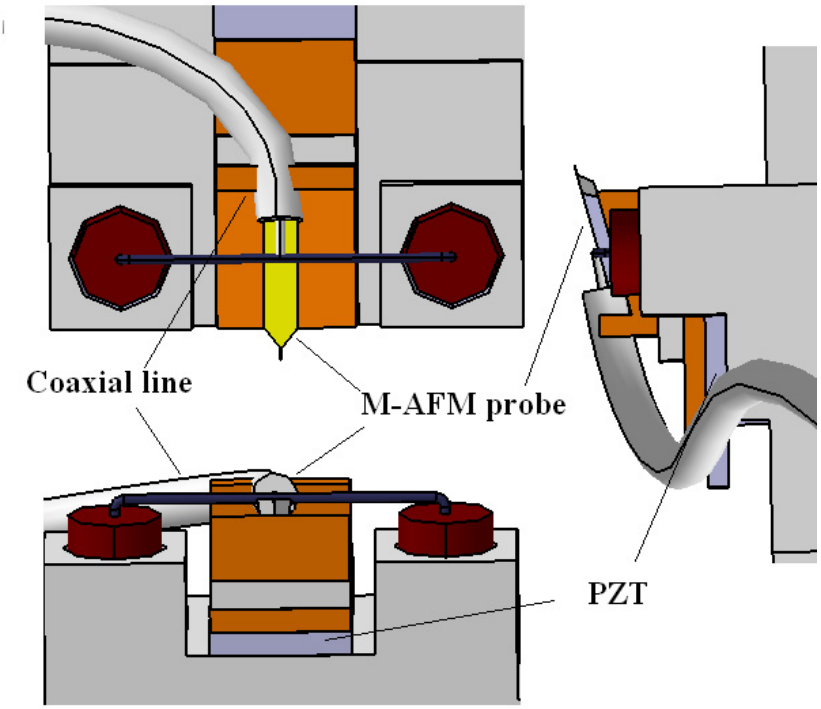

Fig. 3-4 The connection between the M-AF probe and the coaxial line.

We prepared a sample for the scanning test of surface topography and microwave imaging (see **Fig. 3-5**). At first, a resist mask was patterned onto the glass substrate wafer by lithography. After developing the resist pattern, a 200-nm thick Au layer was deposited on the glass substrate by electron beam (EB) evaporation. Finally, the unexposed photo-resists were lifted off in acetone. The resulting Au and glass step

structure is depicted in SEM image of **Fig. 3-6**.

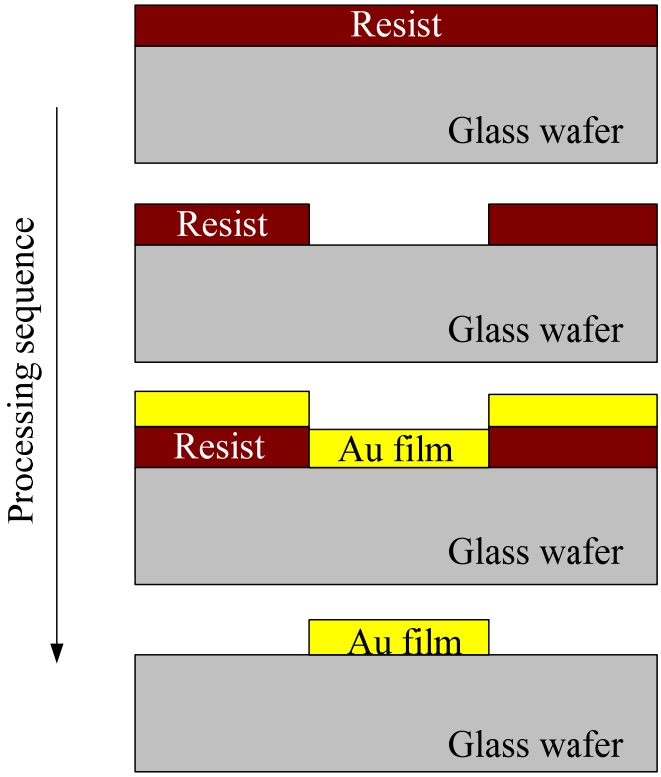

Fig. 3-5 Schematic diagram of the fabrication process of Au/Glass step sample.

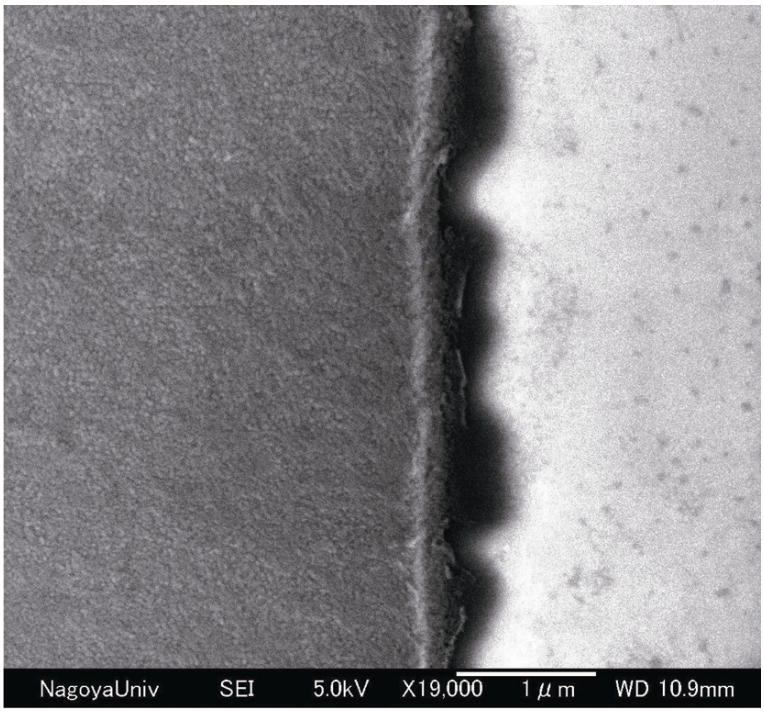

Fig. 3-6 SEM image of measured sample.

3.2 Microwave Image of Au/Glass Step Sample

Figures 3-7 and **3-8** depict the M-AFM scanning results of the sample at the step area between the Au coating film and the glass wafer substrate. The measurements were performed in the air, and the M-AFM worked in non-contact mode, with a working environment temperature of 24.5 °C and a relative humidity of 38.4%. The resonance frequency of M-AFM probe was 133 kHz and the *Q*-value of it was 295. The scan area was 10×10 μm^2, scanning speed was 5 μm/s. **Fig.3-7(a)** depicts the surface topography of the M-AFM-measured sample. In this image, the left side represents the Au film, whereas the right side is the glass substrate. As can be seen in the scanning profile depicted in **Fig.3-7(a)**, the thickness of the Au film was approximately 200 nm on average. In addition, **Fig.3-7(b)** depicts the three-dimensional image with height information that corresponds to **Fig.3-7(a)**.

Figure 3-8(a) depicts the microwave image of the voltage that was converted from the measured microwave signals, which were simultaneously acquired by the M-AFM probe at the corresponding position depicted in **Fig.3-7(a)**. **Figure 3-8(d)** depicts a three-dimensional image with electrical information that corresponds to that depicted in **Fig. 3-8(a)**. This experimental result demonstrates that the microwave image has two spatial phases. Because the standoff distance between the tip of the M-AFM probe and the surfaces of the Au film and glass substrate is constant and controlled by the atomic force, thus, the response of the microwave signals were observed to change based on the different electrical characteristics of the measured materials. As per **Fig. 3-8(a)**, the output voltage over the glass area is larger than that over the Au area, because the scanning started from the Au area with the initial offset from the nulling operation.

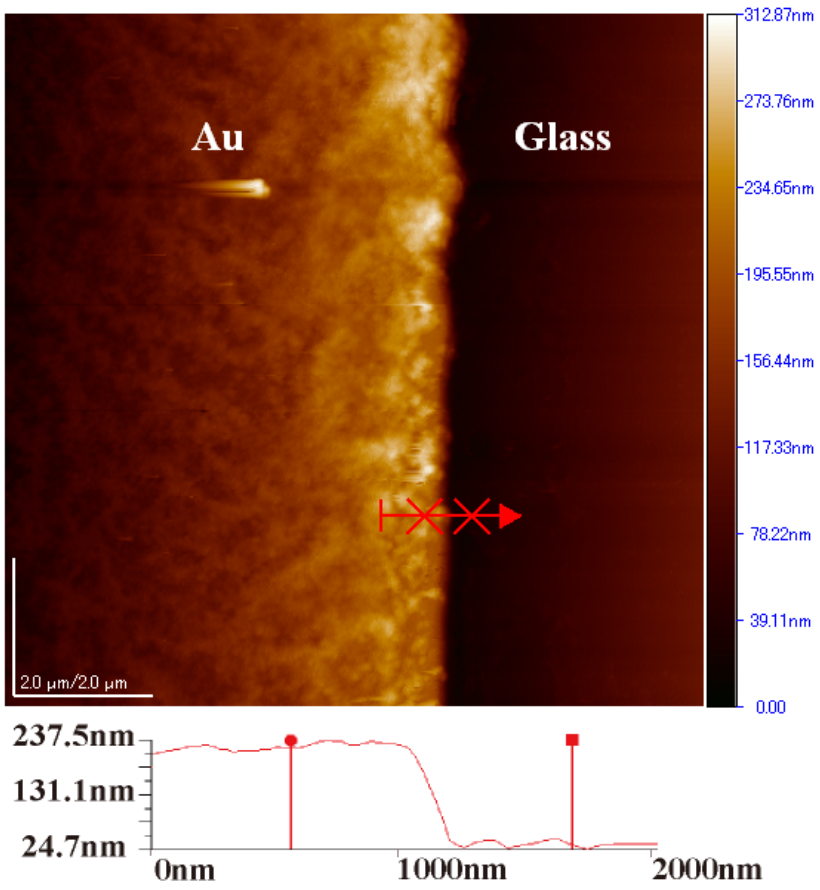

Fig. 3-7(a) AFM topography image of the Au/Glass step sample.

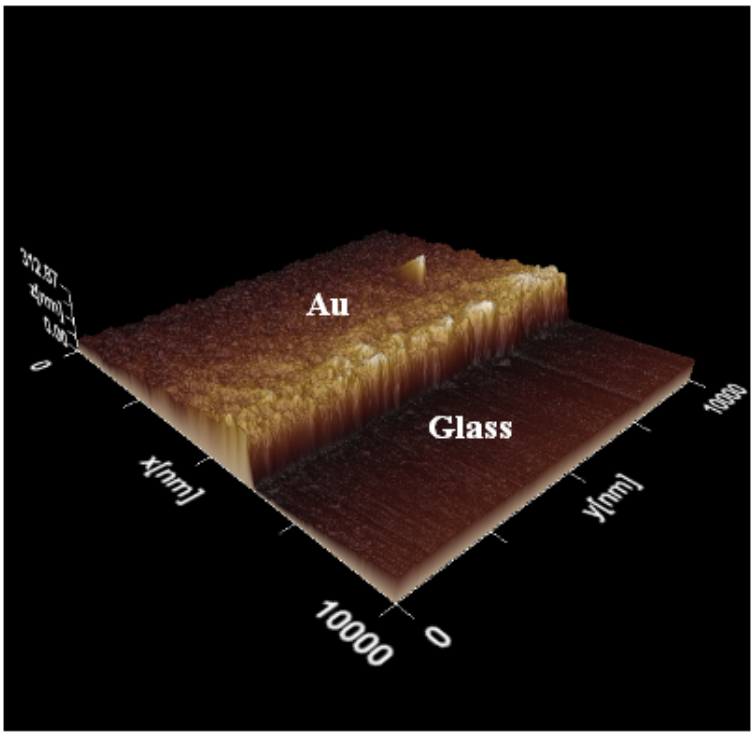

Fig. 3-7(b) A three-dimensional image that corresponds to **Fig. 3-7(a).**

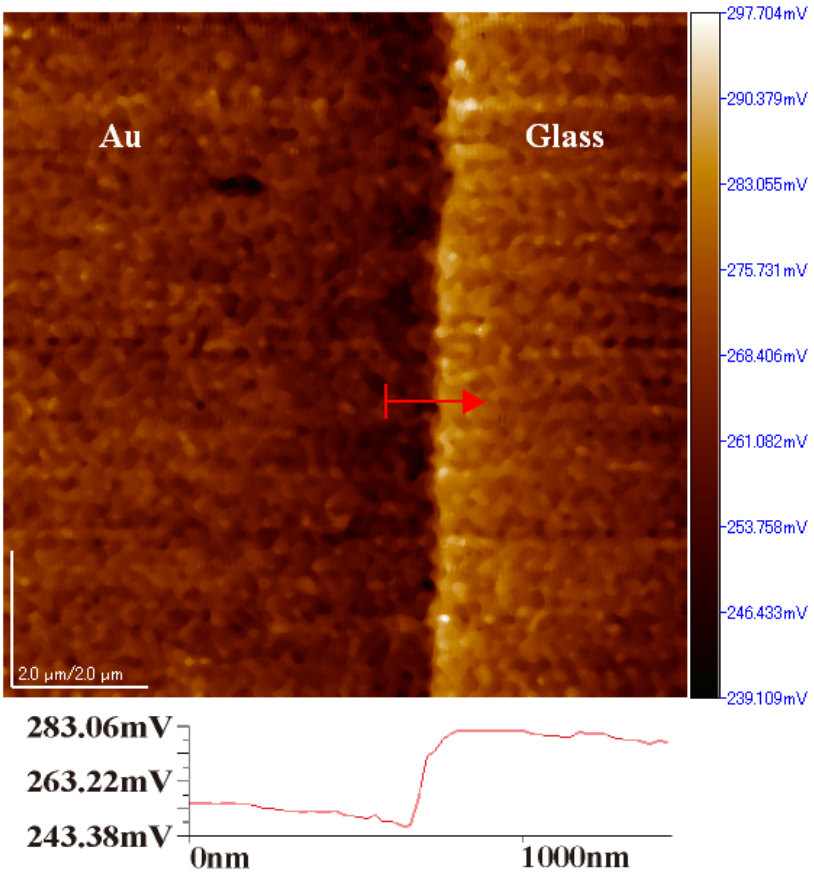

Fig. 3-8(a) Microwave image of the output voltage that was converted from the measured microwave signals.

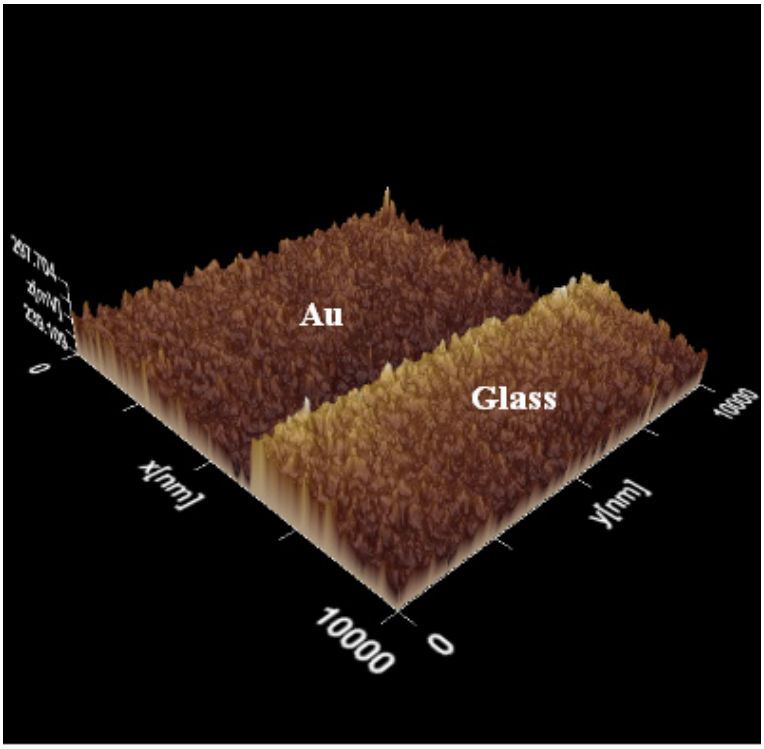

Fig. 3-8(b) A three-dimensional image that corresponds to **Fig. 3-8(a)**.

An analysis of the scanning profile depicted in **Fig. 3-8(a)** demonstrates that the spatial resolution is higher than 120 nm, and that the output voltage measured over the Au and glass areas were 262.5 mV and 281.7 mV, respectively. The difference between the measured voltages between the Au and glass areas is 19.2 mV. Since, the stability of the measurement is high, this value is large enough for evaluating the electrical properties of other materials having the conductivity between Au and glass. As the results presented, the M-AFM should allow us to scan the electrical conductivities of other conductor materials on a nanometer scale. In addition, based on the same principle, it can also be used to measure the permittivities of dielectric materials on a nanometer scale.

3.3 Microwave Image of Au/Au Step Sample

To demonstrate that M-AFM can sense the microwave image based on electrical characteristic of the measured materials and is not affected by the surface shape of the sample, we prepared an Au/Au step sample for the scanning test and performed simultaneous measurements of the surface topography and microwave image of the sample within only one scanning procedure.

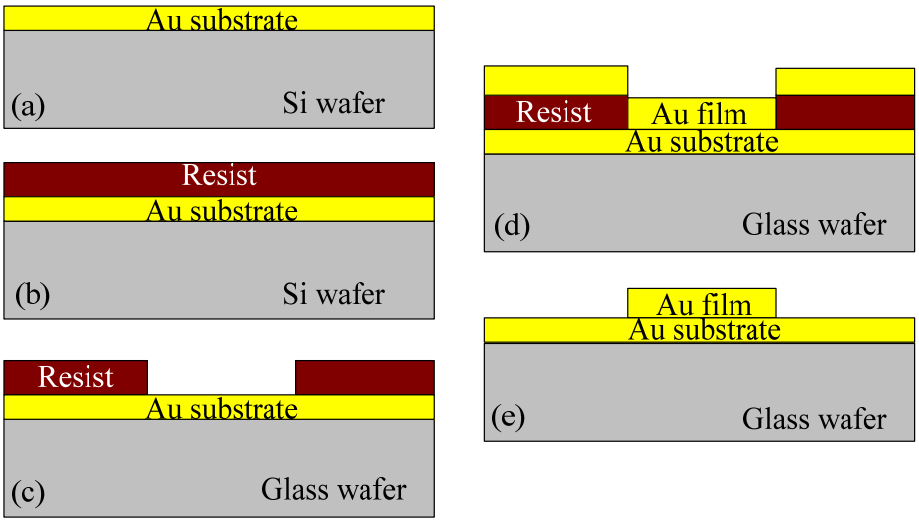

Fig. 3-9 Fabricating procedure of the Au/Au step sample.

Fabricating procedure of the Au step sample was described as follows. At first, a resist mask was patterned onto the Au plate by lithography. After developing the resist pattern, a 100 nm thick Au layer was deposited on the Au plate substrate by EB evaporation. Finally, the unexposed photo-resists were lifted off in acetone (see **Fig. 3-9**).

Figure 3-10 depicts the M-AFM probe scanning the Au step sample in the FM mode (non-contact mode). The measurements were performed in the air, with a working environment temperature of 26.0 °C and a relative humidity of 50%. The resonance frequency of M-AFM probe was 133 kHz, respectively, and the *Q*-value of it was 295. The scan area was 8×8 μm^2, scanning speed was 4 μm/s. **Figure 3-11** shows the surface topography of the sample measured with the M-AFM. As can be seen in the scanning cross-section profile, which is shown in **Fig. 3-11**, the difference between the higher and lower parts of the sample was measured to be 97.1 nm and with a spatial resolution of approximately 100 nm. This result demonstrates the capability of the M-AFM for imaging the surface topography with a spatial resolution on nanometer order. **Figure 3-12** shows the microwave image of the measured voltage that was converted from the detected microwave signals. The image was simultaneously acquired by the M-AFM probe at the corresponding position depicted in **Fig. 3-12**. Because the standoff distance between the tip of the M-AFM probe and the surface of the sample is controlled by the atomic force, the responses of the microwave signals were changed only due to the electrical characteristic of the material. It should be noted that, under the FM mode, the period of the normal vibration of the cantilever is approximately 9.4 μs (frequency: 106.83 kHz), which is approximately 416 times shorter than the scanning time for one pixel (scanning speed: 4 μm/s). Meanwhile, the compact microwave instrument implements a real time measurement and the data measured at each pixel is an average of the microwave signal during 9.4 μs, including 416 times vibrations of the cantilever. Therefore, the influence of the normal vibration to the microwave measurement (image) can be eliminated. Different from the evident difference in heights of different parts of the Au step sample (see **Fig. 3-11**), the voltages measured from the lower and higher parts are

certainly the same (see **Fig. 3-12**). The uniform voltage value can be explained as that higher and lower parts of the Au step sample are composed of the same material, i. e. with the same conductivity. This result indicates that our M-AFM can sense the electrical properties of measured sample regardless of the surface shape. It is noted from **Fig. 3-12** that there is a pulse-shaped signal corresponding to the boundary between the two parts of the Au step sample, the microwave signal was changed abruptly. This phenomenon is due to the acute vibration of the M-AFM probe that occurs when the probe is scanning over the boundary of the two parts. The vibration of the probe leads to a mutation of the microwave signal in a short period according to the scanning speed. But this very short-time mutation just affect the microwave signal at the boundary of Au step sample smaller than 100 nm. Over the broad areas, the microwave signals can keep in a stable situation and not affected by the vibration. These results indicate that the boundary effect will not affect the normal surface measurement of material's conductivity. It is also shown that the spatial resolution of the conductivity measurement is in the order of 100 nm. In addition, the vibration of probe could be restrained or eliminated by controlling the scanning speed. Since there are the much smaller differences among the voltages measured over the broad Au areas with respect to the relative higher voltage created at the step boundary, the microwave image is observed in homogenous significantly in **Fig. 3-12**. It is also noted from **Fig. 3-12** that the measured voltages were presented having high values more than 4 V because that we did not carry out the voltage-offset process to make the initial voltage zero.

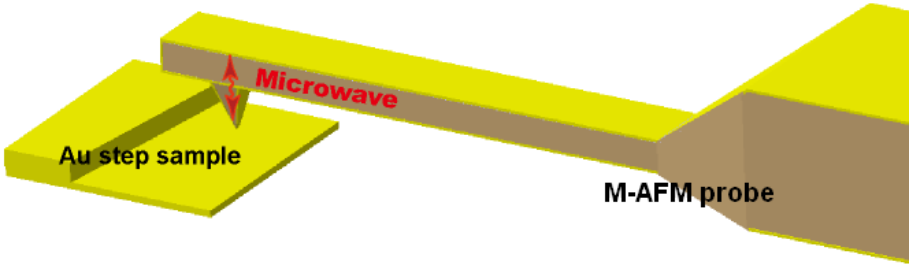

Fig. 3-10 Schematic diagram of the M-AFM probe that was used to measure the Au step sample.

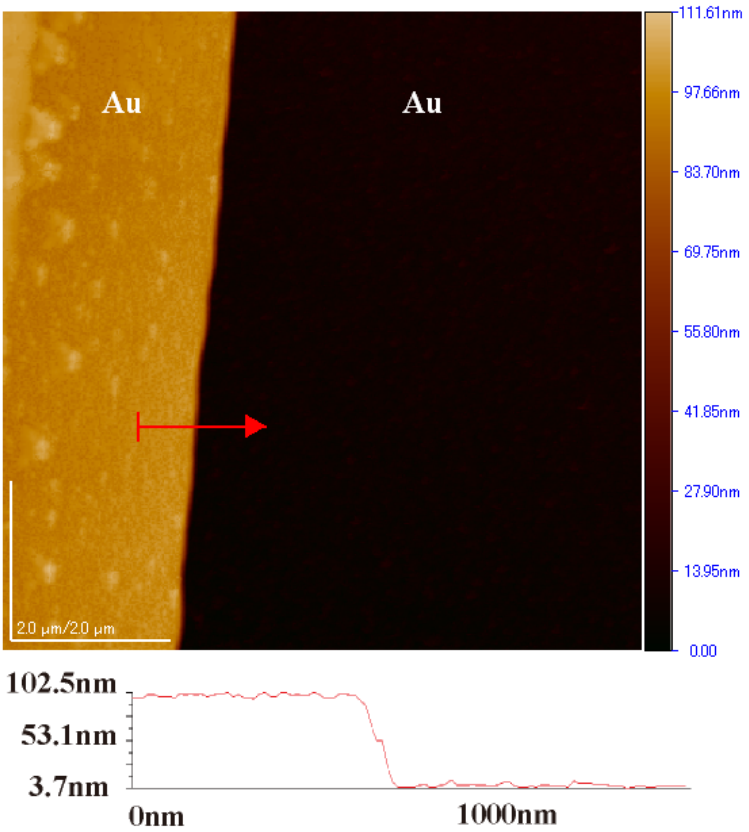

Fig. 3-11 Topography image of the sample with the crossing height profile.

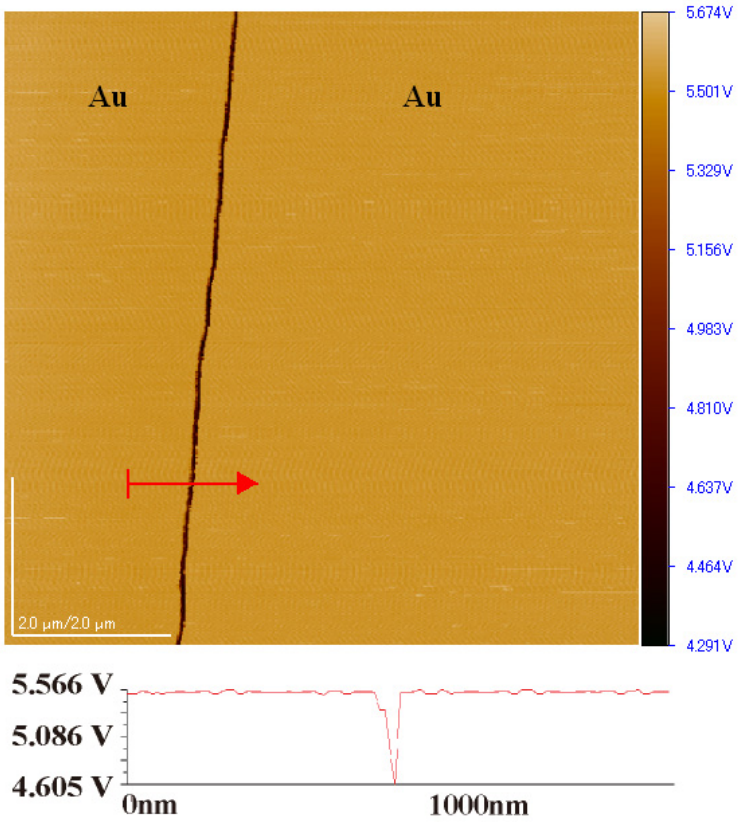

Fig. 3-12 Microwave image obtained from the same scanning process as **Fig. 3-11**, the lower one is the voltage profile.

3.4 Sensitivity in the Measurement of Electrical Properties Affected by the Nano Structure of M-AFM Probe

As previous chapters mentioned, to make microwave propagating properly in the probe, a parallel-plate waveguide was formed by evaporating Au films on the top and bottom surfaces of the M-AFM probe. The Au films on the both side are connected at the end of the probe cantilever and there are no Au films on the sides of cantilever and probe holder. Consequently, a homogeneous parallel plate waveguide was fabricated and microwaves are able to propagate along the probe. On the other hand, in order to make microwave signals emit at the apex of the probe tip, a nano-slit at the centre of the probe tip was introduced by focused ion beam (FIB) process, in order to open the short circuit of Au films on the two surfaces of the probe (see **Fig. 3-13**).

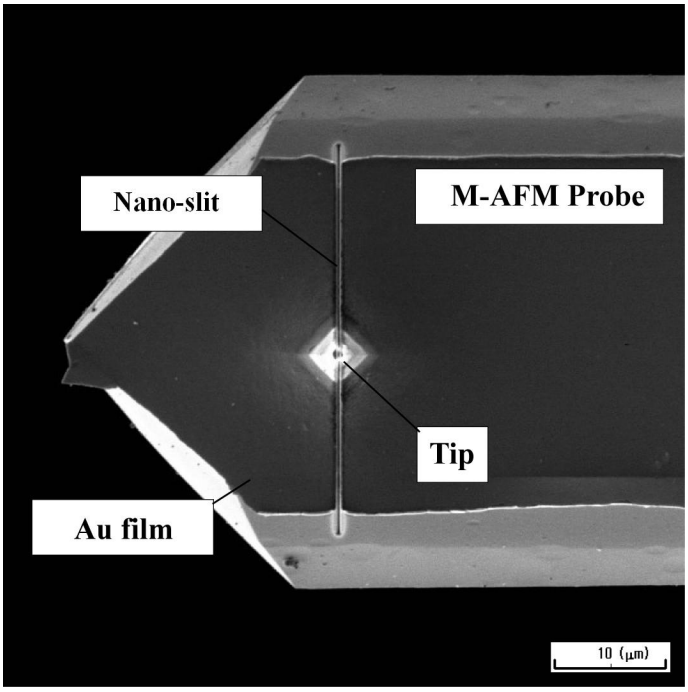

Fig. 3-13 SIM image of top part of M-AFM-probe cantilever, the nano-slit across the tip apex fabricated by FIB process.

The nano-slit plays a very important role in the M-AFM structure, due to the nano-slit is a transmitter to emit the microwave signals to the surface of measured sample, and a detector to get the reflected microwave information. Thus, to research

the sensitivity in the measurement of electrical properties affected by the nano structure of microwave AFM (M-AFM) probe, three kinds of M-AFM probe with a nano-slit on its tip in different width (75 nm, 120 nm and 160 nm) were investigated. As shown in **Fig.3-14**, **Fig.3-15** and **Fig.3-16**, the nano-slits with three different parameters: 75 nm, 120 nm and 160 nm in width were fabricated by FIB, respectively.

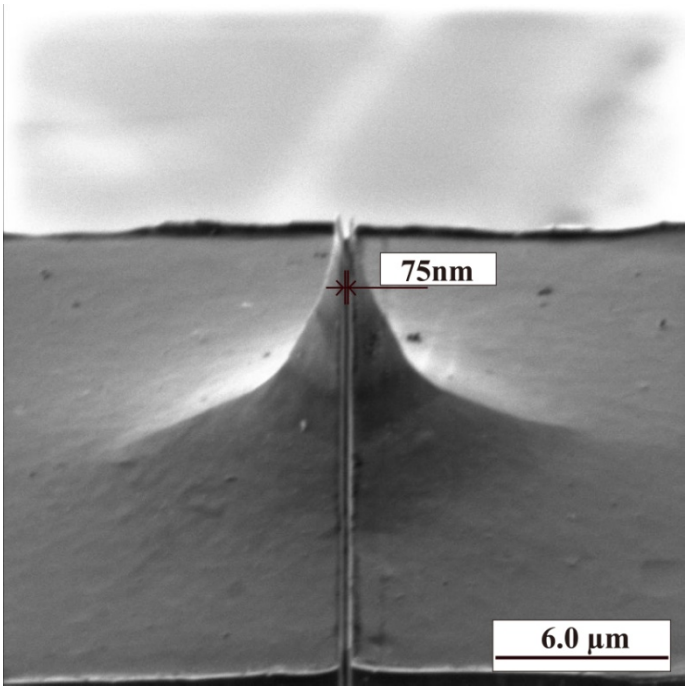

Fig. 3-14 SEM image of M-AFM-probe tip with a 75-nm nano-slit at the apex.

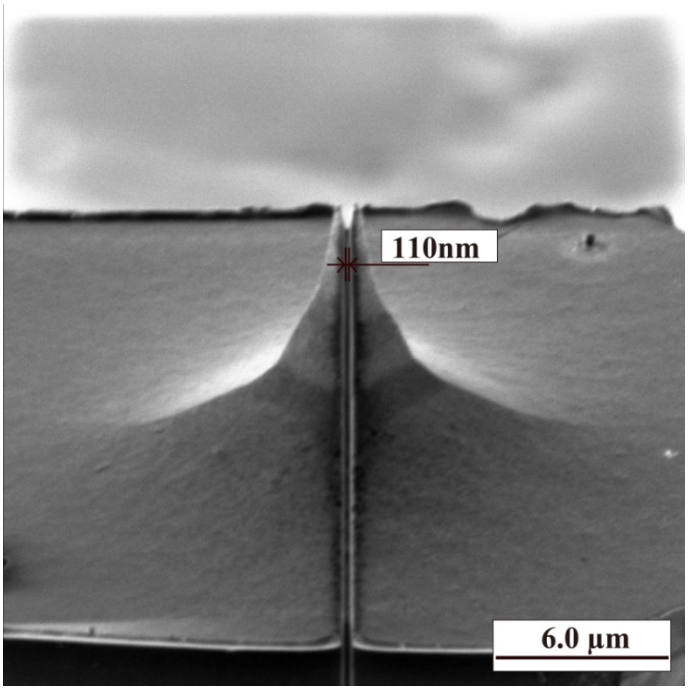

Fig. 3-15 SEM image of M-AFM-probe tip with a 110-nm nano-slit at the apex.

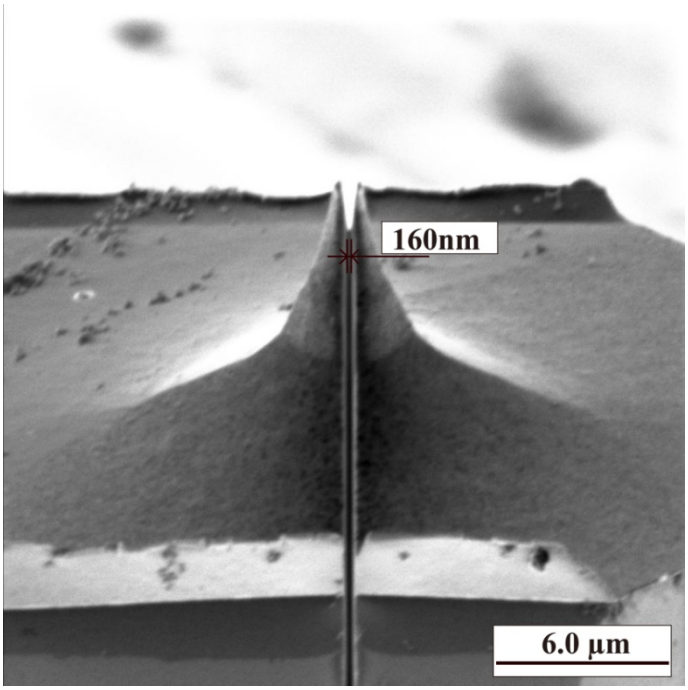

Fig. 3-16 SEM image of M-AFM-probe tip with a 160-nm nano-slit at the apex.

Table 3-1 Experimental microwave imaging results:

Probe	The measured voltage on Au	The measured voltage on glass	Voltage difference
M-FAM probe tip with the 75 nm nano-slit	178.68 mV	233.77 mV	55.09 mV
M-FAM probe tip with the 110 nm nano-slit	276.80 mV	309.15 mV	32.35 mV
M-FAM probe tip with the 160 nm nano-slit	151.98 mV	158.85 mV	6.97 mV

Using the M-AFM probes with the measurement system, the prepared Au and glass samples were measured respectively. **Table 3-1** shows the experimental microwave imaging results. The voltage values were converted from the reflected microwave signal without the calibration, which was obtained by the M-AFM probes. The measurements were performed in the air, and the AFM worked in non-contact

mode, with a working environment temperature of 22.0 °C and a relative humidity of 40%. The resonance frequency of the M-AFM probes (with nano-slits of 75 nm, 120 nm and 160 nm) were 157 kHz,148 kHz and 146 kHz, respectively, and the *Q*-value of them were 481, 641 and 750. The scan area was 1×1 μm^2, scanning speed was 0.5 μm/s.

As shown in **Table 3-1**, for M-AFM probe with 75 nm nano-slit on the tip, the measured voltage over the scanning area of Au sample is 178.7 mV on average, and the voltage over the glass area is 233.8 mV on average. The difference of measured voltage between Au and glass samples is 55.1 mV. In the same way, for M-AFM probe with 120 nm nano-slit on the tip, the measured voltage over the Au and glass areas are 276.8 mV and 309.1 mV on average, respectively. The difference of measured voltage between Au and glass samples is 32.3 mV. For the M-AFM probe with 160 nm nano-slit on the tip, the measured voltage over the Au area is 152.0 mV and glass area 158.9 mV on average. The difference of measured voltage between Au and glass samples is 6.9 mV. In this study, since the tip structure will affect the reference value of microwave signal, the value of the measured voltage for Au and glass samples obtained by different probes are different. It is noted that such difference can be corrected by calibration, therefore it will not affect the evaluation of electrical properties of materials. Comparing the experimental results, it is suggested that the M-AFM probe with 75 nm nano-slit has the highest sensitivity for measuring electrical properties of materials. In addition, it should be noted that the difference of measured voltage between Au and glass samples is 55.1 mV, which is sensitive enough for evaluating the electrical properties of materials. Therefore, the M-AFM probe should allow us to scan the electrical properties of materials on the nanometer scale.

3.5 Summary

(a) We have created an M-AFM-obtained microwave image using a compact microwave instrument that was optimally synchronized with an AFM scanner. The

distinguishing features of M-AFM are its ability to maintain a constant standoff distance between the probe tip and the sample surface and to measure the microwave signal interacted with the sample. Therein, both the topography and electrical-property images of the sample can be simultaneously characterized. Therefore, M-AFM is able to measure, *in situ*, the distribution of electrical properties on a nanometer scale. As shown in the experimental results, we successfully generated a microwave image of a 200-nm Au film coating on a glass wafer substrate with a spatial resolution of 120 nm, and, moreover, we measured the voltage difference between these two materials to be 19.2 mV. We believe that the high spatial resolution and simultaneous measurement capability of this M-AFM system will have important implications to nanotechnology characterization in the immediate future.

(b) We also successfully created a microwave image of an Au/Au step sample with a spatial resolution on nanometer order, which indicates that the microwave measurement is not affected by the surface shape of the material and the standoff distance was well controlled by the atomic force.

(c) To confirm the sensitivity in the measurement of electrical properties affected by the nano structure of microwave AFM (M-AFM) probe, three kinds of M-AFM probe with a nano-slit on its tip in different width (75 nm, 120 nm and 160 nm) were investigated. Au and glass samples were measured by the probes working at a noncontact AFM mode. The M-AFM probe with the nano-slit having the width of 75 nm, by which the difference of the measured voltage between Au and glass samples is 55.1 mV, shows the highest sensitivity for detecting electrical properties of materials. As the result illustrated, the M-AFM probe with smaller width nano-slit on the tip can be considered to be an ideal nano structure.

REFERENCES:

1. Zhang, L.; Ju, Y.; Hosoi, A.; Fujimoto, A. Microwave Atomic Force Microscopy Imaging for Nanometer-scale Electrical Property Characterization. *Rev. Sci. Instrum.* **2010,** *81*, 123708.

2. Zhang, L.; Ju, Y.; Hosoi, A.; Fujimoto, A. Microwave Atomic Force Microscopy:

Quantitative Measurement and Characterization of Electrical Properties on the Nanometer Scale. *Appl. Phys. Express* **2012**, 5, 016602.

3. Ju, Y.; Hamada, M.; Kobayashi, T.; Soyama, H. A Microwave Probe Nanostructure for Atomic Force Microscopy. *Microsyst. Technol.* **2009,** *15*, 1195-1199.

4. Hosoi, A; Hamada, M; Fujimoto, A; Ju, Y. Properties of M-AFM Probe Affected by Nanostructural Metal Coatings. *Microsyst. Technol.* **2010,** *16*, 1233-1237.

4. Quantitative Measurement of the Electrical Properties of Materials on the Nanometer-scale.

4.1 Principle of Microwave Measurement for Electrical Properties

The principle of the method described here is based on the reflection of the microwave from measured materials' surface. Based on the situation of that the reflection from bottom surface can be neglected, the measured reflection coefficient of the microwave signal can be expressed by considering the reflection only from the top surface as [1]

$$\Gamma = \frac{\eta - \eta_0}{\eta + \eta_0}, \tag{4-1}$$

where

$$\eta = \sqrt{\frac{\mu}{\varepsilon - j\frac{\sigma}{\omega}}} \tag{4-2}$$

and

$$\eta_0 = \sqrt{\frac{\mu_0}{\varepsilon_0}}. \tag{4-3}$$

In the above equations, Γ represents the reflection coefficient, and η, σ, μ and ε are intrinsic impedance, conductivity, permeability, and permittivity of materials, respectively, and η_0, σ_0, μ_0 and ε_0 are those of free space. Symbol ω denotes the angular frequency, and $j=\sqrt{-1}$.

For non magnetic materials, considering $\mu = \mu_0$, and using the above equations, the reflection coefficient, Γ, can finally be written as

$$\Gamma = X + jY = \frac{1-\sqrt{\frac{\varepsilon}{\varepsilon_0} - j\frac{\sigma}{\omega\varepsilon_0}}}{1+\sqrt{\frac{\varepsilon}{\varepsilon_0} - j\frac{\sigma}{\omega\varepsilon_0}}}. \tag{4-4}$$

where X is the real part and Y the image part of the reflection coefficient. By solving the simultaneous equations of the real and imaginary parts of Eq.(4-4) and eliminating ε, the conductivity of materials can be expressed as

$$\sigma = \frac{4\omega\varepsilon_0 Y(1-X^2-Y^2)}{[(1+X)^2+Y^2]^2}. \tag{4-5}$$

4.2 Quantitative Measurement of the Electrical Conductivities of samples

For quantitative measurement, the operating frequency of M-AFM is set at 94 GHz. The high-frequency microwaves are easy to propagate in the waveguide and emit from the nano-slit on the probe tip. Since the width of the nano-slit is around 100 nm, the field of microwave interacting with the measured materials can be considered to be in 100 nm order. Thus, if the thickness of measured materials is larger than 100 nm, the reflection from the bottom surface of the sample can be neglected. Therefore, only the reflection from the top surface needs to be considered.

Moreover, the diode detector works in a small signal range, where it is considered to be a square-law detector.[2] Therefore, while keeping the standoff distance between the tip of the M-AFM probe and samples constant, the output reflected voltage V, which varies only with the conductivity of the sample, has a relationship with the squared absolute value of the top surface reflection coefficient, $|\Gamma_s|^2$ as

$$V = k_0|\Gamma_s|^2 + b_0 \tag{4-6}$$

The two undetermined constants k_0 and b_0 can be calibrated with two samples whose conductivities are known.

For good conductors, which are used in this experiment, the surface reflection

coefficient $|\Gamma_s|$ can be written as[3][4]

$$|\Gamma_s| = \left| \frac{1-\sqrt{\sigma / j\omega\varepsilon_0}}{1+\sqrt{\sigma / j\omega\varepsilon_0}} \right| \tag{4-7}$$

where ε_0 and σ represent permittivity of free space and the conductivity of the measured material, respectively, and ω is the angular frequency of the microwave. For semiconductor or isolating materials, similar equations can also be constructed. Then, the conductivity can be determined from Eq. (4-7) as

$$\sigma = \omega\varepsilon_0 \left[4|\Gamma_s|^2 - \left(|\Gamma_s|^2 + 1\right)^2 \right] / \left[\left(|\Gamma_s|^2 + 1\right) \sqrt{4|\Gamma_s|^2 - \left(|\Gamma_s|^2 - 1\right)^2} - 4|\Gamma_s|^2 \right] \tag{4-8}$$

After k_0 and b_0 in Eq. (4-6) are calibrated using two reference samples with known conductivities, the conductivities of any samples can be calculated from the measured voltage. Therefore, the M-AFM allows us to quantitatively evaluate the electrical conductivities of materials on the nanometer scale.

It should be noted that Eq. (4-7) and (4-8) are derived under the plane wave condition, while the probe works in near-field mode. Although near-field analysis may further improve the precision of evaluation results, it requires more reference samples, which will increase the complexity of the measurement. Since the tested material was very close to the open end of the probe-tip (the standoff distance of several nanometers was extremely small as compared with the waveguide width (~100 nm) and the wavelength), this problem can be equivalent to the case that the material surface is terminated at the end of the waveguide, which can be represented by the plane wave model (see **Fig. 4-1**). Therefore, the plane wave approximation is used in this study.

There is a limitation of M-AFM technique we have to face. In the case of that the thickness of measured sample smaller than 100 nm, the reflection of microwave signal from the bottom surface of the sample and the substrate should be considered. Therefore, the M-AFM can not use the previous mentioned equations to obtain the electrical properties of measured sample quantitatively.

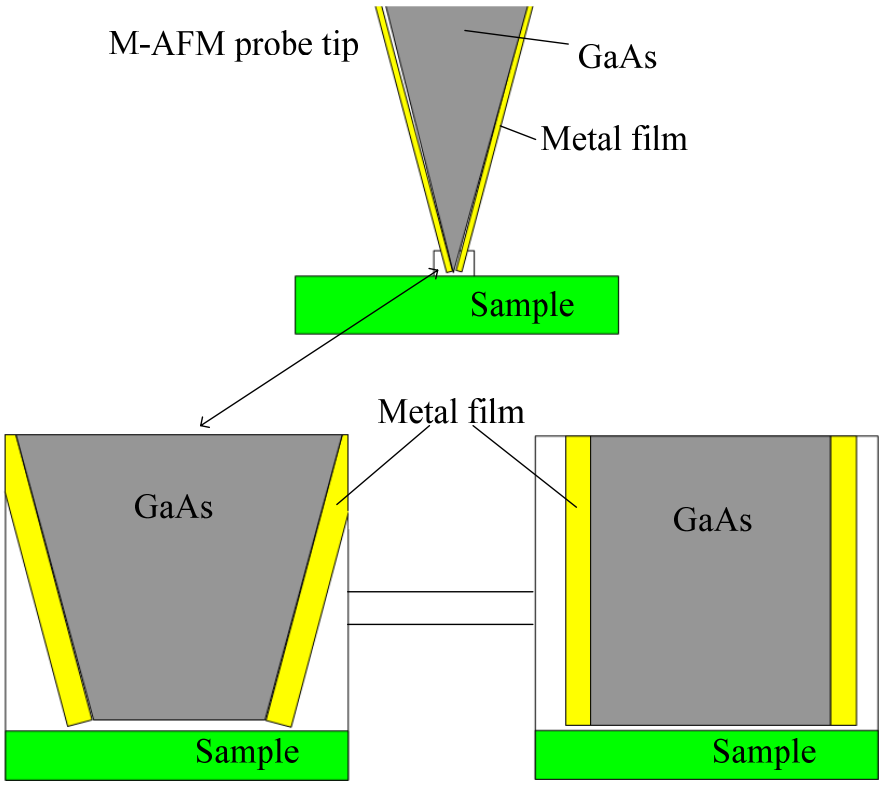

Fig. 4-1 Schematic diagram of the interaction between the M-AFM probe tip and sample surface.

Five different metallic films (Cu, Pb, Al, Co and Zn) with EB fabrication were prepared for the quantitative measurement. The tested electrical conductivities by the four point probe van der Pauw method were obtained as the standard values for calibration and evaluation of M-AFM results.[5] The tested electrical conductivities of these metal films are in the range of 4.46×10^{6} S/m to 5.68×10^{7} S/m. The measurements were performed in the air, and the AFM worked in non-contact mode, with a working environment temperature of 23.0 °C and a relative humidity of 50%. The resonance frequency of M-AFM probe was 107 kHz and the *Q*-value of it was 675. The scan area was 2×2 μm^2, scanning speed was 1 μm/s. Before scanning, we set the original voltage to be zero while maintaining a constant distance of 2.6 μm between the probe tip and the sample. During the scanning process, the standoff distance between the probe tip and samples was fixed at several nanometers by the atomic force, and the voltage corresponding to the inspected sample was measured.

Figures 4-2 to **4-6** show the topographies and microwave images of the five samples. The variations of the measured voltages for the five samples are less than ±0.46 mV, which is much smaller than the dynamic range of the M-AFM. The signal-to-noise ratio of the M-AFM measurements was evaluated to be 20.14 dB on average.

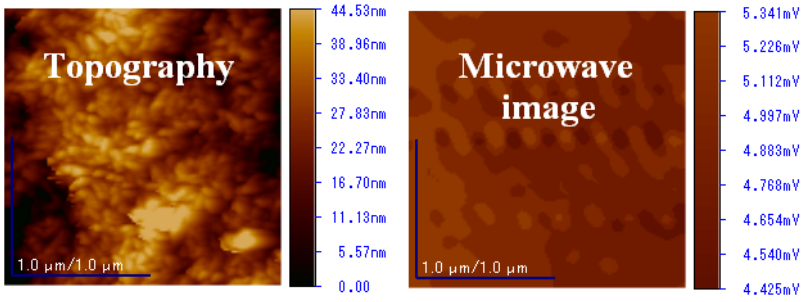

Fig. 4-2 Topography and microwave image of measured Cu sample.

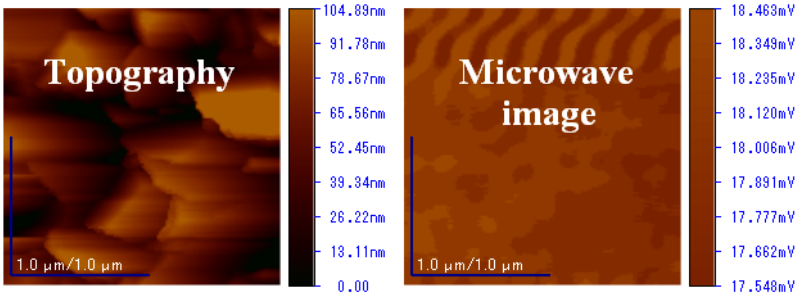

Fig. 4-3 Topography and microwave image of measured Pb sample.

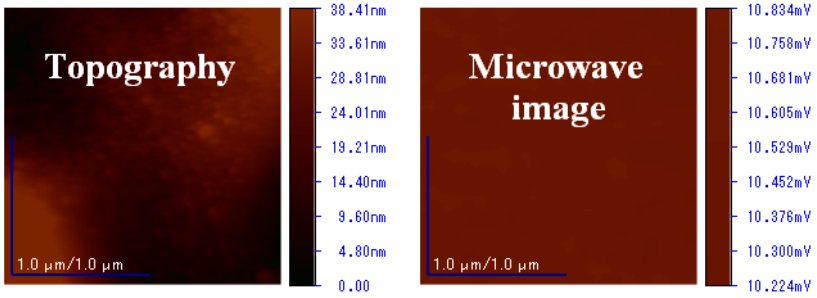

Fig. 4-4 Topography and microwave image of measured Co sample.

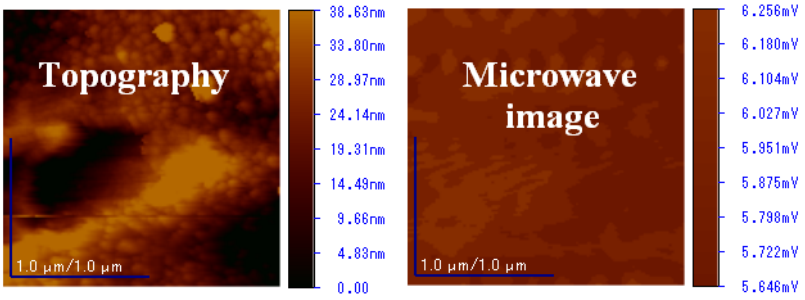

Fig. 4-5 Topography and microwave image of measured Al sample.

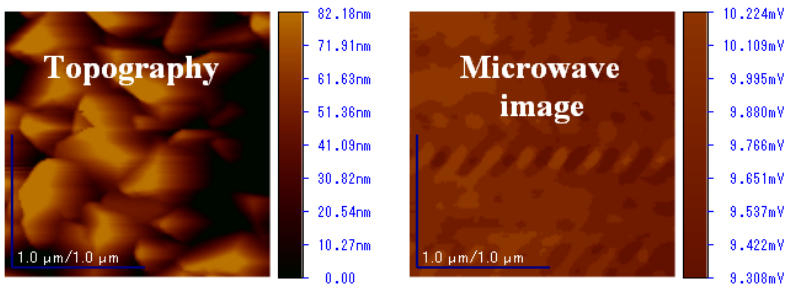

Fig. 4-6 Topography and microwave image of measured Zn sample.

The **Fig. 4-7** shows the variation margins of measured local voltages for samples with different conductivities. Using the measured voltages of two samples obtained from **Figs. 4-2** and **4-3** (4.89 mV for Cu and 18.01 mV for Pb on average) and their tested conductivities (5.68×10^7 S/m for Cu and 4.46×10^6 S/m for Pb) for calibration, the two undetermined constants in Eq. (4-6) were calculated to be k_0=-5.9632 and b_0= 5.9629. Then, the conductivities of Al, Co and Zn samples were evaluated with Eq. (4-6) and Eq. (4-8) by using the measured voltages obtained from **Figs. 4-2** to **4-6**.

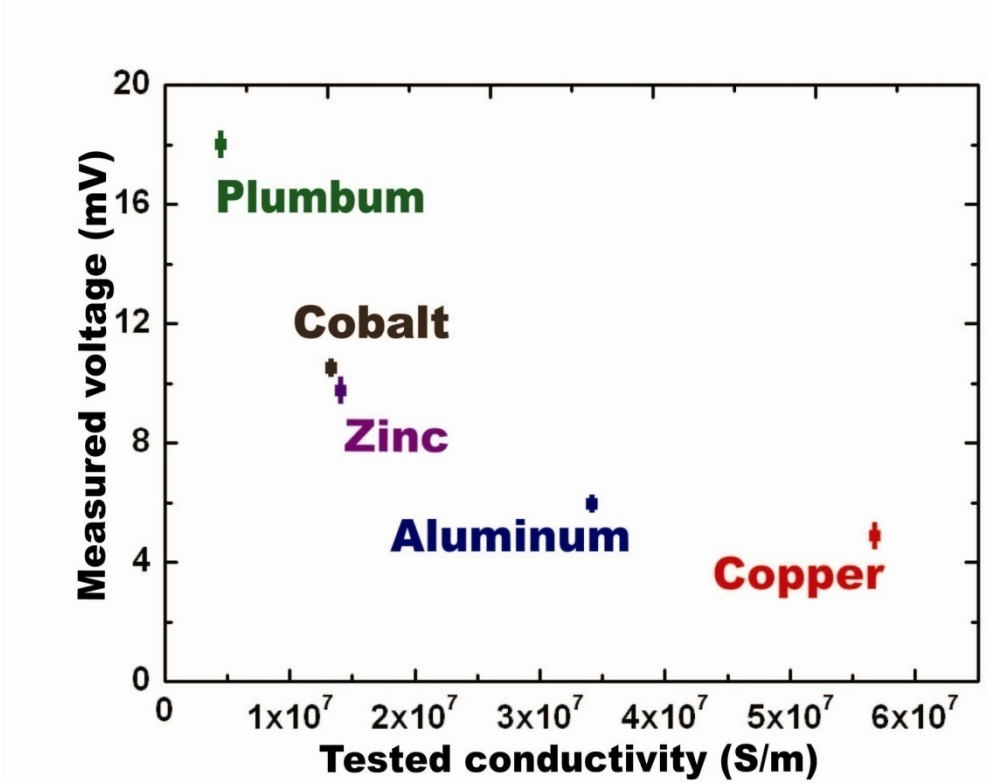

Fig. 4-7 Variation margins of measured local voltages for samples with the different conductivities.

Figure 4-8 shows the variation margins of measured local voltages for samples with the square of surface reflection coefficient ($|\Gamma_s|^2$) of them. As previous mentioned, two undetermined constants in Eq. (4-6) were calculated to be k_0=-5.9632 and b_0=5.9629. That means the method in this work was based on a premise of that the surface reflection coefficient and measured voltage should be kept in a linear relationship. It is noted that the surface reflection coefficient and measured voltage could be provided in a linear relationship (see the fitting straight line in **Fig. 4-8**). Thus, the applicability of the evaluation method in my work can be proved.

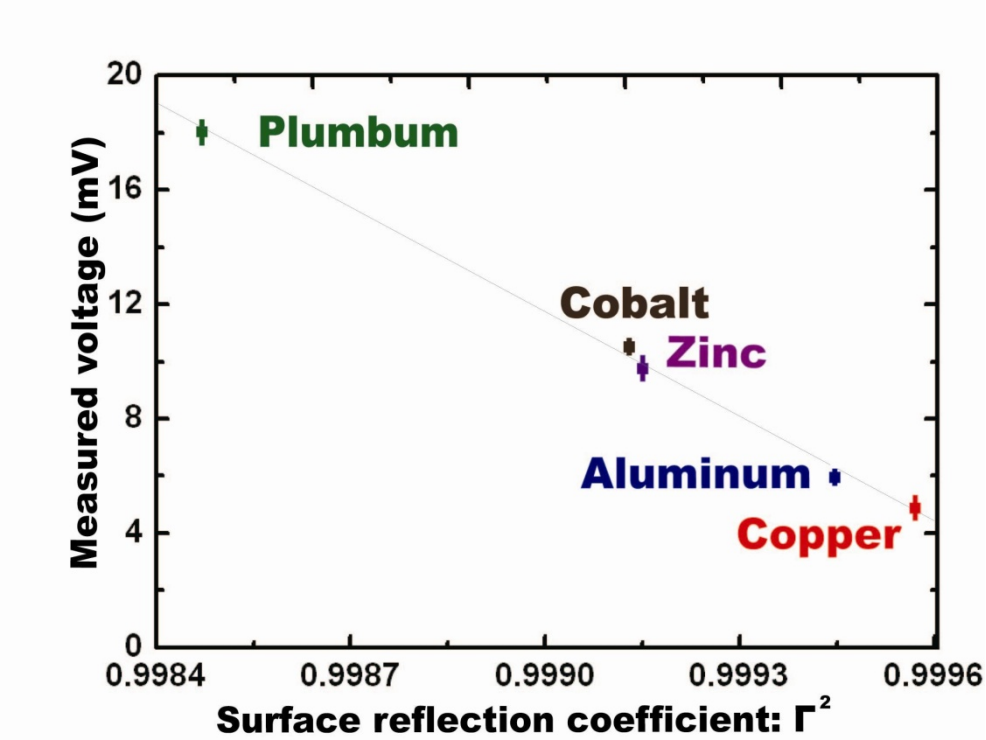

Fig. 4-8 Variation margins of measured local voltages for samples with the square of surface reflection coefficient of them.

Figure 4-9 shows the evaluated results versus the tested values of Al, Co and Zn samples. It is noted from **Figs. 4-2** to **4-6** that no correlation can be observed between the microwave images and their corresponding geometry images. In other words, the variations of the measured local voltages are not caused by the surface morphology. The main causes of error bars of the evaluated conductivities are as follows. Firstly, the film samples prepared by EB evaporation were not homogenous in the microscopic view, and the

distribution of conductivity was location-dependent (local conductivity).

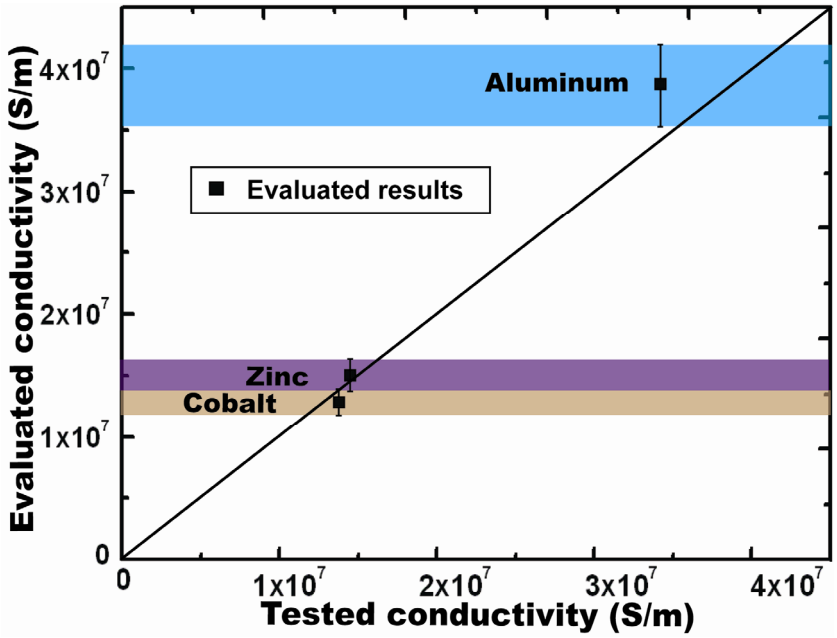

Fig. 4-9 Evaluated conductivities of the samples in comparison with the tested conductivities of them.

It is believed that the variation margins of measured local voltages (see **Fig. 4-7**) by the M-AFM caused the error bars of the evaluated conductivities. Secondly, the microwave signal for conductivity measurement was very small, which might be affected by the measurement environment. Therefore, the uncertainty of the microwave measurement may contribute to the error bars. It is also noted from **Fig. 4-9** that the deviation of evaluated conductivities from the values tested by the Van der Pauw method is 2.03%, 7.24% and 11.6% for the Zn, Co and Al, respectively. One of the causes of this deviation is that the standoff distance variation between different materials may affect the measured voltage, thereby inducing deviation of evaluated conductivity, especially for high-conductivity materials such as Al. Another cause of the deviation may be the evaluation equation which was derived under the plane wave approximation rather than the much more complicated near field analysis. The quantitative evaluation was performed three times, and the similar results as shown in **Fig. 4-7** were obtained.

On the other hand, the evaluated resistivities of the five samples can be presented out as shown in **Fig. 4-10**.

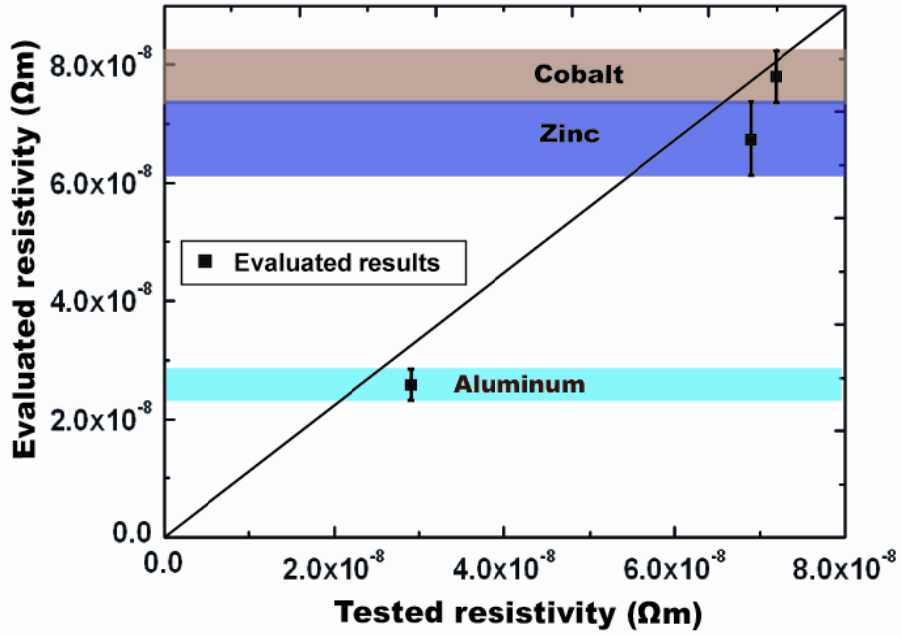

Fig. 4-10 Evaluated resistivities of the samples in comparison with tested c resistivities of them.

4.3 Summary

We also demonstrated a novel evaluation equation and calibration technique for the quantitative measurement of the local conductivity. Based on the analytical and explicit expressions proposed, using two reference samples with known conductivities, the conductivities of any samples can be calculated from the measured voltage. Our results demonstrate that M-AFM is able to quantitatively measure, in situ, the distribution of electrical properties on the nanometer scale.

REFERENCES:

1. Pozer, D. M. *Microwave Engineering 2nd ed.* (Jone Wiley and Sons: New York 1998), p. 32.

2. Ju, Y.; Inoue, K.; Saka, M.; Abé, H. Contactless Measurement of Electrical Conductivity of Semiconductor Wafers Using the Reflection of Millimeter Waves. *Appl. Phys. Lett.* **2002**, *81*, 3585-3587.

3. Ju, Y.; Hirosawa, Y.; Soyama, H.; Saka, M. Contactless Measurement of Electrical

Conductivity of Si Wafers Independent of Wafer Thickness. *Appl. Phys. Lett.* **2005**, *16*, 162102.

4. Liu, L. S.; Ju, Y. Nondestructive Measurement and High-precision Evaluation of the Electrical Conductivity of Doped GaAs Wafers Using Microwaves. *Rev. Sci. Instrum.* **2010**, *81*, 124701.

5. Da Luz, M. S.; Dos Santos, C. A. M.; Shigue, C. Y.; De Carvalho jr, F. J. H.; Mashado, A. J. S. The van der Pauw method of measurements in high-*Tc* superconductors. *Mater Sci-Poland*, **2009**, *27*, 569-579.

5. M-AFM Applications

5.1 Imaging the Nano-Structure Materials

5.1.1 Imaging the Au nanowire by the M-AFM Probe

In general, nanomaterials refer to low-dimensional materials whose crystal structures arrange in zero-dimensional dot, one-dimensional chains or two- dimensional plane, such as nanoparticle, nanowire, nanowhisker, nanorod, nanobelt, nanotube and nanofilm. Among which, the one-dimensional metallic nanostructures display a plethora of electrical, optical, chemical and magnetic properties with diverse applications. For example, the important role of metallic nanowires in semiconductor industry or integrated circuit (IC) may be one of the most attractive topics for scientists and engineers. Recently, the scale of interconnects used in IC is continually shrinking towards dimensions comparable with the electronic mean free path (tens of nanometers) or even smaller.

On the other hand, however, in the nanometer scale, the electrical properties of materials are affected not only by the structure and composition of these materials, but also by the mechanical factors of stress and strain due to lattice vibrations. The electrical properties such as resistivity or conductivity of metallic nanowires will become size-dependent and quite different from that of the bulk materials even at room temperature. Thus it is a great needing toward us to research on the electrical properties of materials on nanometer scale.

The resistance measurement is the most important step for electrical properties' evaluation, in which the preparation of nanowire with electrodes connected to a circuit is limited by manipulation difficulties in nano-scale. When the nanowire and electrodes are well connected, resistance measurement can be carried out by four-point probe (FPP) method which is able to cancel the influences of contact resistances. However, the probes should be connected to the nanowires directly or to electrodes deposited on the nanowires. The process will become somewhat complex

for free-standing nanowires.

Comparing the traditional four-point method, which needs finding some nanowires in suitable positions for conductivity measurement by dispersing the nanowires onto an insulated substrate with electrodes arrays, the M-AFM can spot the nano-structure (such as free standing nanowires and nanotubes) out directly and measure the electrical properties with the topography simultaneously.

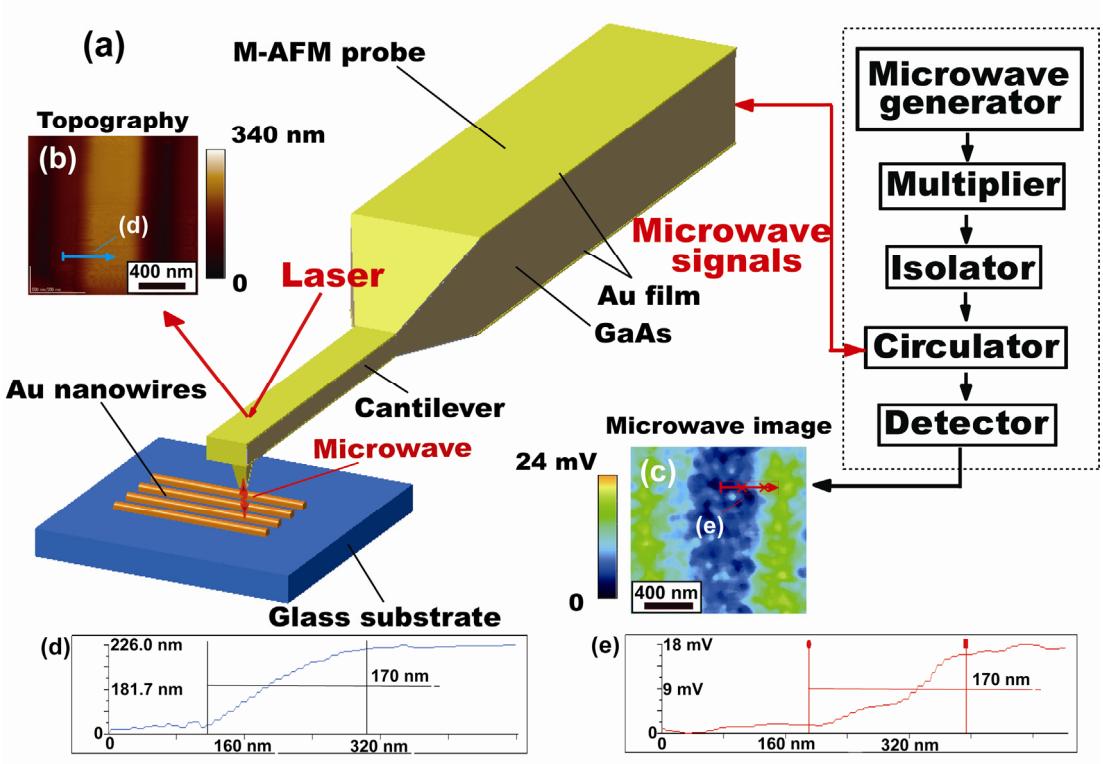

Fig. 5-1 Microwave atomic force microscopy setup and typical surface topography and microwave image of a nanowire sample: (a) schematic graph of the AFM compact microwave instrument setup and schematic diagram of the Au nanowires scanned using the M-AFM probe; (b) topography image of measured sample; (c) microwave image of the nanowire created from the voltage of the measured microwave signals; (d) crossing profile corresponding to the arrow in the topography image; (e) crossing profile of the selected area in the microwave image.

Figure 5-1 shows schematically the integrated measurement system of M-AFM. As mentioned in previous chapters, When the M-AFM probe is located above a sample surface (a Au nanowire in this work), the measured signals are synchronized with the

position information obtained from the AFM scanner, and the topography and microwave image can be generated. **Figure 5-1(b)** shows the measured width and height of a single Au nanowire on a glass substrate to be 480 and 210 nm, respectively, as obtained with M-AFM. The Au nanowires were formed by partially etching the Au film using FIB with a width of 500, where the Au film was coated on a glass-wafer substrate of 200 nm thickness by EB evaporation (the fabrication process of the was shown in **Fig. 5-2**).

Figure 5-1(c) shows the microwave image of the Au nanowire, where the voltage was measured from the reflected microwave signal without calibration. The M-AFM worked in frequency modulation (FM) mode (noncontact mode). The resonance frequency of M-AFM probe was 106 kHz and the *Q*-value of it was 570. The measurements were performed in air ambient, with a working environment temperature of 26.0 °C and a relative humidity of 50%. The scanning area and scanning speed were 1.5×1.5 μm^2 and 500 nm/s, respectively. In **Fig. 5-1(e)**, it is noted that the difference in the measured voltages of the Au and glass substrate is approximately 16 mV, and the spatial resolution is 170 nm. This result illustrates that M-AFM is capable of sensing the microwave image of a nanostructure. In contrast to the traditional four-point method, which requires some nanowires to be in suitable positions for conductivity measurements by dispersing the nanowires onto an insulated substrate with electrode arrays, M-AFM can spot the nanostructures directly and measure the microwave image and topography simultaneously.

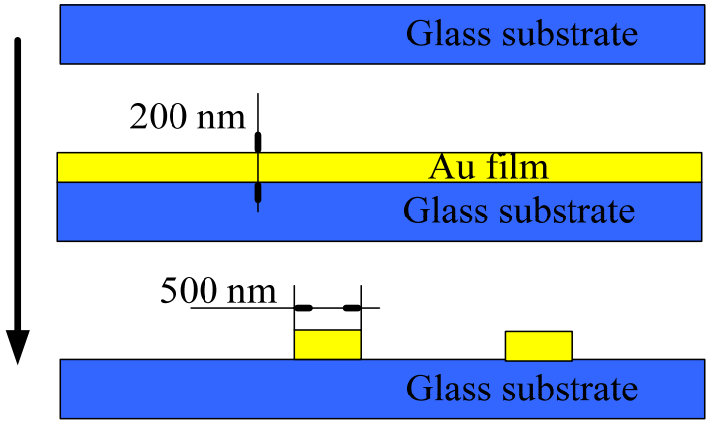

Fig. 5-2 The crossing view of fabrication process of the Au nanowires.

5.1.2 Imaging Results' Precision Affected by Scanning Speed

To study the interaction relationship between the scanning speed and the imaging results, based on a standard sample, the scanning process of M-AFM with three kinds of scanning speed was investigated.

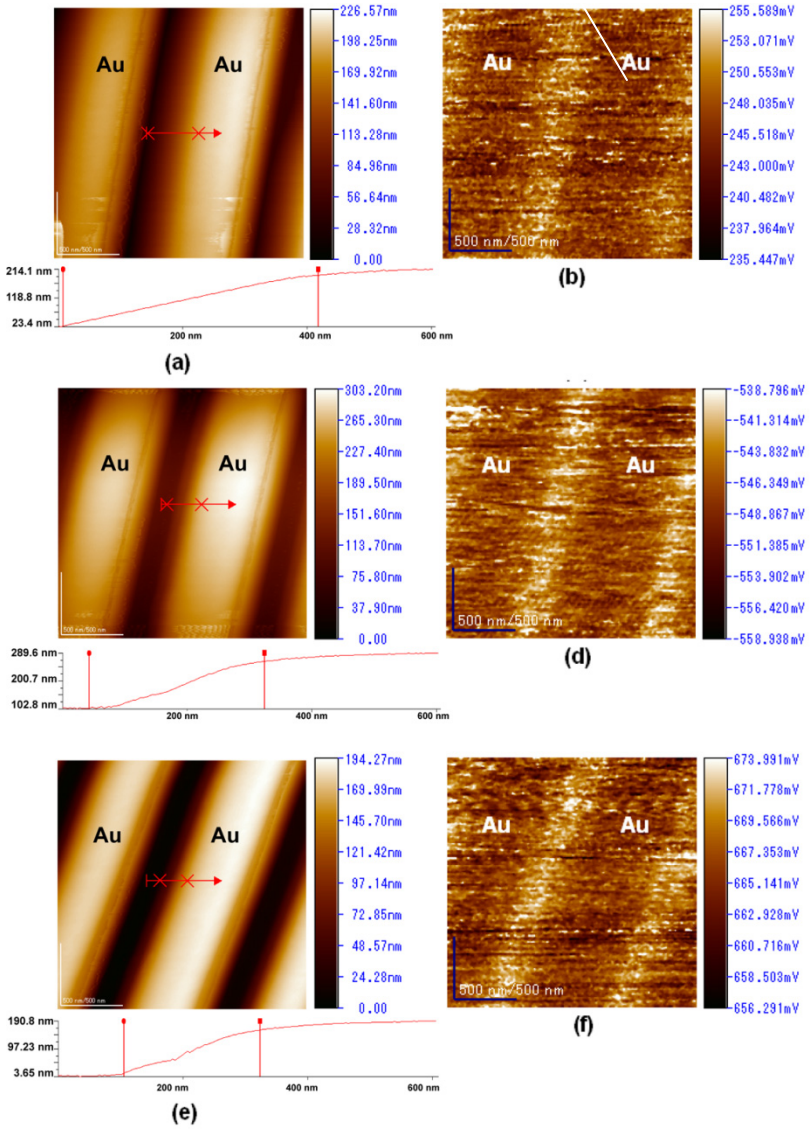

Fig. 5-3 (a) and (b) AFM topography image with the profile and microwave image of the Au-nano-belts obtained by the M-AFM probe with a scanning speed of 500 nm/s; (c) and (d) AFM topography image with the profile and microwave image of the Au-nano-belts obtained by the M-AFM probe with a scanning speed of 1000 nm/s; (e) and (f) AFM topography image with the profile and microwave image of the Au-nano-belts obtained by the M-AFM probe with a scanning speed of 2000 nm/s.

Using the M-AFM probes with the compact-measurement system, a special sample of Au nano-structure was sensed. The Au-nano-belts with the dimension of 400×200 nm arranged on a glass substrate was prepared. The fabrication method of Au-nano-belts was similar with the fabrication method of the Au nanowire in previous chapter. **Figure 5-3** shows the scanning results of topographies and the microwave images. The measurements were performed in the air, and the AFM worked in non-contact mode, with a working environment temperature of 25.0 °C and a relative humidity of 40%. The resonance frequency of M-AFM probe was 153 kHz and the *Q*-value of it was 760. The scan area was 2×2 μm^2, and the scanning speeds were 500 nm/s, 1000 nm/s, and 2000 nm/s, respectively.

Comparing the experimental results, it is suggested that with the scanning speed is decreasing more and more (form 2000 nm/s to 500 nm/s, in this work), the spatial resolution is going to be much better (see the profiles in **Fig. 5-3**). Based on the results in the **Fig. 5-3 (a), (c),** and **(e)**, the sensed shape was presented as much better with the scanning speed decreasing (see **Fig. 5-3 (e)**). However, on the other hand, the precision of microwave image was not change much during the scanning speed was decreasing. The reason can be explained as that comparing with the scanning speed (taking the maximal scanning speed of 2000 nm/s in this work for example), the microwave signal with a very high frequency, the data measured at each pixel is an average of the microwave signal during 9.4 μs, i.e. compact microwave instrument can always implements a real time measurement and the variation of scanning speed cannot put the influence in the microwave measurement (image). As the result, our M-AFM can be used to measure the electrical properties of materials with a high operating efficiency.

It is also noted that, in this work, the value of the measured voltage for the sample of Au-nano-belts obtained in the different scanning process are much different (see **Fig. 5-3 (b), (d),** and **(f)**). The reason can be explained as that before the scanning process, without the original nulling setup, in the other word, the original testing voltage were different. However, such difference can be corrected by the calibration

process with a zero setting, therefore it will not affect the evaluation of electrical properties of materials.

5.2 Imaging the Nano-Structure Materials

Recently, the researches about electrical characteristics of metallic film and membrane on a nano-scale have become the hot topics more and more. However, if the surface of the metallic film or membrane is covered by a thin oxide layer, the traditional method will fail in evaluating the electrical property of material under the oxide layer, because it is difficult to make direct contacts to the material under test. On the contrary, M-AFM can be used to solve this problem, because the microwave signals emitted from the tip of M-AFM can penetrate the dielectric film, and have an interaction with the underlying materials. By analyzing the reflected microwave signals, the electrical properties of underlying materials can be evaluated. In this paper, some special samples with different thickness of dielectric films which plays the role of oxide layer created on the material surface were fabricated, and the measurement of electrical properties of materials under the oxide layer by the M-AFM was investigated in details.

5.2.1 Improved the Compact Microwave Instrument

In order improve the sensitivity of the microwave evaluation system, the compact microwave instrument was modified. In this work, the compact microwave instrument which is composed of an amplifier, a magic-Tee, an attenuator, a tunable short, and a diode detector, as shown in **Fig. 5-4**. **Figure 5-4(a)** shows the flow chart of the operating microwave signals for measurements. The microwave signals working at a frequency f＝94 GHz (same with previous), which was generated by a microwave generator. Then the microwave signals were separated into two branches by the magic-tee (a four-port, 180 degree hybrid splitter, realized in waveguide). One branch signal was sent to the M-AFM probe to sense the samples and then the reflected signal was received by the probe tip, as shown in **Fig. 5-4(b)**. Another branch signal was sent to the attenuator and then to the tunable-short to form a reference signal with

a constant phase difference and a similar amplitude comparing with the reflected signal from the sample. The reference signal was determined by setting the output voltage of the detector to be a definite value when the M-AFM was set in air without the approaching, and this was carried out by adjusting the attenuator and the tunable-short.

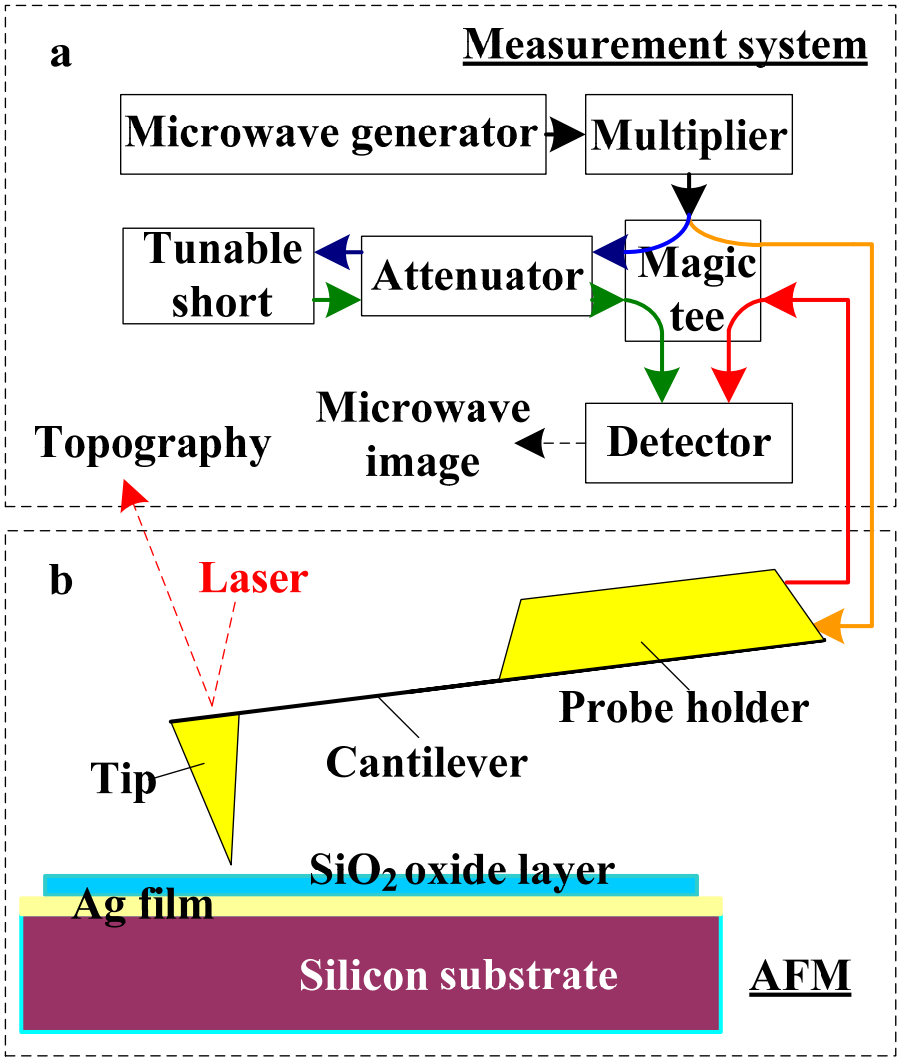

Fig. 5-4 Schematic diagram of the M-AFM measurement system.

The reflected signal and the reference signal were finally synthesized by the magic-Tee, and the coherent signals were measured by the detector. The detector used in the experiment was a square-law detector, and the output voltage has a linear relationship with the squared complex modulus of the reflection coefficient. When the

sample was scanned by the M-AFM probe, the reflected signal which carries some useful information of the sample's electrical property was received and converted to the voltage value. **Figure 5-5** shows the photo image of the M-AFM measurement system.

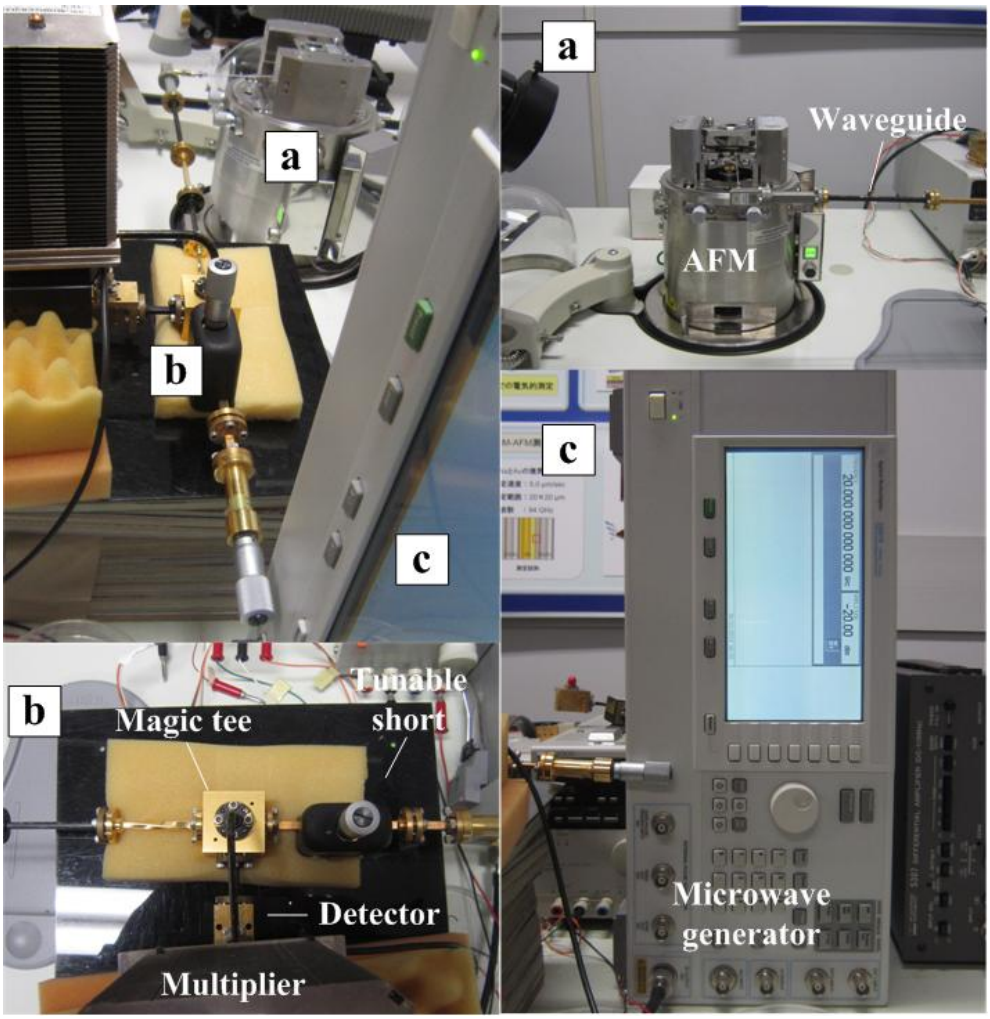

Fig. 5-5 Photo image of the M-AFM measurement system.

5.2.2 Experimental Conditions and Samples

Figure 5-6 indicates the interaction of microwave signals with the sample under test. The incident microwave signals propagated in M-AFM probe and then were emitted at the top of probe tip. Considering the configuration and dimensions of the probe tip and the nano-slit from which microwave signals are emitted, the measurement was

dominated by the interaction between the near-field microwave and a shallow surface layer of the sample. Therefore, if the distance between M-AFM probe tip and the sample under test exceeds the interaction range of the near-field microwave, the microwave cannot sense the sample and no useful information of the sample's electrical property is presented in the reflected microwave signals. In this study, we researched on the relationship between the thickness of oxide layer on a metallic film and the reflected microwave signals. It can be demonstrated from our study that the M-AFM is able to measure the electrical property of material under a thin oxide layer.

The samples under test are prepared as follows. A thin Ag film with thickness of 100 nm on average was deposited on the Si wafer by electron beam (EB) evaporation. Then, SiO_2 films with different thickness were evaporated on the Ag film respectively, as shown in **Fig. 5-6(b)**. These SiO_2 films play the role of oxide layer created on the surface of the metallic film. In this way, we obtained five samples with the SiO_2 films having the thickness from 20 nm to 100 nm with the increment of 20 nm and another one without the SiO_2 film.

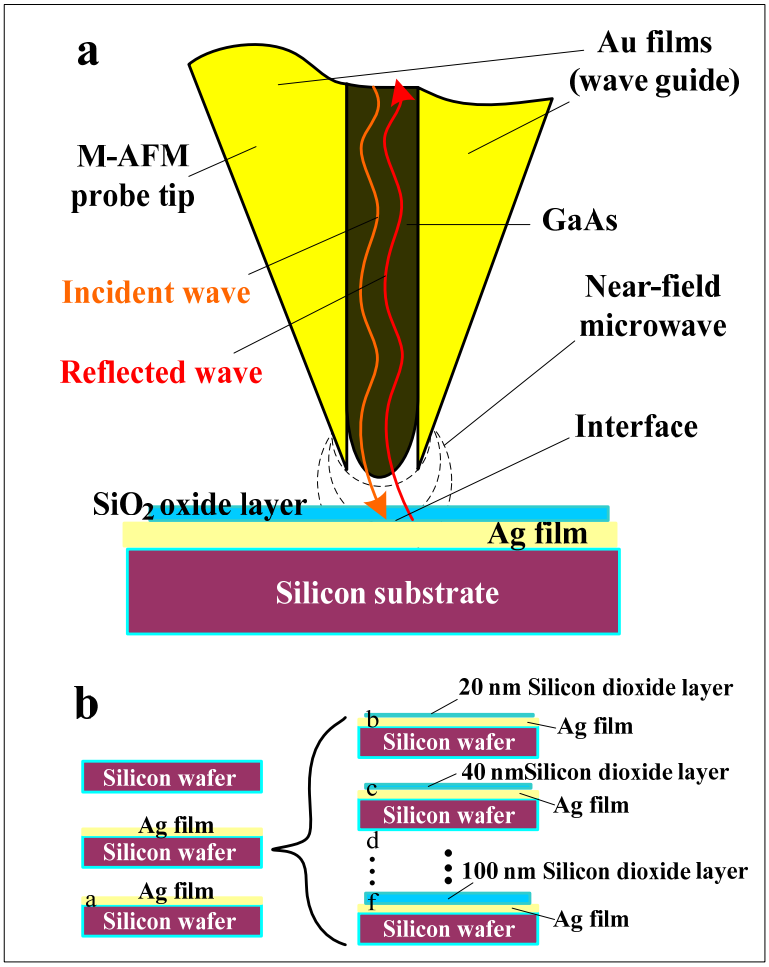

Fig. 5-6 Schematic diagrams, a: interaction of near-filed microwave with the sample under test; b: the fabrication process of samples used in this study.

Since the thickness of Ag film in this study was 100 nm, which is much larger than the skin depth of Ag for microwave at the frequency of 94 GHz, only the microwave signal reflected from the top face of the Ag film can affect the measurement results. The M-AFM worked in frequency modulation (FM) mode (noncontact mode). The resonance frequency of M-AFM probe was 106 kHz and the *Q*-value of it was 570. The measurements were performed in air ambient, with a working environment temperature of 25.0 °C and a relative humidity of 50%. The scanning area and scanning speed were 2×2 μm^2 and 1000 nm/s, respectively.

5.2.3 Experiment Results of Measuring the Samples

Figure 5-7(a) depicts the schematic diagram of experiment of measuring the samples.

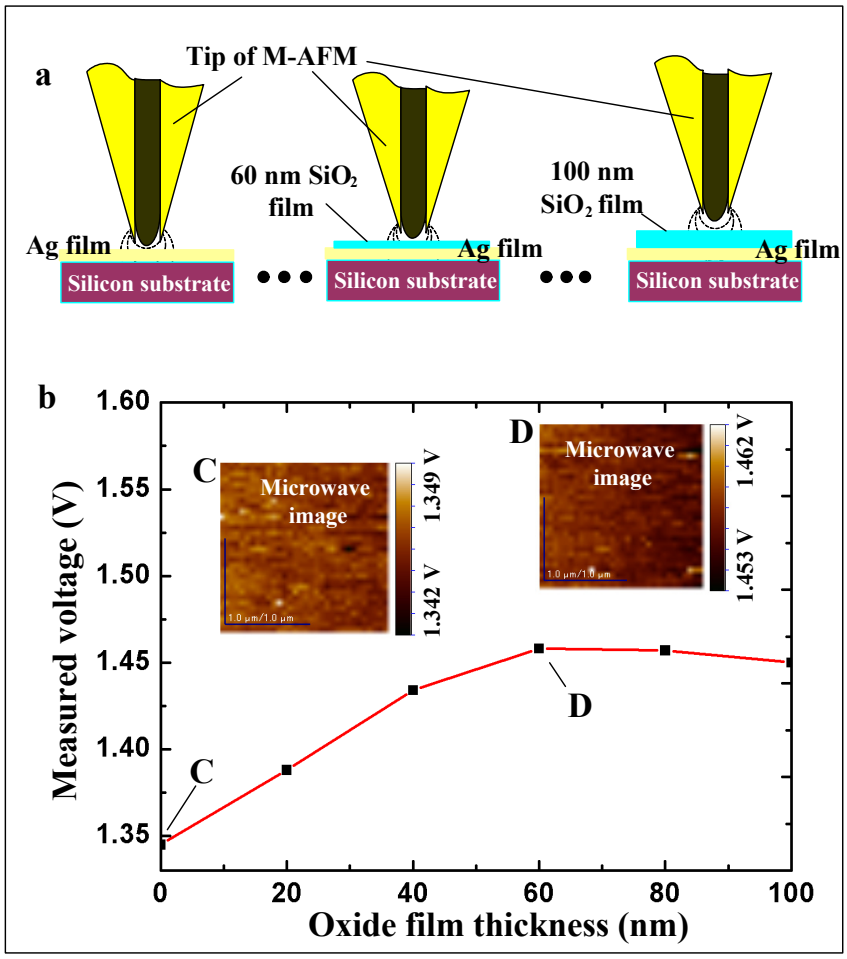

Fig. 5-7 (a): schematic diagram of the scanning process of samples covered by oxide films with different thickness;(b): the relationship between the measured voltage and the thickness of oxide film. Inset C and D are the microwave images of Ag film and Ag film covered by a 60 nm oxide layer measured by the M-AFM.

Since this study is going to use the M-AFM probe to scan the Ag samples under 6 different thickness of oxide film (SiO_2), the whole experiment was separated into 6 times. In order to make all the steps can be kept in same initial measurement conditions, before the scanning processes for all the samples, we firstly set the initial voltage to 1.5 V (by the voltage-offset function of pre-amplifier) at the situation of keeping a constant distance of 2.6 μm between the probe tip and measured sample. Then, during the

scanning process, the stand-off distance between the probe tip and scanning surface was fixed in several nanometers by the atomic force and the voltage corresponding to the inspected sample was measured and recorded. **Figure 5-7(b)** shows the relationship between the thickness of oxide film and the measured voltage, which was converted from the reflected microwave signals.

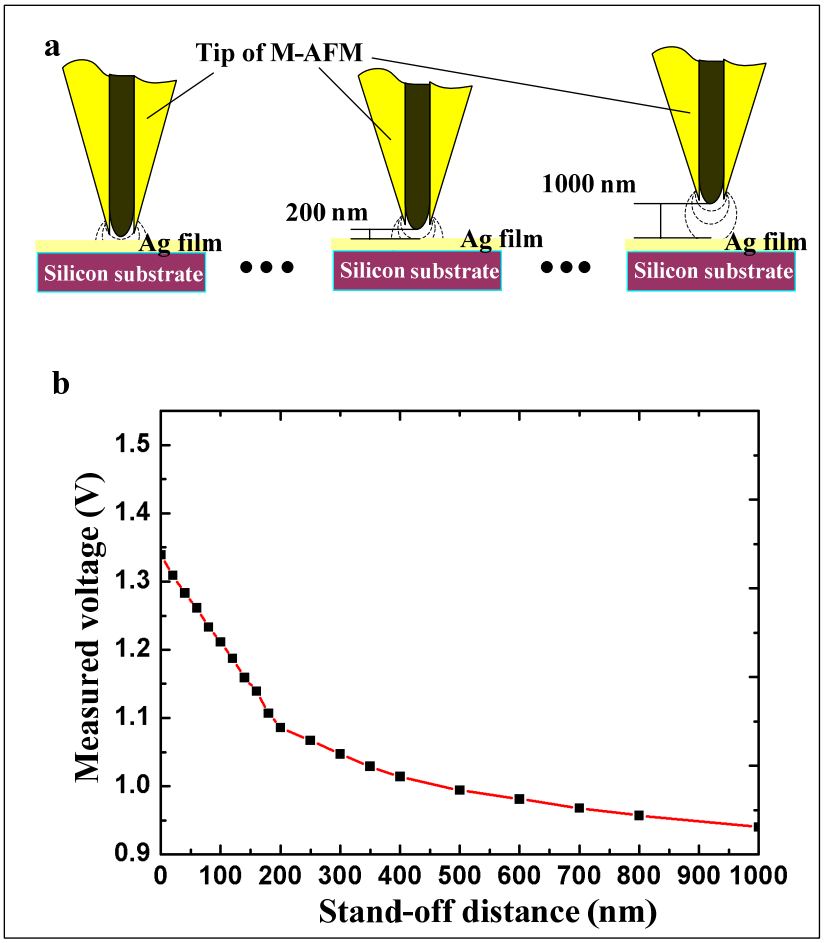

Fig. 5-8 (a) The M-AFM probe scanned the samples of Ag film 20 times with different standoff distances ranging from 0 to 1000 nm. (b) the relationship between measured voltage values and the standoff distances.

In order to verify the creditability of the measurements, calibration experiment was also carried out (see **Fig. 5-8**). The M-AFM as well as the AFM is able to adjust the standoff distance to different values and keep it constant during the scanning process. By recording the scanning route of scanning topography, the cantilever of probe could be lifted up a set value with nano-meter order. Lifting the cantilever on the each

scanning contour, the M-AFM probe performs up-and-down motion line by line. Then, the stable topography and microwave image can be acquired in twice scanning process. In this study, we input the height value to lift up the M-AFM tip from the normal feedback position of topography image with a positive value from 20 nm to 1000 nm. All the other experimental conditions are kept the same as mentioned for the previous works.

5.2.4 Discussion

As shown in **Fig. 5-7(a)**, the measured voltage is monotone increasing when the thickness of oxide layer is smaller than 60 nm. However, when the thickness of oxide layer covered on the Ag film becomes larger than 60 nm, the measured voltage almost keeps constant regardless of different thickness of oxide layer. This result illustrates that the electrical property of Ag film under the oxide layer would affect the reflected microwave signals and thus can be extracted from the measured voltage when the SiO_2 layer is thinner than 60 nm. However, if the thickness of oxide layer is larger than 60 nm, the microwave signals will spread to other directions rather than penetrate the oxide layer to sense the covered sample. Thereby, the electrical property of the sample under a thick oxide layer can not be extracted from the measured voltage. In the calibration experiment, the similar phenomenon was observed. When the standoff distance is larger than 200 nm, the change in the measured voltage becomes very small. It means that the effective detection range of the M-AFM probe tip in air is almost 3 times larger than that in the SiO_2 layer. The reason can be explained as that considering the relative dielectric constants (ε_r) of air and SiO_2 are 1.000585 and 3.9, respectively, the $\varepsilon_{r air}$ is much smaller than the $\varepsilon_{r SiO_2}$. The microwave wavelength in the air is longer than the one in the oxide layer. Thus, the effective detection range (interaction range) of microwave signal and measured material has a relationship of positive correlation with the wavelength.

The results suggest that the M-AFM can be used to measure the electrical property of

material under a thin oxide layer, but the thickness and electromagnetic parameters of the oxide layer should be considered in a quantitative measurement.

5.3 Osteoblast-like Cells Analysis on Nanometer Scale

The cell is the functional basic unit of life. It is the smallest unit of life that is classified as a living thing, and is often called the building block of life. The interior of a cell is the part inside the cell membrane, consisting of the cytoplasm and all organelles within it. Biochemical studies reveal that all biological structures are made up of combinations of proteins, carbohydrates, lipids and nucleic acids. These compositions carry out complicated biochemical and physiological process inside the cell. In order to study these complicated process, acquiring the morphological and fundamental function of these intracellular structures become an indispensible process.

With the development of biotechnology, more and more approaches have been developed to investigate the intracellular structures. Immunofluorescent staining was the most widely used method to detect the changes of microfilaments in studying the behavior of cytoskeleton.[1-2] Some cellular organelle such as chloroplast have been isolated from plant cells and investigated morphological structures and functions in the process of photosynthesis. In order to observe the intracellular structures, some special microscopes have been designed. Tokita and cooperators have developed a new kind of microscope that able to observe the internal structure of living cells.[3] Researchers from Caltech try to see the arrangement of individual proteins inside cells in a lifelike state with the electron cryomicroscope.[4] Transmission electron microscopy (TEM) and scanning electron microscope (SEM) also play an important role in cellular research. Compared with those approaches above, in this study, we try to visualize the intracellular structures with AFM.

Advances in our understanding of molecular and cellular biology were and still are dictated by the development of new techniques, allowing the structural and functional study of living materials. The nano-scale surface analysis of microbial cells represents

a significant challenge of current microbiology and is critical for developing new biotechnological and biomedical applications. The exploration of microbes using atomic force microscopy (AFM) is an exciting research field that has expanded rapidly in the past years. Since the invention of the AFM in 1986,[5] amazing progress has been made in the imaging and manipulation of bio-molecules. AFM topographies of plant [6-7], bacteria [8] and other cells [9-12] have been acquired by different groups, which make it easier to study cells on nanometer-scale. Recently, researchers have successfully used AFM to measure the elasticity and adhesion forces of cells [13-15]. AFM can be used not only for mechanical imaging but also for nanometer level mechanical manipulations of biological samples through its capability of pushing and pulling them with a sharp tip prefabricated on a thin cantilever. Afrin and Han have tried to deliver small molecules and DNA in to living cells with tip modified AFM [16-17]. Results indicated that AFM can be an effective tool for gene/molecule delivery. However, few papers reports on the application of AFM to study the intracellular structures of cells, with a new type of novel M-AFM, we try to observe and measure the intracellular microstructures of cells. M-AFM probe is operated in a non-contact mode, which provides anon-invasive measurement. Therefore, the measurement could be utilized for various materials, such as metals, organic and inorganic samples and bio-specimens.

Figure 5-9(a) shows the flow chart of the operating microwave signals for measurements. When the sample was scanned by the M-AFM probe, since the cell membrane which's range from 7 to 8 nm in thickness, the microwave signal can transmit membrane (see **Fig. 5-9** (c)).The reflected signal which carries some useful information of the sample's electrical property was received and converted to the voltage value. The M-AFM worked in frequency modulation (FM) mode (noncontact mode). The resonance frequency of M-AFM probe was 132 kHz and the *Q*-value of it was 500. The measurements were performed in air ambient, with a working environment temperature of 25.0 °C and a relative humidity of 50%. The scanning area and scanning speed were 20×20 μm^2 and 10μm /s, respectively.

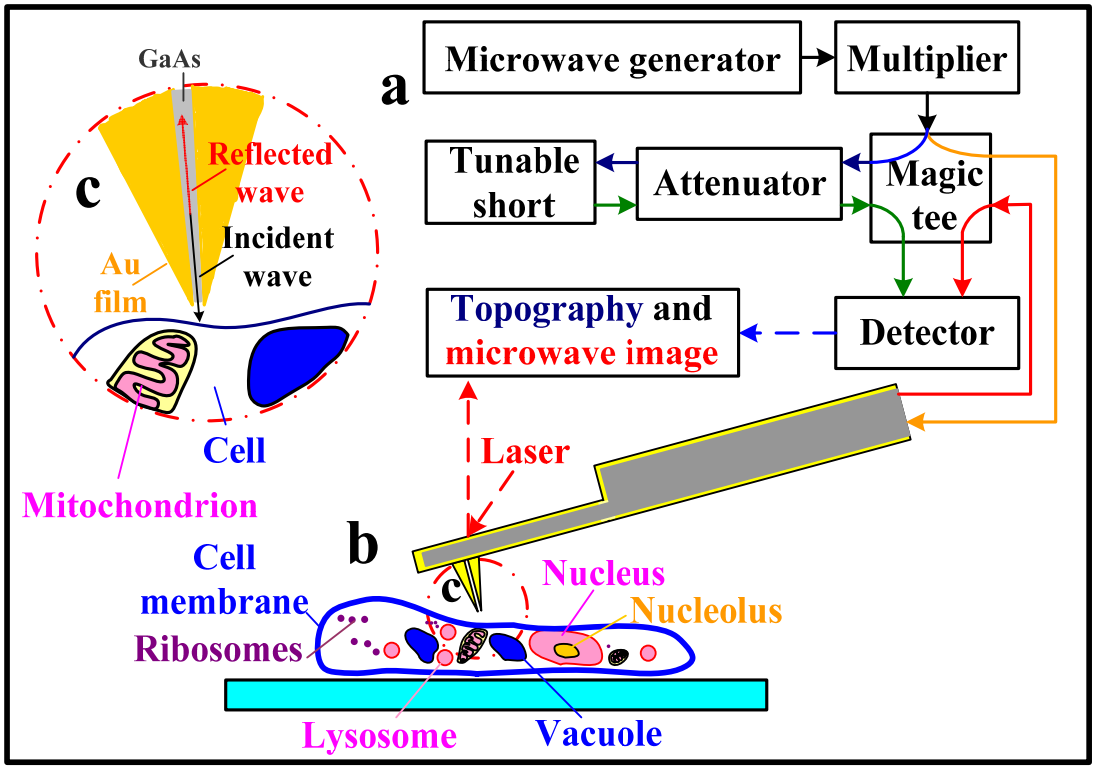

Fig. 5-9 Schematic of the M-AFM set up and the osteoblast-like cells composed of organelles: (a and b) schematic graph of the AFM compact microwave instrument setup and the schematic diagram of the osteoblast-like cell scanned by the M-AFM probe; (c) High-magnification image of interaction part of M-AFM-probe tip and cell organelles.

AFM imaging of thus prepared samples revealed single osteoblast-like cell with diameters of up to 20 μm. **Figure 5-10** depicts an optical microscope image of osteoblast-like cells spread on a glass substrate. **Figure 5-11(a)** shows the surface topography of an osteoblast-like cell with the M-AFM. **Figure 5-11(b)** is the three dimensional image corresponding to **Fig. 5-11(a)**. **Figure 5-12(a)** shows the microwave image of the measured voltage that was converted from the detected microwave signals. The image was simultaneously acquired by the M-AFM probe at the corresponding position depicted in **Fig. 5-11(a)**. **Figure 5-12(b)** is the three dimensional image of **Fig. 5-12(a)**.

In **Figure 5-11**, the topography image showing the outline of an osteoblast-like cell was chosen so that the total height of the membrane and its structures could be

determined. Three different height levels are clearly detectable. The first level has a value of 65 nm PFA coating film associated with the 10 nm-height of the lipid bi-layer (cell membrane).

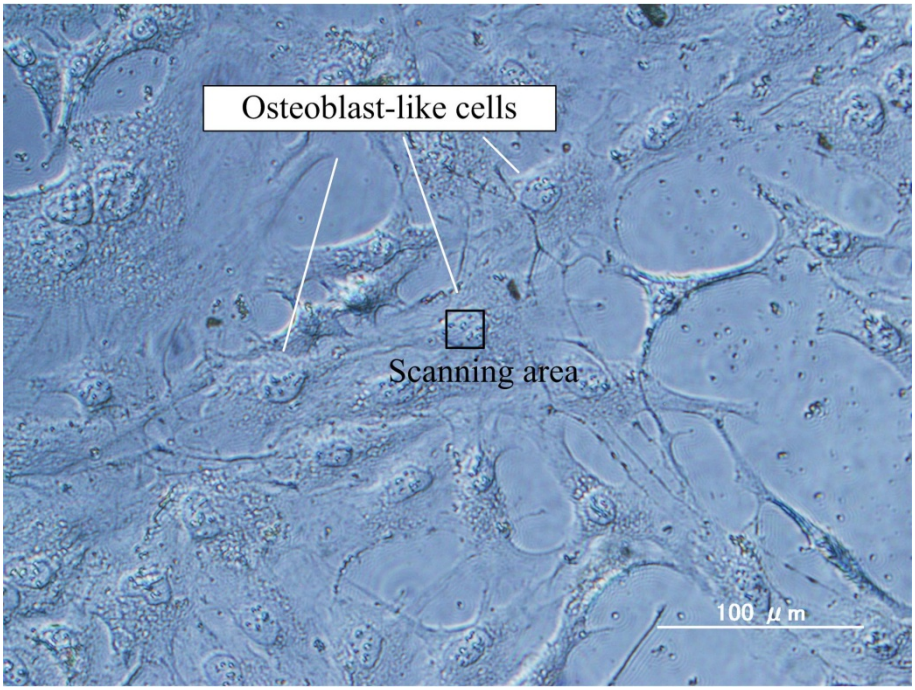

Fig. 5-10 The osteoblast-like cells wereobserved with optical microscope.

The second level corresponds to the height of the residual body of cytoplasm with exception of nucleus and mitochondria protruding from the inner surface of the membrane. Finally, the third level shows the nucleus and mitochondria. The protruding nucleus appears with height of 460 nm. Moreover, please notice that, in **Fig. 5-11(a)** the second level and third level (see **Fig. 5-11(a)**) in appear with different heights. However, in **Fig. 5-12(a)**, at the corresponding area, the microwave images of nucleus and mitochondria were distinguished, but the residual body of other cytoplasm with no response. The reason can be explained as that the, the reflected microwave signals over nucleus and mitochondria much than other scanning area. Mitochondria are found in nearly all eukaryotes, thus in microwave image the mitochondria also can be found. It also should be noted that the apparent shape of the them is usually found to be semi-ellipsoidal (see **Fig. 5-11(a)**) with smooth probing contour, which means that under the non-contact mode, the M-AFM can eliminate the

fact that lateral dimensions of the base of individual proteins are well estimated as the result of M-AFM-probe.

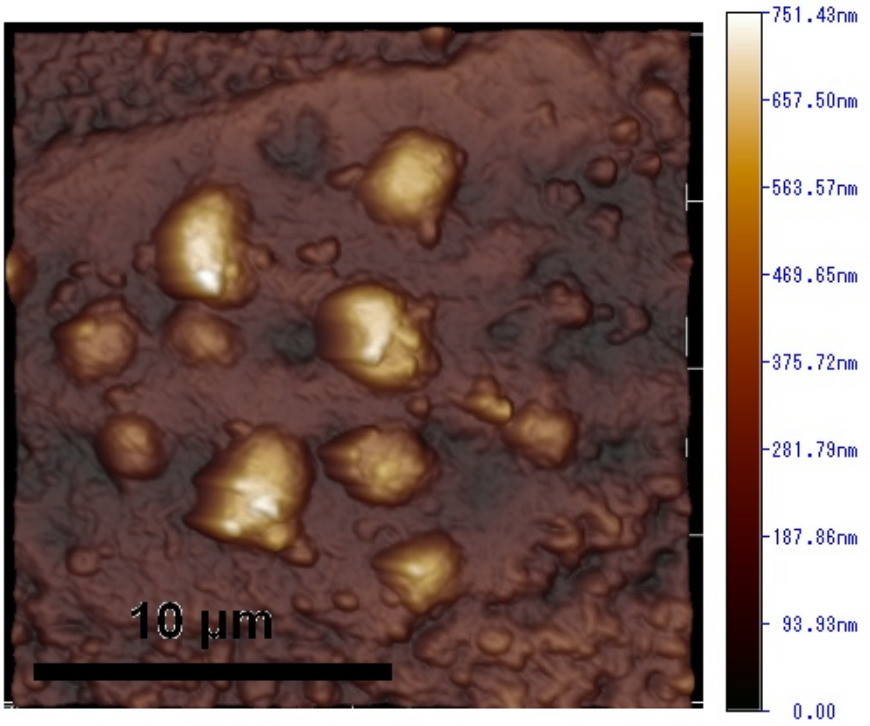

Fig. 5-11(a) AFM topography image of the osteoblast-like cell.

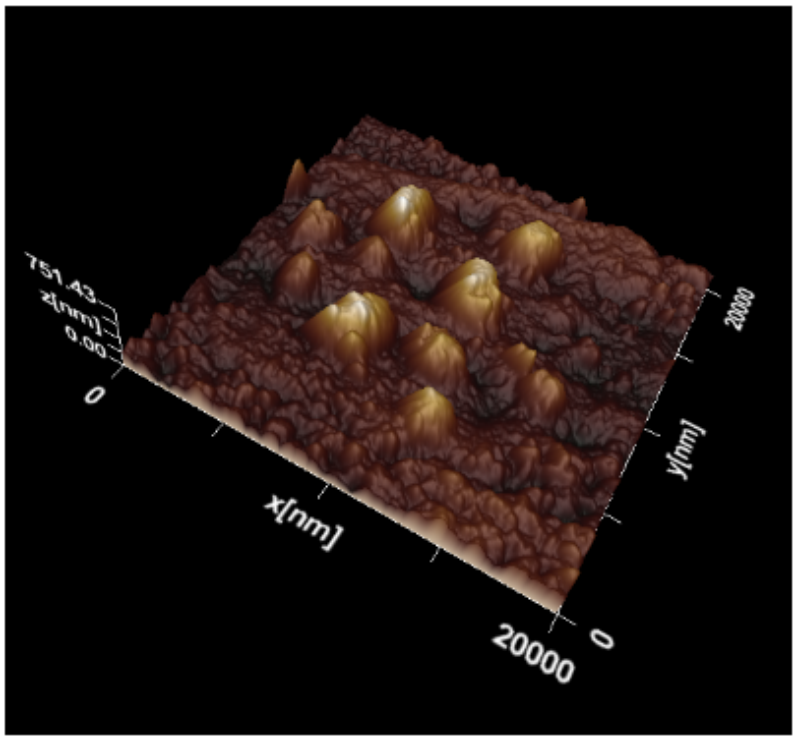

Fig. 5-11(b) 3D-AFM topography image of the osteoblast-like cell.

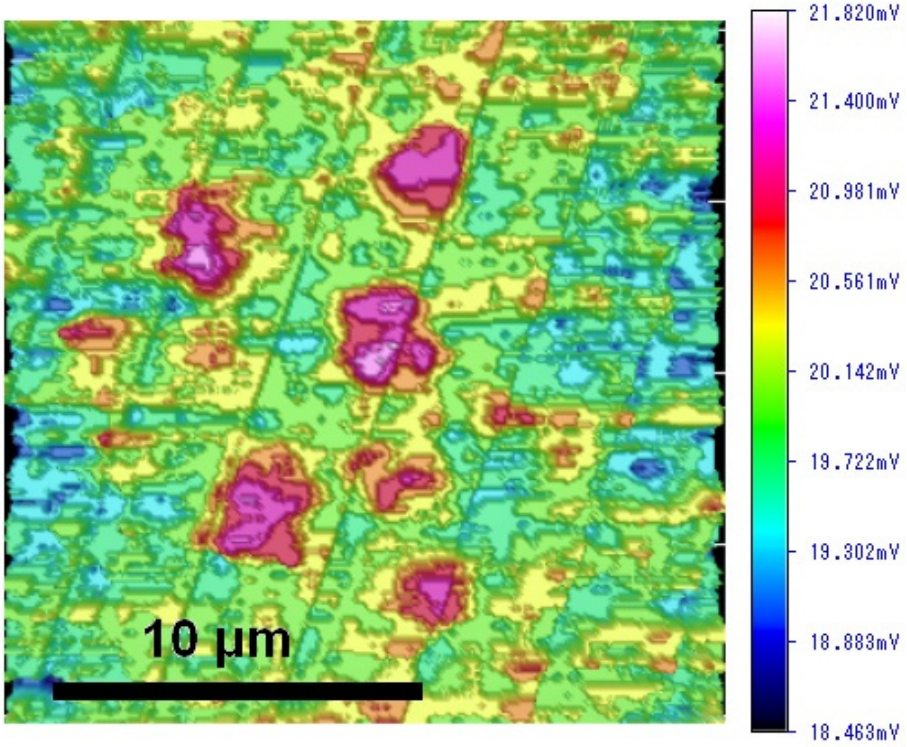

Fig. 5-12(a) Microwave image obtained from the the osteoblast-like cell.

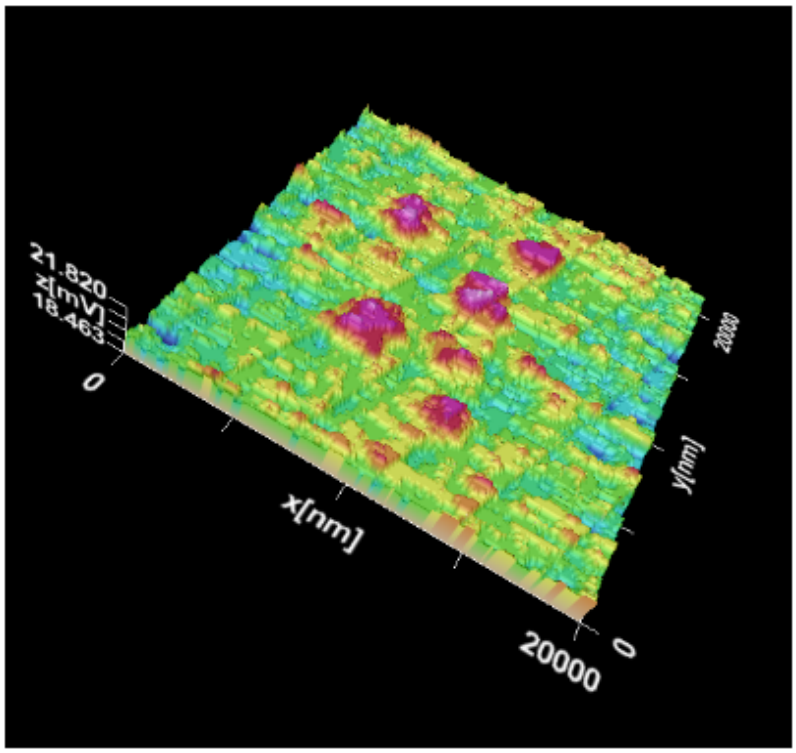

Fig. 5-12(b) 3D-Microwave image obtained from the the osteoblast-like cell.

The electrical information images of osteoblast-like cell obtained with the M-AFM

were accomplished, and the scanning results are very reproducible. Further, in non-contact mode, the M-AFM-probe tip is scanned above the cell surface, maintaining a constant stand-off distance. The created lateral forces are too small to sweep away or deform the fragile biomolecules. The technique M-AFM may serve as a suitable method for imaging the ocsteoblast-like cells. Quantification such as determining the number and distribution oforganelles andproteins as well as their dimension and electrical information becomes possible. Theunique potentials of M-AFM to image biological substrates with nanoscale resolution under physiological conditions on a non-damaging manner, where the original structure and function of the biomolecules under investigation are preserved, make this technique very attractive to biologists in near future.

5.4 Summary

(a) Under the non-contact mode, the surfacce topography and microwave image of a single Au nanowire were obtained by the M-AFM probe, simultaneously. The deference of the measured voltage between the Au and glass substrate is approximately 16 mV. These results illustrate that the M-AFM is capable of sensing the microwave image of a nano-structure. In contrast to the traditional four-point method, which requires some nanowires to be in suitable positions for conductivity measurements by dispersing the nanowires onto an insulated substrate with electrode arrays, the M-AFM can spot the nano-structures directly and measure the microwave image and topography simultaneously.

(b) Using the M-AFM probes with the compact-measurement system, the sample of Au-nano-belts was sensed with three kinds of scanning speed: 500 nm/s, 1000 nm/s, and 2000 nm/s, respectively. Comparing the experimental results, it is suggested that with the scanning speed is decreasing, the spatial resolution is going to be much better. However, on the other hand, the precision of microwave image was not change much during the scanning speed was decreasing. Because M-AFM with the compact microwave instrument can always implements a real time measurement, and the

variation of scanning speed cannot put the influence in the microwave measurement (image).Which means that the M-AFM can be used to measure the electrical properties of materials with a high operating efficiency.

(c) To improve the sensitivity of the microwave evaluation system, the compact microwave instrument was modified. The improved compact microwave instrument is composed of an amplifier, a magic-Tee, an attenuator, a tunable short, and a diode detector. The microwave signal was separated into two routes, one branch signal was sent to the M-AFM probe to sense the samples and then the reflected signal was received by the probe tip. Another branch signal was sent to the attenuator and then to the tunable-short to form a reference signal with a constant phase difference and a similar amplitude comparing with the reflected signal from the sample. The reflected signal and the reference signal were finally synthesized by the magic-Tee, and the coherent signals were measured by the detector. As the result, the environment noise can be eliminated, and the system accuracy control could get a much improvement.

(d) We carried out a group of experiment to verify the M-AFM with the capacity of measuring the electrical information of underlying materials. Some special samples with different thickness of dielectric films (SiO_2) which plays the role of oxide layer creating on the material surface were fabricated. The thickness of oxide-layer is from 20 nm to 100 nm with 20 nm increase in this work. Based on the results, the M-AFM can be used to measure the electrical property of material under a thin oxide layer with a limited thickness of 60 nm, and the thickness and electromagnetic parameters of the oxide layer should be considered in a quantitative measurement.

(e) M-AFM can sense the topography and microwave image of cells in one scanning process, simultaneously. Under the non-contact AFM mode, a microwave image of osteoblast-like cell on nanometer-scale spatial resolution was created by the M-AFM. By analysis the results, quantification such as number and distribution of organelles and proteins of osteoblast-like cell as well as their dimension and electrical information can be characterized.

APPENDIX：

Cell culture: Osteoblast-like cells MG-63 (cellbank) was used in this study, which has a number of characteristic features of osteoblasts. The MG63 cells were cultured in Dulbbeco's modified Eagle's medium (DMEM, Gibco). 10% fetal bovine serum (FBS) and 1% penicillin/streptomycin were added to culture media. hMSCs were seeded in 25 cm^2 culture flasks (Becton Dickinson Labware, USA) and kept in humidified incubator (SANYO, Japan) at 37ºC under 5% CO_2 atmosphere. The culture medium was changed every 3 days. After reaching confluence, cells were detached with 0.25 % trypsin/ mM EDTA (Takara Bio Inc., Japan). Sample preparation: After MG-63 cells were cultured on the cover glass for 2 days, the surfaces were rinsed with PBS and the cells attached on the surfaces were fixed with 2.5% glutaraldehyde (Wako, Japan) in PBS for 1 h at room temperature. After thorough washing with PBS, the cells on the surfaces were dehydrated in ethanol graded series (50%, 60%, 70%,80%, 90%, 95% and 100%) for 15 min each and air-dried at room temperature.

REFERRENCE

1. Tumminia, S. J.; Mitton, K. P.; Arora, J; Zelenka, P.; Epstein, D. L; Russell, P. Mechanical Stretch Alters the Actin Cytoskeletal Network and Signal Transduction in Human Trabecular Meshwork Cells. *IOVS*, **1998,** *39*, .1361-1371.

2. Xu, B.; Song, G.; Ju, Y. Effect of Focal Adhesion Kinase on the Regulation of Realignment and Tenogenic Differentiation of Human Mesenchymal Stem Cells by Mechanical Stretch. *Connect Tissue Res*. **2011**, 52, 373-379.

3. Matsuura-Tokita, K.; Takeuchi, M.; Ichihara, A.; Mikuriya, K.; Nakano, A. Live imaging of yeast Golgi cisternal maturation. *Nature*, **2006**, *441*, 1007-1010.

4. Briegela, A.; R. Ortegac, D. R.; Tochevaa, E. I.; Wuichetd, K.; Lia, Z.; Chena, S.; Müllere, A.; Iancua, C. V.; Murphya, G. E. Dobroa, M. J.; Zhulind, I. B.; Jensena, G. J. Universal architecture of bacterial chemoreceptor arrays. *PNAS,* **2009,** *05,* 181106.

5**.** Binnig, G; Rohrer, H; Gerber, C; Weibel, E. Surface Studies by Scanning Tunneling Microscopy. *Phys. Rev. Lett.* **1982,** *49*, 57-61.

6. McMaster, T.J.; Winfield, M.O.; Karp, A.; Miles, M.J. Analysis of cereal

chromosomes by atomic force microscopy. *Genome*, **1996**, *39*, 439–444.

7. Winfield, M.O.; McMaster, T.J.; Karp, A.; Miles, M.J. Atomic force microscopy of plant chromosomes. *Chromosome Res*. **1995**, *3*, 128–131.

8. Qian, L.; Xiao, H.; Zhao, G.; He, B. Synthesis of modified guanidine-based polymers and their antimicrobial activities revealed by AFM and CLSM. *ACS Appl Mater Interfaces.* **2011**, *3*,1895-1901.

9. Zhou, X. T.; Zhang, F.; Hu, J.; Li, X.; Ma, X. M.; Chen, Y. Cell imprinting and AFM imaging of cells cultured on nanoline patterns. *Microelec. Eng.* **2010***, 87,* 1439-1443.

10. Segura-Valdez, M. L.; Zamora-Cura, A.; Nadia Gutiérrez-Quintanar, N.; Ernesto VillalobosNájera, E.; Rodríguez-Vázquez, J. B.; Galván-Arrieta, T. C.; Rodríguez, D. J.; Agredano-Moreno, L. T.; Lara-Martínez, R.; Jiménez-García , L . F. Visualization of cell structure in situ by atomic force microscopy. *Microscopy,* **2010,** *Sci. Technol, Appl. and Edu.,* 441-448.

11. Ushiki, T.; Yamamoto, S.; Hitomi, J. Atomic Force Microscopy of Living Cells. *Jpn. J. Appl. Phys.* **2000**, *39,* 3761-3764.

12. Tsilimbaris, M.K.; Lesniewska, E.; Lydataki, S.; Le Grimellec, C.; Goudonnet ,J.; P.; Pallikaris, I. G. The Use of Atomic Force Microscopy for the Observation of Corneal Epithelium Surface. *Invest Ophthalmol Vis Sci.,* **2000**, *41*, 680-686.

13. Schaer-Zammaretti, P.; Ubbink, J. Imaging of lactic acid bacteria with AFM—elasticity and adhesion maps and their relationship to biological and structural data. *Ultramicroscopy* **2003**, *97*, 199–208.

14. Rosrcha, C.; Braetb, F.; Wisseb, E.; Radmacher, M. AFM imaging and elasticity measurements on living rat liver macrophages. *Cell Biol Int.,* **1997,** *21*, 685-96.

15. Kirmizis, D.; Logothetidis, S. Atomic force microscopy probing in the measurement of cell mechanics. *Int. J. Nanomed.*, 2010, *5*, 137 -145.

16 Afrin, R.; Zohora, U. S.; Uehara, H.; Watanabe-Nakayama, T.; Ikai, A. Atomic force microscopy for cellular level manipulation: imaging intracellular structures and DNA delivery through a membrane hole. *J Mol Recognit.* **2009**, *22*, 363-372.

17 Hana, S. W.; Nakamuraa, C.; , Obatayaa, I.; Nakamuraa, N.; Miyakea, J. A

molecular delivery system by using AFM and nanoneedle. *Biosensors and Bioelectronics,* **2005***, 20,* 2120-2125.

6. Conclusion

(a) We invented out a novel device named of microwave atomic force microscope (M-AFM), which is a combination of the principles of the scanning probe microscope and the microwave-measurement technique. M-AFM can maintain the constant stand-off distance between the M-AFM-probe tip and scanned sample surface, by detecting the deflection of the atomic force between them, and measure the electrical properties of materials with nanometer scale spatial resolution.

(b) Microwave-AFM probes were fabricated on the GaAs wafer by using the wet etching process. A waveguide was introducing on the probe by evaporating Au film on the both surfaces of the probes. The open structure (the nano-slit) of the waveguide at the tip apex of the M-AFM probe was obtained by using FIB fabrication. SEM was used to observe the fabricated M-AFM probes. As the results, the average dimensions of the cantilever and the body of the M-AFM probes are typically 252×31×14 μm and 2742×723×339 μm, respectively. Based on these dimensions, the characteristic impedance of the M-AFM probes is, on average, 49.3 Ω. In this way, the M-AFM probe could match well with the co-axial line, which has an impedance of 50 Ω. The observed tip is located near the front edge of the cantilever and the tip is approximately 7 μm high, and the nano-slit is approximately 100 nm in width.

(c) The AFM topography of two grating sample having 2000 line/mm and 18 nm step height were measured by the fabricated M-AFM probe. AFM measurements were performed by comparing with the commercial Si AFM probe. The results indicated that GaAs microwave probe has a capability to catch AFM topography of grating samples and having a high accuracy for lateral and height evaluation, similar as the commercial AFM probe.

(d) We have created an M-AFM-obtained microwave image using a compact microwave instrument that was optimally synchronized with an AFM scanner. The distinguishing features of M-AFM are its ability to maintain a constant standoff distance between the probe tip and the sample surface and to measure the microwave

signal interacted with the sample. Therein, both the topography and electrical-property images of the sample can be simultaneously characterized. Therefore, M-AFM is able to measure, *in situ*, the distribution of electrical properties on a nanometer scale. As shown in the experimental results, we successfully generated a microwave image of a 200-nm Au film coating on a glass wafer substrate with a spatial resolution of 120 nm, and, moreover, we measured the voltage difference between these two materials to be 19.2 mV. We believe that the high spatial resolution and simultaneous measurement capability of this M-AFM system will have important implications to nanotechnology characterization in the immediate future.

(e) We also successfully created a microwave image of an Au/Au step sample with a spatial resolution on nanometer order, which indicates that the microwave measurement is not affected by the surface shape of the material and the standoff distance was well controlled by the atomic force.

(f) The sensitivity in the measurement of electrical properties affected by the nano structure of microwave AFM (M-AFM) probe was confirmed. Three kinds of M-AFM probe with a nano-slit on its tip in different width (75 nm, 120 nm and 160 nm) were investigated. Au and glass samples were measured by the probes working at a noncontact AFM mode. The M-AFM probe with the nano-slit having the width of 75 nm, by which the difference of the measured voltage between Au and glass samples is 55.1 mV, shows the highest sensitivity for detecting electrical properties of materials. As the result illustrated, the M-AFM probe with smaller width nano-slit on the tip can be considered to be an ideal nano structure.

(g) We also demonstrated a novel evaluation equation and calibration technique for the quantitative measurement of the local conductivity. Based on the analytical and explicit expressions proposed, using two reference samples with known conductivities, the conductivities of any samples can be calculated from the measured voltage. Our results demonstrate that M-AFM is able to quantitatively measure, in situ, the distribution of electrical properties on the nanometer scale.

(h) Under the non-contact mode, the surfacce topography and microwave image of a single Au nanowire were obtained by the M-AFM probe, simultaneously. The

deference of the measured voltage between the Au and glass substrate is approximately 16 mV. These results illustrate that the M-AFM is capable of sensing the microwave image of a nano-structure. In contrast to the traditional four-point method, which requires some nanowires to be in suitable positions for conductivity measurements by dispersing the nanowires onto an insulated substrate with electrode arrays, the M-AFM can spot the nano-structures directly and measure the microwave image and topography simultaneously.

(i) Using the M-AFM probes with the compact-measurement system, the sample of Au-nano-belts was sensed with three kinds of scanning speed: 500 nm/s, 1000 nm/s, and 2000 nm/s, respectively. Comparing the experimental results, it is suggested that with the decrease of scanning speed, the spatial resolution becomes much better. However, on the other hand, the precision of microwave image was not change much during the decrease of scanning speed. Because M-AFM with the compact microwave instrument can always implements a real time measurement, and the variation of scanning speed cannot put the influence in the microwave measurement (image), the M-AFM can be used to measure the electrical properties of materials with a high operating efficiency.

(j) We carried out a group of experiment to verify the M-AFM with the capacity of measuring the electrical information of underlying materials. Some special samples with different thickness of dielectric films (SiO_2) which plays the role of oxide layer creating on the material surface were fabricated. The thickness of oxide-layer is from 20 nm to 100 nm with 20 nm increase in this work. Based on the results, the M-AFM can be used to measure the electrical property of material under a thin oxide layer with a limited thickness of 60 nm, and the thickness and electromagnetic parameters of the oxide layer should be considered in a quantitative measurement.

(k) M-AFM can sense the topography and microwave image of cells in one scanning process, simultaneously. Under the non-contact AFM mode, a microwave image of osteoblast-like cell on nanometer-scale spatial resolution was created by the M-AFM. By analysis the results, quantification such as number and distribution of organelles and proteins of osteoblast-like cell as well as their dimension and electrical

information can be characterized.